GAUSSIAN NON-CLASSICAL CORRELATIONS IN BIPARTITE DISSIPATIVE CONTINUOUS VARIABLE QUANTUM SYSTEMS

Niall Quinn

A Thesis Submitted for the Degree of PhD
at the
University of St Andrews

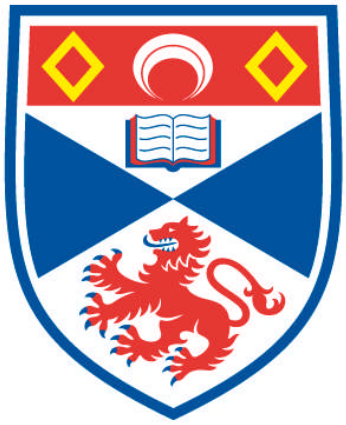

2015

Gaussian Non-Classical Correlations in Bipartite Dissipative Continuous Variable Quantum Systems

Niall Quinn

University of
St Andrews

This Thesis is submitted in partial fulfilment for the degree of Ph.D
at the
University of St Andrews

March 2015

Abstract

This Thesis probes the usefulness of non-classical correlations within imperfect continuous variable decoherent quantum systems. Although a consistent function and practical usefulness of these correlations is largely unknown, it is important to examine their characteristics in more realistic dissipative systems, to gain further insight into any possible advantageous behaviour. A bipartite separable discordant state under the action of controlled loss on one subsystem was considered. Under these conditions the Gaussian quantum discord not only proved to be robust against loss, but actually improves as loss is intensified. Harmful imperfections which reduce the achievable level of discord can be counteracted by this controlled loss. Through a purification an explanation of this effect was sought by considering system-environment correlations, and found that a flow of system-environment correlations increases the quantumness of the state. Entanglement recovery possibilities were discussed and revealed the importance of hidden quantum correlations along bi-partitions across the discordant state and a classically prepared "demodulating" system, acting in such a way as to partially cancel the entanglement preventing noise. Entanglement distribution by separable states was studied by a similar framework, in an attempt to explain the emergence of quantum entanglement by a specific flow of correlations in the globally pure system. Discord appears to play a less fundamental role compared to the qubit version of the protocol. The strengthening of non-classical correlations can be attributed to a flow of classical and quantum correlations. This work proves that discord can be created in unique ways and, in select circumstances, can act to counteract harmful imperfections in the apparatus. Due to this advantageous behaviour discord indeed may ultimately aid in more applicable "real world" applications, which are by definition decoherent.

Declarations

1. Candidate's declarations :
I, Niall Quinn, hereby certify that this thesis, which is approximately 27,000 words in length, has been written by me, and that it is the record of work carried out by me, or principally by myself in collaboration with others as acknowledged, and that it has not been submitted in any previous application for a higher degree.

I was admitted as a research student in October 2011 and as a candidate for the degree of Doctor of Philosophy; the higher study for which this is a record was carried out in the University of St Andrews between 2011 and 2015.

Signature of Candidate:

Date:

2. Supervisor's declaration :
I hereby certify that the candidate has fulfilled the conditions of the Resolution and Regulations appropriate for the degree of Doctor of Philosophy in the University of St Andrews and that the candidate is qualified to submit this thesis in application for that degree.

Signature of Supervisor:

Date:

3. Permission for publication :
In submitting this thesis to the University of St Andrews I understand that I am giving permission for it to be made available for use in accordance with the regulations of the University Library for the time being in force, subject to any copyright vested in the work not being affected thereby. I also understand that the title and the abstract will be published, and that a copy of the work may be made and supplied to any bona fide library or research worker, that my thesis will be electronically accessible for personal or research use unless exempt by award of an embargo as requested below, and that the library has the right to migrate my thesis into new electronic forms as required to ensure continued access to the thesis. I have obtained any third-party copyright permissions that may be required in order to allow such access and migration, or have requested the appropriate embargo below. Access to printed copy and electronic publication of Thesis through the University of St. Andrews.

Signature of Candidate:

Signature of Supervisor:

Date:

Contents

Acknowledgements

First and foremost I would like to thank my supervisor Dr Natalia Korolkova for her support, guidance, and most importantly patience over the past years. I would like to extent my gratitude to Dr Ladislav Mišta for his help throughout this work and for the numerous insightful discussions. Thank you also to Callum Croal for endless constructive discussions throughout the years in the office. My progression was greatly helped by my predecessors Dr Richard Tatham and Dr Darran Milne, who entertained my constant tangential musings. Finally, I would like to thank my family and friends, who have graciously listened to my ramblings and provided endless support and unforgettable memories over this time.

Publications

The following is a list of publications that have arisen as a result of the research of this Thesis.

V. Chille, N. Quinn, C. Peuntinger, C. Croal, L. Mišta, Jr., Ch. Marquardt, G. Leuchs, N. Korolkova.
Quantum nature of Gaussian discord: Experimental evidence and role of system-environment correlations.
Phys. Rev. A, **91**:050301(R), (May 2015).

N. Quinn, C. Croal, V. Chille, C. Peuntinger, L. Mišta, Jr., Ch. Marquardt, G. Leuchs, N. Korolkova.
Robustness of Non-classical Correlations in Dissipative Gaussian Systems due to coupling to Environment.
In preparation (expected 2015).

N. Quinn, N. Korolkova.
Flow of quantum correlations through a tripartite open system and entanglement distribution by separable ancilla.
In preparation (expected 2015).

Conference Presentations

The following lists the conferences in which I have taken part.

1. 500. WE-Heraeus-Seminar Highlights of Quantum Optics, Bad Honnef, Germany (May 2012), Poster presentation.
2. Quantum Correlations Student Workshop, Nottingham, England (Jul 2012), Poster presentation.
3. Quantum Information, Computing and Control, Aberystwyth, Wales (Aug 2012), Poster presentation.
4. Quantum Atomic and Molecular Physics, Belfast, N. Ireland (Sep 2012), Oral presentation.
5. 20^{th} Central European Workshop on Quantum Optics, Stockholm, Sweden (Jun 2013), Poster presentation.
6. 21^{st} Central European Workshop in Quantum Optics, Brussels, Belgium (Jun 2014), Poster presentation.

For Helen

Young men and maids enjoy yourselves, be happy while you may,
Send round the song and merry dance to drive dull cares away.
Revive old Irish pastimes and the language of the Gael,
And banish foreign fashions from the land of Innishfail.

The times are greatly changed and are changing still I see,
What may they be in forty years, when you're as old as me.
These songs may then be out of date, they may be heard no more,
But they were the songs our fathers loved in the fighting days of yore.

T'was an Island of saints and scholars, here scholars from Europe did come,
To drink from its fountains of knowledge, enthralled by its music and song.
The Irishman's home is in Ireland, that beautiful Isle in the west,
That Island made verdant and holy, by the footsteps of saints on its breast.

Patrick Farrell (1856 – 1938)

Part I

Foundational Material

Chapter 1

Introduction

The undoubtable crowning achievement of modern science is the construction of a simple and elegant description of the universe, as composed of seemingly inexplicable and esoteric phenomena. The complexities of the macroscopic world can be remarkably attributed to the behaviour of just three particles and four forces.

All physical objects are constructed from varying configurations of three particles: neutrons, protons and electrons, later discovered to be themselves composed of smaller entities known as quarks. Underpinning these building blocks is quantum theory. Three of the four forces, namely the strong and weak nuclear forces in operation within the atomic nucleus and the electromagnetic force holding atoms and molecules together, can be best described by quantum theory. The fourth force is perhaps the most commonly known but is one for which, as yet, there is no sufficient and satisfactory quantum description, the force of gravity.

Quantum theory was based on a foundation of unexpected and bewildering natural phenomena not explained by any existing scientific framework at the time of its conception. The term 'quantum' was introduced into physics in 1901 by Max Planck in context of "quanta of matter and electricity". Lightly speaking, Planck concluded from his work on black body radiation that light must be emitted in packets of energy called 'quanta' [1], originating from the Latin referring to a discrete quantity. Whilst this concept was considered as a purely mathematical manoeuvre, it was later supported by the work of Albert Einstein on the photoelectric effect, thus concluding that light appears to exhibit legitimate particle properties [2]. This was revolutionary since the only existing description of light was based on the unquestionable work of James Clerk Maxwell, that light is an electromagnetic wave propagating through space [3]. Combining these discoveries lead to what is referred to as the *wave-particle duality* of light. Duality is mathematically represented by a combination of Planck's postulation of the proportionality between the frequency of a quanta of light (or photon) and its energy, $E = \hbar\omega$, and de Broglie's relation between momentum and wavelength, $\lambda = \hbar/p$ later proposed in 1925.

In 1926, Schrödinger published his wave equation based on classical energy conservation

using quantum operators, solutions of which are the wave functions for the quantum system,

$$i\hbar\frac{\partial}{\partial t}\Psi = \hat{H}\Psi$$

where the wavefunction formulation treats the particle as a quantum harmonic oscillator. This marks the inspiration for the *Copenhagen interpretation* of quantum mechanics, relating the squared modulus of the wave function, to the probability density of measuring a particle at a given time and place.

A generalisation of the wavefunction description of a quantum state is the density operator. This is used to include the possible uncertainty in state preparation. The density operator is defined using a statistical ensemble of quantum states $\{|\Psi_n\rangle\}$ in Hilbert space with probabilities $\{p_n\}$ as

$$\hat{\rho} = \sum_n p_n |\Psi_n\rangle\langle\Psi_n|.$$

By choosing an arbitrary basis $\{|i\rangle\}$, one can define the density matrix as a positive semi-definite[1], normalised Hermitian matrix,

$$\rho = \sum_{ij} |i\rangle\langle i|\hat{\rho}|j\rangle\langle j|.$$

A density matrix is seen to describe the two general classes of state, those that are considered as *pure states* with $\mathrm{Tr}[\rho^2] = 1$, and a statistical mixture of pure states known as *mixed states* with $0 \leq \mathrm{Tr}[\rho^2] < 1$.

Born from quantum theory was the concept of quantum information. The birth of quantum information is considered to be in the paper published by Einstein, Podolsky and Rosen in 1935 [4] which introduced questions leading the concept of *quantum entanglement* — although this term was later officially coined by Schrödinger [5]. The thought experiment considered a so-called EPR state of two systems A and B, each described by two conjugate quantities, which interact briefly and then sent to two separate locations. The aim of the thought experiment was to conclude the incompleteness of *Heisenberg's uncertainty principle* [6], which states that if one quantity is measured and thus fully determined, then the other conjugate quantity of the same system must become indeterminate. The EPR paradox concluded that it was possible that if one conjugate quantity of A is determined, then the corresponding quantity of system B will be undetermined even if no contact occurs between the two systems. The conclusion of this result was that the total information of a bipartite system AB is not merely composed of the joint information of the two individual systems. This "spooky action at a distance" is what is defined as quantum entanglement.

Imperative work by Ben Schumacher lead to the revolutionary interpretation that quantum information is physical, and as such can be measured and quantified [7]. Quantum information is measured in units of *qubits (or quantum bits)*, a quantum analogy to the classical bit. A qubit is seen as an informational representation of a physical particle itself, and since any physical object can be described by its information, a qubit is treated as a one-to-one correspondence to a physical particle. Much like a classical bit, a qubit has two

[1] A positive semi-definite matrix M is one which satisfies $x^* M x \geq 0$ for all complex matrices x.

possible states denoted $|0\rangle$ and $|1\rangle$, however the most notable difference is that a qubit may be in both configurations simultaneously. It is possible for a qubit to be in a linear combination of states $|\psi\rangle = \alpha|0\rangle + \beta|1\rangle$, more commonly known as a *superposition state*, which is at the heart of quantum entanglement in larger systems containing two or more qubits. α and β are complex numbers and their square modulus define the probability of being in either of the two extreme configurations. With having two states, which form an orthonormal basis of a two-dimensional vector space, qubits are said to exist in a finite dimensional Hilbert space. A combination of many qubits then exists in a larger Hilbert space defined as $\mathcal{H} = \bigotimes_{i=1}^{n} \mathcal{H}_i$.

One indispensable description in quantum information processing is the *von Neumann entropy* defined as

$$\mathcal{S}(\rho) = -\mathrm{Tr}[\rho \log \rho], \tag{1.1}$$

with ρ being the density matrix of a state. The entropy provides an indication to the level of disorder within a system such that if $\mathcal{S}(\rho) = 0$, the state is considered to be pure, hence the entropy of a system indicates its departure from a pure state system, or the degree of mixing present. This tool is in turn used to define the entire information contained within a bipartite state beyond that described by the joint entropy of the two individual systems alone, termed the *total quantum mutual information*, i.e.,

$$\mathcal{I}_q(\rho_{AB}) = \mathcal{S}(\rho_A) + \mathcal{S}(\rho_B) - \mathcal{S}(\rho_{AB}). \tag{1.2}$$

Developed from the concept of entropy and mutual information was *quantum discord*. Discord is a measure of correlations in a bipartite mixed state which are classified as non-classical and so includes quantum entanglement. There however exist a set of states which, although are strictly non-classical, do not possess quantum entanglement. The ultimate usefulness and practical implications of these states have been a topic of immense interest and continue to attract much attention. The following Thesis aims to provide new insight to the functionality of states which possess these class of correlations, particularly within dissipative systems with numerous sources of loss.

The outline of this Thesis is as follows: The necessary foundational material will be contained within Part I divided into Chapter 2 which will provide an essential introduction to the extension into infinite-dimensional Hilbert space in the form of continuous variable quantum optical principles; Chapter 3 will give an extensive explanation of quantum entanglement including methods of quantification; Chapter 4 will elaborate on the possible correlations by discussing non-classicality in general, including quantum discord. The knowledge of these Chapters will then be applied in Part II. Chapter 5 will introduce an original scheme involving a bipartite dissipative system, serving as the main focus of this Thesis. Relating to this, in the latter half of Chapter 5 a previously unconsidered insight will be given to the protocol for entanglement distribution via separable ancilla. Chapter 6 will then contain some concluding remarks and highlight the main results and insights introduced.

Chapter 2

Continuous Variable Systems

With the rapid development of quantum information science in recent years, and the goal of realisable quantum technologies in the near future, it is inspiring how the quantum interpretation of the physical world has progressed. In particular, the revolutionary development of the quantum mechanical interpretation of light. Until Einstein in 1905, light was solely thought of as a classical object with the behaviour of a wave. It was not until Lanard's work on the photoelectric effect that later prompted Einstein to propose that light, instead of completely filling space, possesses a "grainy" structure. Of course we now know these 'grains' to be wave packets of light known as *photons*. Consequentially, light exhibits both the properties of a wave and also of being composed of particles [2]. This was the first formal proposal of a quantum effect and earned Einstein a Nobel Prize in 1921.

Now in the 21^{st} century further revelations are ever-occurring particularly with the fields of optical computing and transformation optics. The content of this Chapter is designed to provide a fundamental introduction to the quantum properties and mathematical representation of light crucial to studies in later Chapters. We begin by introducing the field of quantum optics in general and the main connections to quantum informational concepts. Until finally converging to a distinct set of states of which we are concerned, namely, *Gaussian states*. Everything introduced in this Chapter (and much more) has been covered extensively in literature such as [8–12].

2.1 Introductory Quantum Optics

Quantisation of Multimode Free Electromagnetic Field

During the years of 1861 and 1862, Maxwell introduced a set of intrinsic partial differential equations relating the electric and magnetic fields [3]. Maxwell was one of the first to determine that the speed of propagation of an electromagnetic wave was the same as the speed of light, thus contributing to the conclusion that electromagnetic waves and visible light were one and the same. The electric field $\mathbf{E}$ will induce a local dipole moment in a dielectric medium since it will cause the charges to move, this will cause an electric displacement field $\mathbf{D} = \epsilon_0 \mathbf{E}$ in free space, where ϵ_0 is the permittivity of free space. The

magnetic field $\mathbf{H}$ and magnetic induction $\mathbf{B}$ are related similarly as $\mathbf{H} = \mu_0\mathbf{B}$, where μ_0 is the permeability of free space. Free space refers to the assumption that there are no present sources of radiation and no charges. The formal presentation of Maxwell's equations are of the form:

$$\nabla \times \mathbf{E} = -\frac{\partial \mathbf{B}}{\partial t}, \quad \nabla \times \mathbf{H} = \frac{\partial \mathbf{D}}{\partial t}, \quad \nabla \cdot \mathbf{B} = 0, \quad \nabla \cdot \mathbf{D} = 0. \tag{2.1}$$

Note that the permittivity, ϵ, and permeability, μ, of the material through which the light travels are unity since we are concerned with free space only. The first relation is *Faraday's law of induction*, the second is *Ampère's law*, amended by Maxwell to include the displacement current, the third and fourth relations are *Gauss' laws* for the electric and magnetic fields.

The quantisation of the electromagnetic field is done by promoting the classical fields to operators and impose commutation relations, thus establishing the interpretation that a classical field is an expectation value of a quantum observable. The promoted field operators $\hat{\mathbf{E}}, \hat{\mathbf{D}}, \hat{\mathbf{H}}, \hat{\mathbf{B}}$ thus now describe a quantum field. The electric and magnetic induction fields may now be cast in terms of their vector potential $\hat{\mathbf{A}}$, which satisfies the wave equation and the Coulomb gauge condition

$$\nabla^2 \hat{\mathbf{A}} - \frac{1}{c^2}\frac{\partial^2 \hat{\mathbf{A}}}{\partial t^2} = 0 \quad \text{and} \quad \nabla \cdot \hat{\mathbf{A}} = 0, \tag{2.2}$$

where

$$\hat{\mathbf{E}} = -\frac{\partial \hat{\mathbf{A}}}{\partial t} \quad \text{and} \quad \hat{\mathbf{B}} = \nabla \times \hat{\mathbf{A}}. \tag{2.3}$$

subject to the boundary conditions that the fields will be negligible at infinity. Note that the speed of light c in the wave equation (2.2) is related to free space parameters as $c = (\epsilon_0\mu_0)^{-1/2}$. The classical vector potential can be written as a superposition of plane waves, given in the form

$$\mathbf{A}(\mathbf{r}, t) = \sum_{\mathbf{k},s} \mathbf{e}_{\mathbf{k}s} \left[A_{\mathbf{k}s}(t) e^{i\mathbf{k}\cdot\mathbf{r}} + A^*_{\mathbf{k}s}(t) e^{-i\mathbf{k}\cdot\mathbf{r}} \right], \tag{2.4}$$

where $A_{\mathbf{k}s}(t)$ is the amplitude of the field, with $\mathbf{k}$ the wave vector, and $\mathbf{e}_{\mathbf{k}s}$ the real polarisation vector of two orthogonal, independent polarisations, s and s'. The quantised vector potential is then recast as

$$\hat{\mathbf{A}}(\mathbf{r}, t) = \sum_{\mathbf{k},s} \left(\frac{\hbar}{2\omega_k \epsilon_0 V} \right)^{\frac{1}{2}} \mathbf{e}_{\mathbf{k}s} \left[\hat{a}_{\mathbf{k}s}(t) e^{i\mathbf{k}\cdot\mathbf{r}} + \hat{a}^\dagger_{\mathbf{k}s}(t) e^{-i\mathbf{k}\cdot\mathbf{r}} \right], \tag{2.5}$$

where ω_k is the frequency of the mode. Continuing from this, the electric and magnetic field operators can be written, using Eq.'s (2.3), as

$$\begin{aligned} \hat{\mathbf{E}}(\mathbf{r}, t) &= i \sum_{\mathbf{k},s} \left(\frac{\hbar\omega_k}{2\epsilon_0 V} \right)^{\frac{1}{2}} \mathbf{e}_{\mathbf{k}s} \left[\hat{a}_{\mathbf{k}s} e^{i(\mathbf{k}\cdot\mathbf{r} - \omega_k t)} - \hat{a}^\dagger_{\mathbf{k}s} e^{-i(\mathbf{k}\cdot\mathbf{r} - \omega_k t)} \right], \\ \hat{\mathbf{B}}(\mathbf{r}, t) &= \frac{i}{c} \sum_{\mathbf{k},s} \left(\frac{\hbar\omega_k}{2\epsilon_0 V} \right)^{\frac{1}{2}} \left(\frac{\mathbf{k}}{|\mathbf{k}|} \times \hat{\mathbf{e}}_{\mathbf{k}s} \right) \left[\hat{a}_{\mathbf{k}s} e^{i(\mathbf{k}\cdot\mathbf{r} - \omega_k t)} - \hat{a}^\dagger_{\mathbf{k}s} e^{-i(\mathbf{k}\cdot\mathbf{r} - \omega_k t)} \right], \end{aligned} \tag{2.6}$$

respectively, the operator $\hat{a}_{\mathbf{k}s}$ is defined such that

$$\hat{A}_{\mathbf{k}s} = \left(\frac{\hbar}{2\omega_k \epsilon_0 V}\right)^{\frac{1}{2}} \hat{a}_{\mathbf{k}s}. \tag{2.7}$$

The total energy of the electromagnetic field is given by the Hamiltonian

$$\hat{H} = \frac{1}{2}\int_V \left(\epsilon_0 \hat{\mathbf{E}}^2 + \frac{1}{\mu_0}\hat{\mathbf{B}}^2\right) dV, \tag{2.8}$$

which, by substituting in Eq.'s (2.6) is recast as

$$\hat{H} = \frac{1}{2}\sum_{\mathbf{k},s} \hbar\omega_k \left(\hat{a}^\dagger_{\mathbf{k}s}\hat{a}_{\mathbf{k}s} + \hat{a}_{\mathbf{k}s}\hat{a}^\dagger_{\mathbf{k}s}\right). \tag{2.9}$$

These operators in turn satisfy the commutation relations,

$$\begin{aligned} [\hat{a}_{\mathbf{k},s},\ \hat{a}_{\mathbf{k}',s'}] &= [\hat{a}^\dagger_{\mathbf{k},s},\ \hat{a}^\dagger_{\mathbf{k}',s'}] = 0, \\ [\hat{a}_{\mathbf{k},s},\ \hat{a}^\dagger_{\mathbf{k}',s'}] &= \delta_{\mathbf{k}\mathbf{k}'}\delta_{ss'}, \end{aligned} \tag{2.10}$$

with $\hat{a}_{\mathbf{k},s}$ and $\hat{a}^\dagger_{\mathbf{k},s}$ being defined as the photon annihilation and creation operators respectively. Acting together to define the photon number operator as $\hat{n}_{\mathbf{k}s} = \hat{a}^\dagger_{\mathbf{k},s}\hat{a}_{\mathbf{k},s}$. The photon number is raised and lowered by the creation and annihilation operators respectively, placing the state into a different eigenstate, $|n\rangle$, of the photon number operator. It is important to note that, when considering a vacuum, the energy of the state $|0\rangle$ is non-zero, i.e., it contains random fluctuations. This can be interpreted as an analogue of the zero point oscillations in a harmonic oscillator in its ground state.

The Fock (or number) states, $|n\rangle$ are defined as the eigenstates of the number operator $\hat{n}$. The Fock state then represents a state of n photons. Let us consider now application of the creation and annihilation operators to a single-mode Fock state,

$$\begin{aligned} \hat{a}|n\rangle &= \sqrt{n}|n-1\rangle, \quad \text{where} \quad \hat{a}|0\rangle = 0, \\ \hat{a}^\dagger|n\rangle &= \sqrt{n+1}|n+1\rangle. \end{aligned} \tag{2.11}$$

Note that when the annihilation operator is applied to the ground state $|0\rangle$, this must return zero. Intuitive as this is the lowest energy state containing zero photons and thus cannot be brought to a lower energy state with $n < 0$. From this, the photon number n can then be interpreted as the number of excitations above the vacuum state, i.e.,

$$|n\rangle = \frac{\left(\hat{a}^\dagger\right)^n}{\sqrt{n!}}|0\rangle. \tag{2.12}$$

In order to progress with the quantisation of the field, the canonically conjugate operators $\hat{x}_{\mathbf{k},s}$ and $\hat{p}_{\mathbf{k},s}$ must be introduced, modelling observable quantities and satisfying the

following similar commutation relations,

$$\begin{aligned}[\hat{x}_{\mathbf{k},s},\ \hat{x}_{\mathbf{k}',s'}] &= [\hat{p}_{\mathbf{k},s},\ \hat{p}_{\mathbf{k}',s'}] = 0, \\ [\hat{x}_{\mathbf{k},s},\ \hat{p}_{\mathbf{k}',s'}] &= i\hbar\delta_{\mathbf{k}\mathbf{k}'}\delta_{ss'}.\end{aligned} \tag{2.13}$$

Within the multimode setting, the so-called annihilation and creation operators can be defined in terms of these canonically conjugate operators as,

$$\begin{aligned}\hat{a}_{\mathbf{k}s} &= (2\hbar\omega_k)^{-\frac{1}{2}}\left[\omega_k\hat{x}_{\mathbf{k},s} + i\hat{p}_{\mathbf{k},s}\right] \\ \hat{a}^\dagger_{\mathbf{k}s} &= (2\hbar\omega_k)^{-\frac{1}{2}}\left[\omega_k\hat{x}_{\mathbf{k},s} - i\hat{p}_{\mathbf{k},s}\right]\end{aligned} \tag{2.14}$$

respectively, with the Hamiltonian of the electromagnetic field in Eq. (2.9) becoming recast as

$$\begin{aligned}\hat{H} &= \sum_{\mathbf{k},s}\hbar\omega_k\left(\hat{a}^\dagger_{\mathbf{k}s}\hat{a}_{\mathbf{k}s} + \frac{1}{2}\right), \\ &= \sum_{\mathbf{k},s}\hbar\omega_k\left(\hat{n}_{\mathbf{k}s} + \frac{1}{2}\right),\end{aligned} \tag{2.15}$$

using the definition of the photon number operator $\hat{n}_{\mathbf{k}s} = \hat{a}^\dagger_{\mathbf{k}s}\hat{a}_{\mathbf{k}s}$.

Fock (Number) States

The generalised Fock state of a multimode field is the product of all the Fock states in the field and so is of the form,

$$|\{n_j\}\rangle = \prod_j \frac{\left(\hat{a}^\dagger_j\right)^{n_j}}{\sqrt{n_j!}}|\{0\}\rangle, \tag{2.16}$$

where $\{n_j\}$ is the set of all Fock states for j modes. The energy of a Fock state is given by eigenvalues of the Hamiltonian,

$$\hat{H}|n_j\rangle = E_j|n_j\rangle = \sum_j \hbar\omega_j\left(n_j + \frac{1}{2}\right), \tag{2.17}$$

hence the energy of the vacuum state is $E_0 = \frac{1}{2}\hbar\omega_0$. An important property of Fock states is that they form a complete set of orthonormal states, i.e.,

$$\langle n_j|n_k\rangle = \delta_{j,k} \quad \text{and} \quad \sum_j |n_j\rangle\langle n_j| = 1. \tag{2.18}$$

Quadrature States

To begin we must reintroduce the operators $\hat{x}$ and $\hat{p}$ termed as *quadrature operators* defined in the most simple form using Eq.'s (2.14) with $\hbar = 1$ as,

$$\begin{aligned} \hat{x} &= \frac{1}{\sqrt{2}}\left(\hat{a}^\dagger + \hat{a}\right), \\ \hat{p} &= \frac{i}{\sqrt{2}}\left(\hat{a}^\dagger - \hat{a}\right), \end{aligned} \tag{2.19}$$

which appear in the real and imaginary components of the "complex" amplitude $\hat{a}$ as,

$$\hat{a} = \frac{1}{\sqrt{2}}\left(\hat{x} + i\hat{p}\right), \tag{2.20}$$

In quantum optics the common interpretation of these operators are as the conjugate "position" and "momentum" of a quantum system in phase-space due to the commutation relation it satisfies,

$$[\hat{x}, \hat{p}] = i. \tag{2.21}$$

However, in actuality they are loose interpretations of these physical quantities, since for a single photon the concept of position and momentum are not easily defined. These labels are chosen as these operators exhibit a similar connection as between position and momentum. Alternate definitions of these quadratures are as the "amplitude" and "phase" of light, since they satisfy the same commutation relation. The quadrature states are defined as the eigenstates of the quadrature operators and similarly to Fock states (discussed above) are orthogonal and complete

$$\begin{aligned} &\hat{x}|x\rangle = x|x\rangle, \quad \langle x|x'\rangle = \delta(x - x'), \quad \int_{-\infty}^{\infty} |x\rangle\langle x| dx = \mathbb{1}, \\ &\hat{p}|p\rangle = p|p\rangle, \quad \langle p|p'\rangle = \delta(p - p'), \quad \int_{-\infty}^{\infty} |p\rangle\langle p| dx = \mathbb{1}. \end{aligned} \tag{2.22}$$

From these quadrature operators it is possible to define the position and momentum distributions associated with a state with wavefunction $\psi(x)$ as

$$\psi(x) = \langle x|\psi\rangle, \quad \tilde{\psi}(p) = \langle p|\psi\rangle, \tag{2.23}$$

where the quadrature states are simply related by a Fourier transform. More generally speaking, the position and momentum distributions for the n^{th} Fock state are defined as,

$$\begin{aligned} \psi_n(x) = \langle x|n\rangle &= \frac{H_n(x)}{\sqrt{2^n n!}\pi^{1/4}} e^{-\frac{x^2}{2}}, \\ \tilde{\psi}_n(p) = \langle p|n\rangle &= \frac{H_n(p)}{\sqrt{2^n n!}\pi^{1/4}} e^{-\frac{p^2}{2}}, \end{aligned} \tag{2.24}$$

where H_n are the Hermite polynomials.

Coherent States

Coherent states are a set of states seen to give rise to the most sensible classical limit, and thus are termed the "most classical" quantum states [13–15]. Coherent states are defined with respect to the creation and annihilation operators as follows

$$\hat{a}|\alpha\rangle = \alpha|\alpha\rangle, \quad \langle\alpha|\hat{a}^\dagger = \alpha^*\langle\alpha|, \tag{2.25}$$

where α is an arbitrary complex number defined as $\alpha = |\alpha|e^{i\theta}$ with $|\alpha|$ and θ the amplitude and phase respectively. The normalised form of a coherent state is provided through the completeness of Fock states as,

$$|\alpha\rangle = \sum_{n=0}^{\infty} c_n|n\rangle = \exp\left(-\frac{|\alpha|^2}{2}\right)\sum_{n=0}^{\infty}\frac{\alpha^n}{\sqrt{n!}}|n\rangle. \tag{2.26}$$

Substituting Eq. (2.12) we have an expression for the coherent state as,

$$|\alpha\rangle = \exp\left(-\frac{|\alpha|^2}{2}\right)\exp(\hat{a}^\dagger\alpha)|0\rangle. \tag{2.27}$$

Since it can be written that $\exp(-\alpha^*\hat{a})|0\rangle = |0\rangle$, the coherent state can be recast as,

$$|\alpha\rangle = \hat{D}(\alpha)|0\rangle, \quad \text{with} \quad \hat{D}(\alpha) = \exp\left(-\frac{|\alpha|^2}{2}\right)\exp(\hat{a}^\dagger\alpha)\exp(-\alpha^*\hat{a}). \tag{2.28}$$

The operator $\hat{D}(\alpha)$ is a unitary operator,

$$\hat{D}^\dagger(\alpha) = \hat{D}(-\alpha) = [\hat{D}(\alpha)]^{-1}, \tag{2.29}$$

which acts as a *displacement operator*. Hence a coherent state is interpreted as a displaced vacuum state, or displaced form of the ground state of the harmonic oscillator.

Properties of the coherent states that are of note are:

- the probability of finding n photons in a coherent state $|\alpha\rangle$ is given by a Poisson distribution, namely,
$$p(n) = \frac{\langle n\rangle^n e^{-\langle n\rangle}}{n!} \tag{2.30}$$
where $\langle n\rangle = \langle\alpha|\hat{a}^\dagger\hat{a}|\alpha\rangle = |\alpha|^2$ is the mean photon number.

- the coherent state is a minimum uncertainty state given by the saturated Heisenberg's uncertainty principle, i.e.,
$$\Delta x\Delta p = \frac{1}{2}, \tag{2.31}$$
where Δx is the standard deviation of x such that $\Delta^2 x$ is the variance of x. Uncertainty will be discussed in more depth later in this Section.

- coherent states form an over complete set. This follows from the completeness of Fock states discussed earlier. Summing over n photons is simply the unit operator, such

that

$$\frac{1}{2}\int |\alpha\rangle\langle\alpha| d\alpha = \mathbb{1}, \tag{2.32}$$

which acts as the completeness relation for coherent states. In addition, coherent states are non-orthogonal with,

$$\langle\alpha|\beta\rangle = \exp\left(-\frac{|\alpha|^2}{2} - \frac{|\beta|^2}{2} + \alpha^*\beta\right) \Rightarrow |\langle\alpha|\beta\rangle|^2 = \exp(-|\alpha-\beta|^2)), \tag{2.33}$$

since they are not eigenstates of a Hermitian operator.

Coherent states are of particular interest as they describe the state of ideal laser light and hence allows for the physical interpretation and experimental realisation of quantum concepts.

Uncertainty and Squeezing

The uncertainty of canonically conjugate operators, related by the widely used uncertainty relation presented by Heisenberg, is at the heart of quantum mechanics [6]. Considering the quadrature operators given in Eq. (2.19) with commutation relation in Eq. (2.21) leads to Heisenberg's uncertainly relation for quadrature observables as

$$\Delta x \Delta p \geq \frac{1}{2}. \tag{2.34}$$

Minimum uncertainty states, e.g. coherent states, are those for which this relation is saturated. Consider now the instance where the uncertainty of one observable is varied within a minimum uncertainty state. If Δx is decreased, in order for Heisenberg's relation to hold, the uncertainty of the corresponding canonically conjugate observable Δp must increase. This proportional change in uncertainty is a process known as "squeezing". As a consequence if $\Delta^2 x$ or $\Delta^2 p < \frac{1}{4}$, then the state is squeezed. Considering now the extremal case where the exact position x in the minimum uncertainty state is known. By Heisenberg's uncertainty principle, the uncertainty of the momentum will be infinity, thus implying that both canonically conjugate quadratures cannot simultaneously be known to an exact certainty at a given time. Perfect (or infinite) squeezing will correspond to an unphysical state. The squeezing is parameterised by the squeezing parameter, r, such that the variances of the quadratures read as

$$\Delta^2 x = \frac{1}{2}e^{-2r} \quad \text{and} \quad \Delta^2 p = \frac{1}{2}e^{2r}. \tag{2.35}$$

Moreover, as will be discussed in the next Section, the squeezing of a state can be implemented as a unitary operation on the vacuum state $|0\rangle$, with the *squeezing operator* defined as

$$\hat{S}(r) = \exp\left[\frac{r}{2}\left((\hat{a}^\dagger)^2 - \hat{a}^2\right)\right], \tag{2.36}$$

first introduced in [16–18]. In fact all minimum uncertainty states are displaced squeezed vacuum states [19].

Hilbert Space

The Hilbert space was originally introduced as a generalisation to Euclidean three-dimensional space. A set of quantum states known as *pure states* may be represented by unit vectors (or state vectors) residing in a complex *Hilbert space*, also known as the state space. The remaining set of quantum states are known as *mixed states*, corresponding to a statistical mixture of pure states. It is interesting to note that different distributions of pure states can generate physically indistinguishable, equivalent, mixed states. Both pure and mixed states are described by their so-called *density matrix*, ρ, which is a positive, semi-definite Hermitian matrix in Hilbert space. The density matrix is defined by choosing an orthonormal basis $\{|u_n\rangle\}$ such that

$$\rho_{mn} = \sum_i p_i \langle u_m|\psi_i\rangle\langle\psi_i|u_n\rangle = \langle u_m|\hat{\rho}|u_n\rangle \tag{2.37}$$

where $\hat{\rho}$ is the density operator given by

$$\hat{\rho} = \sum_i p_i |\psi_i\rangle\langle\psi_i|, \tag{2.38}$$

where p_i is the probability of the system being in a states $|\psi_i\rangle$. A bipartite state $\rho = \rho_1 \otimes \rho_2$ will then exist in the composite Hilbert space i.e., the tensor product of individual Hilbert spaces, $\mathcal{H} = \mathcal{H}_1 \otimes \mathcal{H}_2$. When discussing continuous variable systems, an infinite-dimensional Hilbert space is considered. Hence a vacuum or coherent state, for example, are pure quantum states in an infinite-dimensional Hilbert space.

Let us now consider the physical description of quantum states and the mathematical space in which they are seen to exist. As mentioned briefly in the description of classes of states, this will involve the introduction of phase-space as well as the probabilistic nature of quantum systems.

2.2 Phase-Space Quasi-Probability Distributions

2.2.1 Wigner Function

Classically it is possible to define a system as being at a single point in phase-space described by a pair of incompatible observables, e.g., position and momentum. However, due to Heisenberg's uncertainty principle, it is not feasible to observe a system's position and momentum simultaneously. If an ensemble of particles is considered, the results would form a statistical representation of the system as probability distributions $P(x)$ and $P(p)$, with the joint distribution describing the entire state. The Wigner function was introduced as the quantum analogue to these distributions and was one of the earliest introduced quasi-probability distributions [20]. The phase space probability distribution has as a one-to-one correspondence with the density matrix. For an arbitrary density operator $\hat{\rho}$ corresponding to a quantum state the Wigner function is defined as

$$\mathcal{W}(x,p) = \frac{1}{2\pi\hbar}\int_{-\infty}^{+\infty} \left\langle x + \frac{q}{2}\right| \hat{\rho} \left| x - \frac{q}{2}\right\rangle e^{ipq/\hbar} dq, \tag{2.39}$$

where $\left|x-\frac{q}{2}\right\rangle$ are the eigenkets of the position operator. This can be derived as the Fourier transform of the Weyl ordered characteristic function. If the state with density matrix ρ is a pure state then the Wigner function will read

$$\mathcal{W}(x,p)=\frac{1}{2\pi\hbar}\int_{-\infty}^{+\infty}\phi^*\left(x+\frac{q}{2}\right)\phi\left(x-\frac{q}{2}\right)e^{ipq/\hbar}dq. \tag{2.40}$$

Integrating over the position (momentum) will yield the probability density for the momentum (position) variable, respectively, i.e.,

$$\begin{aligned}\int_{-\infty}^{+\infty}\mathcal{W}(x,p)dp&=\frac{1}{2\pi\hbar}\int_{-\infty}^{+\infty}\int_{-\infty}^{+\infty}\phi^*\left(x+\frac{q}{2}\right)\phi\left(x-\frac{q}{2}\right)e^{ipq/\hbar}dpdq\\&=\int_{-\infty}^{+\infty}\phi^*\left(x+\frac{q}{2}\right)\phi\left(x-\frac{q}{2}\right)\delta(q)dq\\&=|\phi(x)|^2\end{aligned} \tag{2.41}$$

The position (momentum) space wavefunction can then be transformed into co-ordinate space by a Fourier transform. Although the Wigner function can be decomposed into probability densities of position and momentum, it is however not a true probability distribution as it can become negative for some non-classical states and it is of course not possible to measure both position and momentum simultaneously. It is for these reasons that the Wigner function is termed as a *quasi-probability distribution.*

Key properties that define the Wigner representation are given in [20, 21] and outlined as:

- The Wigner function is real and normalised

$$\iint_{all\ space}\mathcal{W}(x,p)dxdp=1,\qquad \mathcal{W}(x,p)=\mathcal{W}^*(x,p). \tag{2.42}$$

- A rotation in phase-space by a unitary operator $U(\theta)=e^{i\theta}$ is simply given by

$$\begin{aligned}\rho&\to U(\theta)\rho U^\dagger(\theta)\\\mathcal{W}(x,p)&\to\mathcal{W}(x\cos\theta-p\sin\theta,x\sin\theta+p\cos\theta).\end{aligned} \tag{2.43}$$

  The Wigner function is also bounded by the constraint that

$$|\mathcal{W}(x,p)|\leq\frac{1}{\pi}, \tag{2.44}$$

  which stems from expressing the Wigner function using Wigner's formula and the Cauchy-Schwarz inequality[1] so that

$$|\mathcal{W}(x,p)|^2\leq\frac{1}{(2\pi)^2}\int_{-\infty}^{\infty}\left|\left\langle x-\frac{q}{2}|\psi\right\rangle\right|^2dq\int_{-\infty}^{\infty}\left|\left\langle x+\frac{q}{2}|\psi\right\rangle\right|^2dq=\frac{1}{\pi^2} \tag{2.45}$$

[1]The Cauchy-Schwarz inequality states that for two square integrable complex valued functions f and g; $|\int f^*(x)g(x)dx|^2\leq(\int|f(x)|^2dx)(\int|g(x)|^2dx)$.

- One of the more significant properties of the Wigner function is the *overlap formula*. This property is remarkable as it allows to calculate expectation values in a classical fashion. Consider first two operators (not necessarily Hermitian) $\hat{A}_1$ and $\hat{A}_2$,

$$\begin{aligned}\mathrm{Tr}[\hat{A}_1\hat{A}_2] &= 2\pi\int_{-\infty}^{+\infty}\int_{-\infty}^{+\infty}\mathcal{W}_1(x,p)\mathcal{W}_2(x,p)dxdp \\ &= \int_{-\infty}^{+\infty}\int_{-\infty}^{+\infty}\left\langle x+\frac{q}{2}\right|\hat{A}_1\left|x-\frac{q}{2}\right\rangle\left\langle x+\frac{q}{2}\right|\hat{A}_2\left|x-\frac{q}{2}\right\rangle dqdx \\ &= \int_{-\infty}^{+\infty}\int_{-\infty}^{+\infty}\langle x'|\,\hat{A}_1\,|x''\rangle\,\langle x'|\,\hat{A}_2\,|x''\rangle\,dx'dx'' \\ &= \int_{-\infty}^{+\infty}\langle x'|\,\hat{A}_1\hat{A}_2\,|x'\rangle\,dx'.\end{aligned} \tag{2.46}$$

  In setting the operators to a density operator $\hat{\rho}$ and an operator $\hat{A}$ this is recast as,

$$\mathrm{Tr}[\rho\hat{A}] = 2\pi\int_{-\infty}^{+\infty}\int_{-\infty}^{+\infty}\mathcal{W}_\rho(x,p)\mathcal{W}_A(x,p)dxdp. \tag{2.47}$$

  The notability of this is that it will give the expectation values of the state ρ, where $\mathcal{W}_\rho(x,p)$ will represent the classical phase-space density and $2\pi\mathcal{W}_\rho(x,p)$ the physical quantity averaged with respect to $\mathcal{W}_A(x,p)$.

Although the Wigner function is the most predominantly used quasi-probability distribution, others exist which provide alternative advantages. Namely the $\mathcal{Q}$-function [22], the $\mathcal{P}$-function, classified with the Wigner function as s-parameterised quasi-probability distributions [23, 24]. This Thesis will only require the use of the $\mathcal{P}$-function which is introduced in the next Section.

2.2.2 Glauber-Sudarshan $\mathcal{P}$-function

The Glauber-Sudarshan $\mathcal{P}$-function is an alternative representation of the phase-space distribution of a quantum system [25, 26]. Unlike the Wigner function, the $\mathcal{P}$-function is a quasi-probability distribution in which observables are expressed in normal order, i.e., creation operators to the left and annihilation operators to the right. This representation is sometimes preferred over alternative representations describing light in phase-space since typical optical observables, such as the photon number operator, are naturally expressed in normal order, $\hat{n} = \hat{a}^\dagger\hat{a}$. The density matrix of a coherent state is defined using the $\mathcal{P}$-function as,

$$\rho = \int \mathcal{P}(\alpha)|\alpha\rangle\langle\alpha|d^2\alpha, \tag{2.48}$$

where $\mathcal{P}(\alpha)$ is real since ρ is Hermitian, and since it is a probability distribution in phase-space,

$$\mathrm{Tr}(\rho) = \int \mathcal{P}(\alpha)\sum_n\langle\alpha|n\rangle\langle n|\alpha\rangle d^2\alpha = 1. \tag{2.49}$$

If a quantum state has a classical analogue e.g. a coherent state, then $\mathcal{P}(\alpha)$ is non-negative everywhere, typical of an ordinary probability distribution. However, if the quantum system has no classical analogue (it is non-classical), for example an entangled system, then $\mathcal{P}(\alpha)$ is ill-defined. It will be negative somewhere or is more singular than a Dirac delta function. The concept of non-classicality will be discussed in greater detail in Chapter 4. The explicit form of the $\mathcal{P}$-function reads as,

$$\begin{aligned}\mathcal{P}(\alpha) &= \mathcal{W}(\alpha)e^{-\frac{1}{2}|\alpha|^2} \\ &= \frac{e^{-\frac{1}{2}|\alpha|^2}}{\pi}\int \langle -u|\rho|u\rangle \hat{D}(\alpha)\, d^2u \\ &= \frac{e^{\frac{1}{2}|\alpha|^2}}{\pi}\int \langle -u|\rho|u\rangle e^{-u\alpha^*+u^*\alpha}\, d^2u, \quad \text{where} \quad \hat{D}(\alpha) = e^{|\alpha|^2-u\alpha^*+u^*\alpha},\end{aligned} \tag{2.50}$$

where $|u\rangle$ and $|-u\rangle$ are coherent states and $\alpha = a+ib$, achieved by taking the reverse Fourier transform of $\langle -u|\rho|u\rangle$.

Now that an effective representation of quantum states has been presented, let us now converge to a particular and unique set of quantum states classified as *Gaussian*. It is this set of states that this Thesis will focus on, for reasons which will become apparent in the next Section.

2.3 Gaussian States

In quantum information theory there is focus on a specific set of quantum states known as Gaussian states, described by a Gaussian Wigner function. These states are considered for various reasons, the more relevant of which is that Gaussian states and Gaussian maps (maps that transform one Gaussian state to another) can be described by a simple mathematical formalism, known as the *symplectic formalism*. Examples of these are squeezing, displacements, rotations and beamsplitter transformations. Another valid advantage is when considering an experimental setting, Gaussian states are much more readily available in that vacuum and coherent state are Gaussian, and Gaussian maps are easily experimentally achievable. Vast literature exists on Gaussian states, some great sources are provided in Ref. [27–30].

There exists a unique phase-space representation for an N-mode Gaussian state described by a Gaussian Wigner function of the form[2],

$$\mathcal{W}(x_1, p_1, \ldots, x_N, p_N) = \frac{\exp\left[-\left(\mathbf{R}^\top - \mathbf{d}^\top\right)\gamma^{-1}\left(\mathbf{R}-\mathbf{d}\right)\right]}{\pi^N\sqrt{\det\gamma}} \tag{2.51}$$

where $\mathbf{R} = (x_1, p_1, \ldots, x_N, p_N)^\top$ and $\mathbf{d} = (\langle x_1\rangle, \langle p_1\rangle, \ldots, \langle x_N\rangle, \langle p_N\rangle)^\top$ is a vector of the first moments i.e. displacements. The matrix γ is the covariance matrix describing the Gaussian

[2]Note that the commutation relation used here is $[\hat{x}_j, \hat{p}_k] = i\delta_{jk}$, other definitions are used with use of the commutation relation $[\hat{x}_j, \hat{p}_k] = 2i\delta_{jk}$

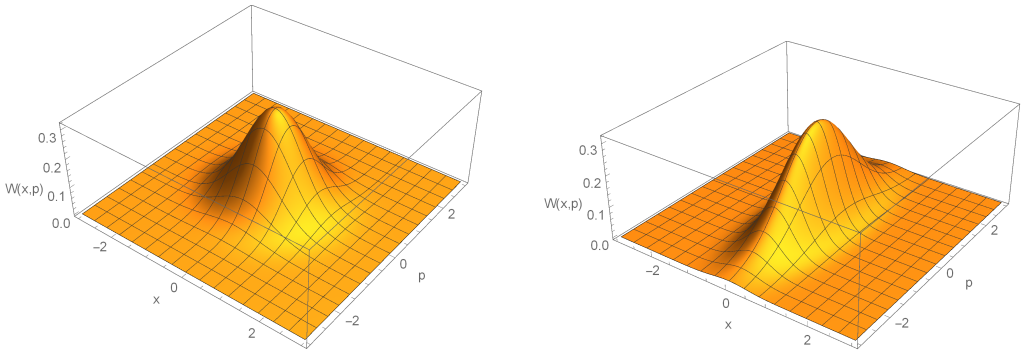

Figure 2.1: Wigner function representations of a vacuum state (left) and squeezed vacuum state in phase-space (right).

state and is defined for $[\hat{x}_i, \hat{p}_j] = i\delta_{i,j}$ as

$$\gamma_{lm} = \left\langle \hat{R}_l \hat{R}_m + \hat{R}_m \hat{R}_l \right\rangle - 2\langle \hat{R}_l \rangle \langle \hat{R}_m \rangle. \tag{2.52}$$

One example of a Gaussian Wigner function representation is that of a squeezed state given by the simple equation

$$\mathcal{W}(x,p) = \frac{1}{\pi} \exp[-x^2 e^{2r} - p^2 e^{-2r}], \tag{2.53}$$

noting that in the case of a vacuum state the squeezing parameter r will be zero, both state representations are illustrated in Fig.'s 2.1.

This gives an indication of the simplicity of the Gaussian formalism since states can be fully characterised by their first and second moments. Remarkably, an implication of the Marcinkiewicz Theorem [31–33] is that to fully describe a continuous variable state, one must either only consider the first two moments (as in the case for Gaussian states) or one must consider all of them.

2.3.1 Gaussian Maps

A quantum channel is defined as a quantum operation which is trace preserving [34]. In the most simple instance these operations are reversible and are described by unitary transformations U such that $U^\dagger U = \mathbb{1}$. A Gaussian unitary channel will thus transform one Gaussian state to another, i.e., it is a Gaussian map.

In the context of phase-space, all Gaussian maps can be represented by a symplectic operation as opposed to a unitary operation in terms of a Hamiltonian. Fig. 2.2 illustrates three transformations of Gaussian states as contours in phase-space, namely a displacement, squeezing and a rotation. In order for a symplectic operation to represent a physical operation it must satisfy the condition

$$S\Omega S^\top = \Omega \qquad \Rightarrow \qquad \det S = 1, \tag{2.54}$$

where a state represented by a covariance matrix γ can then be transformed as $S\gamma S^\top = \gamma'$

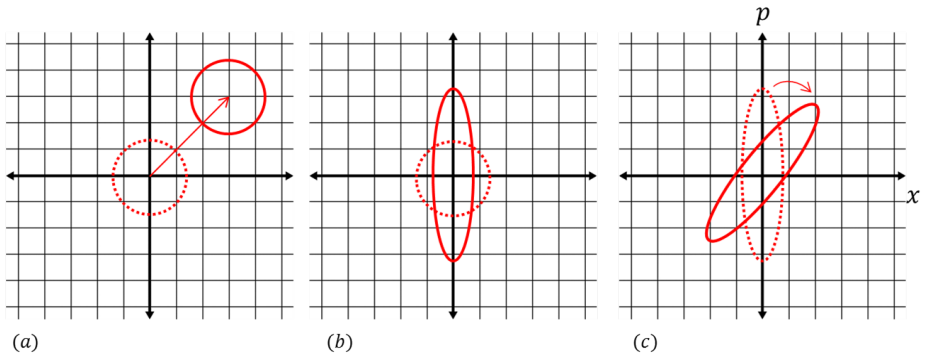

Figure 2.2: Contours of Gaussian state in phase-space following a Gaussian transformation: (a) displacement of vacuum state gives a coherent state, (b) squeezed vacuum state, (c) rotation of squeezed vacuum state. Dotted circle/ellipse indicates original state and solid shape the post-transformation state.

and Ω is the symplectic matrix given by

$$\Omega = \bigoplus_{j=1}^{N} \omega, \qquad \omega = \begin{pmatrix} 0 & 1 \\ -1 & 0 \end{pmatrix}. \tag{2.55}$$

As mentioned previously, some of the most fundamental transformations are Gaussian maps and thus can be represented by a symplectic operation. A rotation in phase-space can be written as

$$S_r(\theta) = \begin{pmatrix} \cos\theta & \sin\theta \\ -\sin\theta & \cos\theta \end{pmatrix}, \tag{2.56}$$

for some phase shift angle θ. The symplectic squeezing operation can be written as

$$S_{sq}(r) = \begin{pmatrix} e^{r} & 0 \\ 0 & e^{-r} \end{pmatrix}. \tag{2.57}$$

where r is the squeezing parameter equivalent to that defined in Eq.'s (2.35).

A slightly more sophisticated operation, which will be utilised throughout this Thesis, is a beamsplitter transformation. This will involve a symplectic transformation on two Gaussian modes. A beamsplitter is an optical device allowing the interaction of two input modes, resulting in two output modes consisting of a combination of the input modes (Fig. 2.3). In general, the beamsplitter can have a variable transmittivity to reflectivity ratio, allowing control of the output modes. However a balanced ratio is generally considered as the most common case. In the Heisenberg picture the beamsplitter will transform the annihilation operators, $\hat{a}, \hat{b}$, via a linear non-unitary Bogoliubov transformation as

$$\begin{pmatrix} \hat{a}' \\ \hat{b}' \end{pmatrix} = \begin{pmatrix} T & R \\ R & -T \end{pmatrix} \begin{pmatrix} \hat{a} \\ \hat{b} \end{pmatrix}, \qquad T^2 + R^2 = 1, \tag{2.58}$$

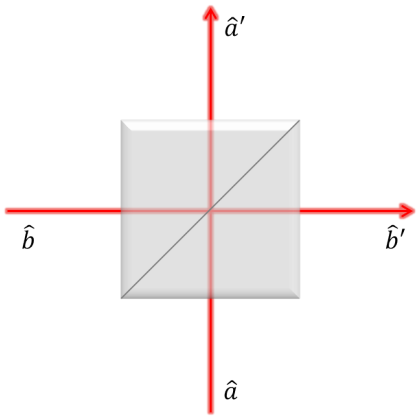

Figure 2.3: Schematic diagram of a beamsplitter with input modes $\hat{a}$, $\hat{b}$ and output modes $\hat{a}'$, $\hat{b}'$. Physically is a cube made from two triangular glass prisms glued together at their base. The thickness of the resin layer is adjusted such that half of the light incident through one port is reflected and the other half is transmitted due to frustrated total internal reflection.

where T and R are the transmittivity and reflectivity of the beamsplitter respectively. The symplectic form of the beamsplitter interacting a two-mode system is written in the most general form as

$$S_{BS}(T,R) = \begin{pmatrix} T & 0 & R & 0 \\ 0 & T & 0 & R \\ R & 0 & -T & 0 \\ 0 & R & 0 & -T \end{pmatrix}, \tag{2.59}$$

where for the most common case of a balanced beamsplitter $T = R = \frac{1}{\sqrt{2}}$. A fundamental state which will be discussed is the *two mode squeezed vacuum* (TMSV) state constructed by the combination, via a balanced beamsplitter interaction, of two orthogonally squeezed vacuum modes, i.e.,

$$\gamma_{TMSV} = S_{BS}\left(1/\sqrt{2}, 1/\sqrt{2}\right)\left(S_{sq}(r)\,\gamma_{vac}\,S_{sq}^{\top}(r) \oplus S_{sq}(-r)\,\gamma_{vac}\,S_{sq}^{\top}(-r)\right) S_{BS}^{\top}\left(1/\sqrt{2}, 1/\sqrt{2}\right). \tag{2.60}$$

Interestingly, from the aforementioned transformations it is possible to simulate the Einstein-Podolsky-Rosen state as a TMSV in which the positions and momenta of the two modes are maximally entangled[3] in the limit of infinite squeezing, $r \to \infty$.

Homodyne and Heterodyne Detection Homodyne and heterodyne are detection processes for arbitrary squeezed light not restricted to the Gaussian scenario. The concept is to mix the signal field, containing the squeezing, with a strong coherent field known as the *local oscillator*. Fig. 2.4 illustrates a schematic of *balanced homodyne detection*. As standard with a balanced beamsplitter, the input states ($\hat{a}$, $\hat{b}$) and output states ($\hat{c}$, $\hat{d}$) following a

[3]The concept of entanglement will be introduced extensively in Chapter 3.

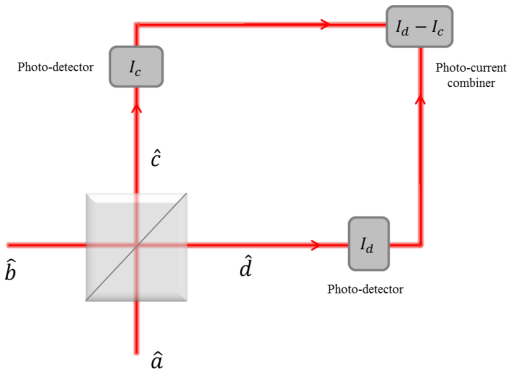

Figure 2.4: Schematic of a balanced homodyne detection with signal $\hat{a}$ and local oscillator $\hat{b}$. Photo-detectors will measure the photo-currents of the output modes and their difference is measured by the photo-current combiner.

beamsplitter interaction are related as

$$\begin{aligned} \hat{a} &= \frac{1}{\sqrt{2}}(\hat{c} - i\hat{d}), \\ \hat{b} &= \frac{1}{\sqrt{2}}(\hat{d} - i\hat{c}). \end{aligned} \tag{2.61}$$

Photo-detectors are placed in the output modes and the difference in their intensities is measured, or more specifically, the expectation values of photon operators are compared, i.e.,

$$\langle \hat{n}_{cd} \rangle = \langle \hat{c}^\dagger \hat{c} - \hat{d}^\dagger \hat{d} \rangle = i \langle \hat{a}^\dagger \hat{a} - \hat{b}^\dagger \hat{b} \rangle, \tag{2.62}$$

by use of Eq.'s (2.61). Now, since mode b is in a coherent state of the form $|\beta e^{-i\omega t}\rangle$, with $\beta = |\beta| e^{-i\psi}$ and $\psi = \theta - \pi/2$, the differences in intensities can be written of the form,

$$\langle \hat{n}_{cd} \rangle = 2|\beta| \left\langle \frac{1}{2} \left\{ \hat{a}_0 e^{-i\theta} + \hat{a}_0^\dagger e^{i\theta} \right\} \right\rangle, \tag{2.63}$$

where $\hat{a} = \hat{a}_0 e^{-i\omega t}$. From this, by changing the phase ψ of the local oscillator $\hat{b}$ and hence the angle θ, it is possible to measure a chosen quadrature of the signal field. This angle is generally chosen to yield the maximum level of quadrature squeezing. Heterodyne detection is a similar method of detecting radiation by non-linear mixing with the fundamental difference that the local oscillator will be shifted in frequency, whereas in homodyne detection, the signal field and local oscillator have identical frequencies.

2.3.2 Symplectic Analysis of Gaussian States

The symplectic formalism was first proposed by Williamson in 1935 [35], stating that a $2N \times 2N$ real symmetric covariance matrix γ representing a feasible physical state will

satisfy Heisenberg's uncertainty relation as

$$\gamma + i\Omega \geq 0, \tag{2.64}$$

as well as postulating that any $2N \times 2N$ positive definite real matrix can be diagonalised and transformed into the so-called symplectic form

$$\gamma_\nu = S\gamma S^\top = \bigoplus_{j=1}^{N} \begin{pmatrix} \nu_j & 0 \\ 0 & \nu_j \end{pmatrix}, \tag{2.65}$$

where ν_j are the *symplectic eigenvalues* defined as the eigenvalues of $|i\Omega\gamma|$. Due to this, the determinant of γ is clearly given by $\prod_j \nu_j^2$. The density matrix representation of a state is connected to symplectic eigenvalues, and by association to the covariance matrix as

$$\rho_{\nu_j} = \bigotimes_{j=1}^{N} \frac{2}{\nu_j + 1} \sum_{n=0}^{\infty} \left(\frac{\nu_j - 1}{\nu_j + 1} \right)^n |n\rangle_j \, {}_j\langle n|. \tag{2.66}$$

Heisenberg's uncertainty principle can be recast according the symplectic eigenvalues implying that for a physical state, $\nu_j \geq 1$ for all j. A particularly important symplectic invariant is the *seralian* [36], defined in terms of the symplectic eigenvalues,

$$\Delta(\gamma) = \sum_{j=1}^{N} \nu_j^2. \tag{2.67}$$

An even more simplistic definition for the symplectic eigenvalues and seralian is available when considering bipartite Gaussian states. But first, later in this Thesis the method of purification of a system will become imperative. Holevo and Werner in [37] outlined a procedure for this based on the fact that thermal states are purified by EPR states and derived that for a N-mode Gaussian state ρ_A, there exist a purifying reference system R such that ρ_{AR} is a pure Gaussian state. The covariance matrix of this pure system is given by some symplectic transformation S such that

$$\gamma_{AR} = \begin{pmatrix} \gamma_A & SC \\ S^\top C^\top & \gamma_\nu \end{pmatrix} \quad \text{where} \quad C := \bigoplus_{j=1}^{N} \sqrt{\nu_j - 1}\sigma_z \tag{2.68}$$

where σ_z is the third Pauli matrix and $\rho_A = \mathrm{Tr}_R[\rho_{AR}]$.

Bipartite Gaussian States

Consider a group of systems split across two locations A and B, having N modes and M modes respectively. The covariance matrix of the entire system can be put into the general form

$$\gamma = \begin{pmatrix} \gamma_A & \gamma_C \\ \gamma_C^\top & \gamma_B \end{pmatrix}, \tag{2.69}$$

where γ_A is a $2N \times 2N$ matrix, γ_B a $2M \times 2M$ matrix and γ_C contains the correlations between modes at locations A and B.

Throughout the course of this Thesis a focus will be put on the instance where only a single mode will be present at location A and B. In this simple case there exists a local symplectic transformation that will transform any covariance matrix into *standard form* defined as

$$\gamma_{sf} = \begin{pmatrix} a & 0 & c_+ & 0 \\ 0 & a & 0 & c_- \\ c_+ & 0 & b & 0 \\ 0 & c_- & 0 & b \end{pmatrix}. \tag{2.70}$$

with the correlation elements satisfying $c_+ = -c_- := c \geq 0$.

The local invariants of the standard form matrix can be expressed in terms of these matrix elements as

$$\det(\gamma_{sf}) = (ab - c_+^2)(ab - c_-^2), \qquad \Delta(\gamma_{sf}) = a^2 + b^2 + 2c_+c_-, \tag{2.71}$$

and the symplectic eigenvalues are given by

$$\nu_\pm = \sqrt{\frac{\Delta \pm \sqrt{\Delta^2 - 4\det(\gamma_{sf})}}{2}} \tag{2.72}$$

The particular significance of these invariants in relation to quantum correlations will become apparent in Chapter 3. Furthermore, purity — or rather the degree of mixedness of the state — can be tested for bipartite systems from its covariance matrix such that if

$$\mu = \frac{1}{\sqrt{\det(\gamma)}} = 1, \tag{2.73}$$

the state is pure and for $0 \leq \mu < 1$ the state is mixed. For systems containing three subsystems the purification of the system is valid if,

$$\Delta_{ij} = \det_{ij} + 1, \tag{2.74}$$

or using entropies

$$\mathcal{S}(\rho_{ij}) = \mathcal{S}(\rho_k), \tag{2.75}$$

hold for all permutations of the subsystems.

It is now necessary to link this quantum mechanical representation of physical states to a fundamental concept and tool within quantum information processing, that of entropy.

2.4 Entropy and Quantum Information

The concept of entropy was first introduced in a thermodynamical context as a measure of the disorder of a quantum system, or simply speaking, a measure of how many ways a thermodynamical system can be arranged [38]. The entropy of a pure state can only ever

increase upon measurement. Mixed states on the other hand have an entropy that can decrease upon measurement. As a result of the disorder of a quantum state, its ability to form correlations increases, therefore the entropy of a system, in an information theoretical context, can be interpreted as the capacity of a system to form correlations. This will be discussed in more detail in Section 4.4.

In dealing with a bipartite quantum system, consisting of systems A and B the total information contained therein can be quantified by the *quantum mutual information*, defined as

$$\mathcal{I}_q(\rho_{AB}) = \mathcal{S}(\rho_A) + \mathcal{S}(\rho_B) - \mathcal{S}(\rho_{AB}), \tag{2.76}$$

where $\mathcal{S}(\rho_A)$ denotes the marginal entropy of subsystem A and $\mathcal{S}(\rho_{AB})$, the joint entropy of states. Specific measures of entropy, both classical and quantum, will be defined in Section 2.4.1. The quantum mutual information thus captures all of the information of states ρ_A and ρ_B composing the larger composite state ρ_{AB}.

The classical correlation in a quantum system is defined as the difference in marginal entropy of one subsystem after a measurement is performed on the remainder of the system, and is operationally related to the amount of perfect classical correlations which can be extracted from the system [39], i.e.,

$$\mathcal{J}(\rho_{AB}) = \mathcal{S}(\rho_A) - \inf_{\{\hat{\Pi}_j\}} \mathcal{H}_{\{\hat{\Pi}_j\}}(\rho_A|\rho_B), \tag{2.77}$$

where $\inf_{\{\hat{\Pi}_j\}} \mathcal{H}_{\{\hat{\Pi}_j\}}(\alpha|\beta)$ corresponds to the quantum conditional entropy, the entropy of the first subsystem subject to a measurement on the second, optimised over all possible measurements. The specific set of measurements that will be considered in the Thesis will be discussed later in Section 4.1.1. A direct result of this is that, in a purely classical system,

$$\begin{aligned} &\mathcal{I}(\rho_{AB}) = \mathcal{J}(\rho_{AB}) \\ \Rightarrow\ &\mathcal{S}(\rho_{AB}) = \inf_{\{\hat{\Pi}_j\}} \mathcal{H}_{\{\hat{\Pi}_j\}}(\rho_A|\rho_B) + \mathcal{S}(\rho_B), \end{aligned} \tag{2.78}$$

thus the joint entropy of the system is the sum of the conditional entropy of subsystem A and the marginal entropy of subsystem B, such that if A is undisturbed by a measurement on B then the joint entropy $\mathcal{S}(\rho_{AB})$ will be zero.

2.4.1 Entropic Measures

So far entropy has been referred to as a general concept and quantity. This Section aims to provide an outline of two significant entropic measures namely the famous von Neumann entropy [40, 41] and the lesser known Rényi-2 entropy, both introduced as special cases of the Rényi-α entropy.

Rényi-α entropies were first introduced by Alfréd Rényi as a generalisation of the usual concept of entropy [42]. These entropies not only encompass the Hartley (or max) entropy, min-entropy and collision entropy, but also the Shannon entropy [43] and consequently, the von Neumann entropy. More recently preliminary work has been done to link the Rényi-α entropy to free energy in [44]. The Rényi-α entropy for classical probability distributions is

defined as

$$\mathcal{H}_\alpha(P) = \frac{1}{1-\alpha}\log_2\left(\sum_{k=1}^{N} p_k^\alpha\right), \qquad \alpha > 0 \text{ and } \alpha \neq 1, \tag{2.79}$$

where P is a distribution $P = (p_1, p_2, \ldots, p_N)$. By implementation of L'Hôpital's Rule [4] in the limit of $\alpha \to 1$, Eq. (2.79) reduces to the Shannon entropy as

$$\mathcal{H}_1(P) = \lim_{\alpha\to 1}\mathcal{H}_\alpha(P) = \sum_{k=1}^{N} p_k \log_2 \frac{1}{p_k}. \tag{2.80}$$

The quantum analogue to the Rényi-α entropy is given by

$$\mathcal{S}_\alpha(\rho) = \frac{1}{1-\alpha}\ln \mathrm{Tr}(\rho^\alpha) \tag{2.81}$$

where ρ is the density matrix describing a quantum state. Considering again the case when $\alpha \to 1$, Eq. (2.81) will reduce to the von Neumann entropy introduced as quantifying the departure of the system from a pure state and defined as

$$\mathcal{S}_1(\rho) = -\mathrm{Tr}[\rho \ln \rho]. \tag{2.82}$$

Consequently, for an N-mode Gaussian state the von Neumann entropy is calculated as

$$\mathcal{S}(\rho) = \sum_{j=1}^{N} f(\nu_j), \tag{2.83}$$

where ν_j are the symplectic eigenvalues and

$$f(x) = \left(\frac{x+1}{2}\right)\ln\left(\frac{x+1}{2}\right) - \left(\frac{x-1}{2}\right)\ln\left(\frac{x-1}{2}\right). \tag{2.84}$$

is a monotonically increasing function of x. The von Neumann entropy has the properties of both subadditivity, given by

$$|\mathcal{S}(\rho_A) - \mathcal{S}(\rho_B)| \leq \mathcal{S}(\rho_{AB}) \leq \mathcal{S}(\rho_A) + \mathcal{S}(\rho_B), \tag{2.85}$$

and strong subadditivity, given by

$$\mathcal{S}(\rho_{ABC}) + \mathcal{S}(\rho_B) \leq \mathcal{S}(\rho_{AB}) + \mathcal{S}(\rho_{BC}) \quad \Leftrightarrow \quad \mathcal{S}(\rho_A) + \mathcal{S}(\rho_C) \leq \mathcal{S}(\rho_{AB}) + \mathcal{S}(\rho_{BC}). \tag{2.86}$$

In recent publications, focus has increasingly been placed on the significance of the case when $\alpha = 2$. It is suggested that this so-called *Rényi-2 entropy* is a much more natural entropic measure of a quantum state, particularly within the Gaussian setting. Considering the instance when $\alpha = 2$, the entropy is of the form $\mathcal{S}_2(\rho) = -\ln \mathrm{Tr}[\rho^2]$. At first glance it is

[4] L'Hôpital's rule states that for two differentiable functions f and g on an open interval I: $\lim_{x\to\infty}\frac{f(x)}{g(x)} = \lim_{x\to\infty}\frac{f'(x)}{g'(x)}$.

clear that this entropy is fundamentally linked to the purity of the state ρ, since a state is pure if $\mathrm{Tr}[\rho^2] = 1$ and mixed otherwise.

The Gaussian Rényi-2 entropy of a state ρ represented by a covariance matrix γ reads as

$$\mathcal{S}_2(\rho) = \frac{1}{2}\ln(\det\gamma), \tag{2.87}$$

which again shows an inherent link to the purity of the state since a state is pure if its covariance matrix satisfies Eq. (2.73).

The question of whether the von Neumann entropy is the most natural of entropies arises from the fundamental conjecture that the minimum output entropy conjecture for bosonic channels, proven for all Rényi-α entropies for $\alpha \geq 2$ [29, 45–47]. Most recently it has also been proven for the case of $\alpha \to 1$ i.e., the von Neumann entropy, by Giovannetti *et al.* [48]. It has been shown in [49] that the Rényi-2 entropy arises naturally from phase-space sampling for Gaussian states as

$$\begin{aligned} H(\mathcal{W}_\rho) &= -\int_{\mathbb{R}^{2N}} \mathcal{W}_\rho(\zeta)\ln\left[\mathcal{W}_\rho(\zeta)\right] d^{2N}\zeta \\ &= \int_{\mathbb{R}^{2N}} \frac{1}{\pi^N\sqrt{\det\gamma}}\exp\left(-\zeta^\top\gamma^{-1}\zeta\right)\left[\zeta^\top\gamma^{-1}\zeta + N\ln\pi + \frac{1}{2}\ln(\det\gamma)\right] d^{2N}\zeta \\ &= \sum_{j=1}^{2N}\frac{\nu_j}{2\nu_j} + N\ln\pi + \mathcal{S}_2(\rho) \\ &= N(1+\ln\pi) + \mathcal{S}_2(\rho) \end{aligned} \tag{2.88}$$

where an integration has been performed in phase-space coordinates ζ such that γ is diagonalised, ν_j are the eigenvalues of the matrix and $N = n_A + n_B$ is the total number of modes of the composite system. This can be extended to represent Shannon relative entropy as

$$\begin{aligned} \mathcal{H}(\mathcal{W}_{\rho_1} \parallel \mathcal{W}_{\rho_2}) &= \int_{\mathbb{R}^{2N}} \mathcal{W}_{\rho_1}(\zeta)\ln\left(\frac{\mathcal{W}_{\rho_1}(\zeta)}{\mathcal{W}_{\rho_2}(\zeta)}\right) d^{2N}\zeta \\ &= -\mathcal{H}(\mathcal{W}_{\rho_1}) + \int_{\mathbb{R}^{2N}} \frac{1}{\pi^N\sqrt{\det\gamma_1}}\exp\left(-\zeta^\top\gamma_1^{-1}\zeta\right)\left[\zeta^\top\gamma_2^{-1}\zeta + N\ln\pi + \frac{1}{2}\ln(\det\gamma_2)\right] d^{2N}\zeta \\ &= \frac{1}{2}\ln\left(\frac{\det\gamma_2}{\det\gamma_1}\right) - N + \sum_{j=1}^{2N}\frac{\gamma_{1,jj}}{2\gamma_{2,j}} \\ &= \frac{1}{2}\left[\ln\left(\frac{\det\gamma_2}{\det\gamma_1}\right) + \mathrm{Tr}\left(\gamma_1\gamma_2^{-1}\right)\right] - N \end{aligned} \tag{2.89}$$

where $\gamma_{n,j}$ denote the eigenvalues of γ, and $\gamma_{n,ij}$ are its individual matrix elements. The validity of the final step is due to the invariance of the quantity $\mathrm{Tr}\left[\gamma_1\gamma_2^{-1}\right]$ under a change of basis.

From this 'Rényi relative entropy' a Gaussian formalism for the quantum mutual information was constructed [50]. Consider a composite system divided into two subsystems ρ_A

and ρ_B. The quantum mutual information between these two subsystems can be written as

$$\begin{aligned}\mathcal{H}(\mathcal{W}_{\rho_{AB}} \parallel \mathcal{W}_{\rho_A\otimes\rho_B}) &= \mathcal{H}(\mathcal{W}_{\rho_A}) + \mathcal{H}(\mathcal{W}_{\rho_B}) - \mathcal{H}(\mathcal{W}_{\rho_{AB}}) \\ &= \frac{1}{2}\ln\left(\frac{\det\gamma_A \det\gamma_B}{\det\gamma_{AB}}\right) \\ &= \mathcal{S}_2(\rho_A) + \mathcal{S}_2(\rho_B) - \mathcal{S}_2(\rho_{AB}) \\ &= \mathcal{I}_2(\rho_{A:B}),\end{aligned} \tag{2.90}$$

since $\mathrm{Tr}\left[\gamma_1\gamma_2^{-1}\right] = 2N$. It is clear that this is analogous to the von Neumann definition of mutual information Eq. (2.76). This Gaussian Rényi-2 mutual information is positive semi-definite as it coincides with the Shannon mutual information of the Wigner function of ρ_{AB} and has the operational interpretation of the total quadrature correlations of the composite state ρ_{AB} since Eq. (2.90) describes the required extra amount of discrete information to be transmitted over a continuous variable channel which will allow the construction of the complete joint Wigner function of ρ_{AB} as opposed to the two marginal Wigner functions.

In Ref. [50] the development of the Gaussian Rényi-2 formalism was extended further to include a quantum conditional entropy optimised over all single mode Gaussian measurements. Any measurement considered is described by positive operator valued measure (POVM)[5] of the general form on n_B modes

$$\Pi_B(\eta) = \pi^{-n_B}\left[\prod_{j=1}^{n_B}\hat{W}_{B_j}(\eta_j)\right]\rho_B^{\Pi}\left[\prod_{j=1}^{n_B}\hat{W}_{B_j}^{\dagger}(\eta_j)\right] \tag{2.91}$$

where $\hat{W}$ is the Weyl displacement operator

$$\begin{aligned}&\hat{W}_B(\eta_j) = \exp\left(\eta_j\hat{b}_j^{\dagger} - \eta_j^*\hat{b}_j\right), \\ &\hat{b}_j = \frac{1}{\sqrt{2}}\left(\hat{q}_{B_j} + i\hat{p}_{B_j}\right), \\ &\pi^{-n_B}\int\prod_B(\eta)d^{2n_B}\eta = \mathbb{1}\end{aligned} \tag{2.92}$$

and ρ_B^{Π} is the density matrix of a n_B-mode mixed Gaussian state with covariance matrix $\mathbf{\Gamma_B^{\Pi}}$. The covariance matrix of the conditional state of A when a measurement is performed on subsystem B is given by the Schur complement

$$\tilde{\gamma}_A^{\Pi} = \gamma_A - \gamma_C(\gamma_B + \mathbf{\Gamma}_B^{\Pi})^{-1}\gamma_C^{\top}. \tag{2.93}$$

[5] A positive operator valued measure (POVM) is a measure with elements which are non-negative self-adjoint operators on a Hilbert space.

From this the Gaussian Rényi-2 classical correlations can be written in the form

$$\begin{aligned}\mathcal{J}_2\left(\rho_{A|B}\right) &= \mathcal{S}_2(\rho_A) - \mathcal{S}_2(\rho_{A|\eta}), \\ &= \sup_{\mathbf{\Gamma}_B^{\Pi}} \frac{1}{2} \ln\left(\frac{\det \gamma_A}{\det \tilde{\gamma}_A^{\Pi}}\right).\end{aligned} \tag{2.94}$$

In general Rényi-α entropies for $\alpha \neq 1$ are not subadditive, thus implying that quantities such as the quantum mutual information, in Eq. (2.90), can become negative, and so is then a meaningless correlation measure. However, Rényi-2 entropy satisfies a strong subadditivity inequality for all Gaussian states ρ_{ABC},

$$\begin{aligned}\mathcal{S}_2(\rho_{AB}) + \mathcal{S}_2(\rho_{BC}) &\leq \mathcal{S}_2(\rho_{ABC}) + \mathcal{S}_2(\rho_B), \\ \Rightarrow \frac{1}{2} \ln\left(\frac{\det \gamma_{AB} \det \gamma_{BC}}{\det \gamma_{ABC} \det \gamma_B}\right) &\geq 0.\end{aligned} \tag{2.95}$$

The consequence of this is that the core of quantum information theory can be consistently recast within the Gaussian scenario, using the simpler and physically natural Rényi-2 entropy as opposed the von Neumann entropy.

This Chapter has introduced the basic mathematical framework necessary to understand the continuous variable implementation of quantum information. This included a discussion on Gaussian states, which are a key set of quantum states physically realisable and mathematically convenient due to their unique covariance matrix description. A short discussion was also held regarding some essential quantum optical transformations and an alternative entropic measures. The Chapters to come will utilise this framework to introduce some key concepts such as quantum entanglement and quantum discord of which this Thesis is concerned.

Chapter 3

Quantum Entanglement

The birth of quantum entanglement is considered to have taken place in 1935 when Einstein, Podolsky and Rosen published a paper entitled "*Can quantum-mechanical description of physical reality be considered complete?*", of which the answer was no [4]. It was considered that if in the case of two physical quantities described by non-commuting operators (position and momentum), the knowledge of one precludes the knowledge of the other, then the quantum mechanical theory of physical reality must be incomplete. At the time of the EPR paper, the quantum mechanical interpretation of physical reality was challenged by *local realism*. "Realism" implies the existence of a probability distribution dependent on how the global state is generated and thus that there must be a pre-existing outcome for any possible measurement before the measurement is made. "Locality" implies that a measurement choice and outcome of one subsystem should not impact the result of a measurement on the remaining subsystem. This interpretation was proved to be contradicted by the EPR paradox. The concept explored in this thought experiment is: given two quantum systems, if the information contained in the entire system cannot simply be described by each subsystem individually, then the additional information contained therein defines quantum entanglement. By this, it can be stated that one subsystem cannot be fully understood without considering its counterpart. Einstein found the apparent "spooky action at a distance" (or *"spukhafte Fernwirkung"*) [51] to be contradictory to reality and was fundamentally uncomfortable with the concept of its validity. The same year, in the journal Naturwissenschaften, Schrödinger coined the term *"Verschränkung"*, meaning "entanglement". Schrödinger developed his famous thought experiment of a cat, which exists simultaneously in a state of being alive and dead, to help illustrate the difference in classical and quantum mechanics, and in turn the concept of quantum superposition exhibited by an entangled state [5].

In 1952, building on earlier work by de Broglie [52], Bohm suggested a deterministic interpretation of quantum theory that incorporates "hidden variables" [53], the values of which effectively determine, from the moment of separation, the outcomes of the measurement. Implying that each particle carries all the necessary information and no information is required to be transmitted from one system to the other at the time of measurement.

It was then in 1964 that Bell proposes his famous theorem allowing researchers to later experimentally, and definitively, rule out any hidden variables operating locally to justify

quantum entanglement outcomes [54–57]. The outcome of this is that if the theorem holds, then entanglement could be explained through purely local effects. If violated, some amount of non-locality must be occurring, as standard quantum mechanics would predict. Bell's theorem was experimentally tested for the first time in 1972 in Berkeley by measuring the polarisations of a pair of photons [58]. Although the inequality is indeed found to be violated, some loopholes existed in the experiment. It was not until 1982 that the French physicist Alain Aspect performed an even stronger test of entanglement, confirming that non-local effects do exist [59–61].

Fundamental applications of quantum entanglement were then introduced from 1984 in the form of quantum cryptography, which would use photons from an entangled system to create a secure key [62]. It was also found in 1993 that entanglement can be used to teleport a particle's quantum information from one place to another [63], first experimentally verified separately by Zeilinger and De Martini groups (1997–1998) [64, 65]. The distance record of sending entangled photons across 144 kilometers, between two of the Canary Islands, was set in 2007 by Zeilinger's group [66].

The improved comprehension of quantum entanglement has been remarkable in the past two decades. The phenomenon is no longer one which exists between photons or electrons, the effects of quantum entanglement have been witnessed between vibrational states of two spatially separated, millimetre-sized diamonds at room temperature [67]. The dimensional limit to which entanglement can persist appears to be expanding with quantum properties such as wave-particle duality been found in molecules the size of Buckminsterfullerenes (or Bucky-balls)[1] [68]. Research involving practical purposes of quantum entanglement are becoming ever more popular as the world edges closer to the inevitable development of physical quantum technologies, including quantum computers [69] and quantum cryptography [70, 71].

3.1 Characterising Bipartite Entanglement

3.1.1 Bell's Inequality and Local Realism

Let us consider a hypothetical world in which local realism is the valid interpretation of the physical world and focus on a bipartite system within this world. Each system S_A and S_B will have two parameters assuming the values $s_{(n,1)}$ and $s_{(n,2)}$ respectively, which are independent of observation, where n corresponds to an individual system. In this instance Bell's CHSH inequality [55] will read as

$$|\langle s_{(A,1)}s_{(B,1)}\rangle + \langle s_{(A,1)}s_{(B,2)}\rangle + \langle s_{(A,2)}s_{(B,1)}\rangle - \langle s_{(A,2)}s_{(B,2)}\rangle| \leq 2 \tag{3.1}$$

where $\langle s_{(A,j)}s_{(B,k)}\rangle$ is the average over the case where $s_{(A,j)}$ is measured, and simultaneously, $s_{(B,k)}$ is also measured. This inequality is born from the probability distribution dependent on how the global state is generated. However in quantum mechanics, in the majority of cases if the system possesses entanglement, Bell's inequality will be violated yielding a value

[1] Bucky-balls are spherical fullerene molecules with a cage-like structure made of twenty hexagons and twelve pentagons, with a carbon atom at each vertex and a bond along each edge.

of $2\sqrt{2} > 2$, although there exist so-called Werner state for which this is not the case. The set of states which provide a saturation of this inequality, appropriately known as *Bell states*. These represent maximally entangled bipartite states, defined as,

$$|\Phi^{\pm}\rangle = \frac{1}{\sqrt{2}}(|s_{(A,1)}s_{(B,1)}\rangle \pm |s_{(A,2)}s_{(B,2)}\rangle), \tag{3.2a}$$

$$|\Psi^{\pm}\rangle = \frac{1}{\sqrt{2}}(|s_{(A,1)}s_{(B,2)}\rangle \pm |s_{(A,2)}s_{(B,1)}\rangle). \tag{3.2b}$$

3.1.2 Definition of an Entangled State

The definition of quantum entanglement was put forward as a contradiction. That is, an entangled state is one which cannot be considered as separable and thus written as a tensor product of the density matrices of its subsystems [72, 73][2],

$$\rho_{AB} = \sum_j p_j \rho_{A,j} \otimes \rho_{B,j}, \tag{3.3}$$

where $\rho_{n,j}$ is the density matrix of subsystem n and p_j is its associated probability. Hence it appears that entanglement is equivalent to non-separability.

Within the covariance matrix formalism for Gaussian states, it was shown by Werner and Wolf [74] that a bipartite state is considered separable if it can be expressed as a direct sum of the covariance matrices of the subsystems, i.e. a product state

$$\gamma_{AB} \geq \begin{pmatrix} \gamma_A & 0 \\ 0 & \gamma_B \end{pmatrix}. \tag{3.4}$$

In the case of the inequality being saturated, the covariance matrix will correspond to a state which solely possesses classical correlations and thus exhibits no quantum entanglement. This qualitative definition holds only with respect to pure states, however the more complex case of mixed sates is discussed in Chapter 4.

Local Operations and Classical Communication (LOCC)

One of the most important properties of quantum entanglement is its Local Operations and Classical Communication (LOCC) constraint. Considering two states which are perfectly entangled, the presence of entanglement would be synonymous to a perfect quantum communication channel. In actuality however, noise will inevitably play a detrimental role to this communication channel. One option to counteract these noisy channels is to use LOCC, which can be used to form classical correlations. If a bipartite quantum state is then used to successfully perform a particular task which cannot be explained by classical correlations alone, the solution must be that the ability to perform the task must be due

[2]In Ref. [72] Werner used the words "classically correlated", but the term "separable" was chosen by Peres in Ref. [73] and is more frequently used nowadays.

to some unconsidered quantum correlations present in the state. Therefore LOCC cannot create entanglement. The set of possible LOCC operations is vast, with the possible classical correlations being implemented before or after a local operation. As a result, there is no complete and simplified characterisation of LOCC operations, as a consequence, other classes of operations possessing traits pertaining to local operations must be considered.

Although separable states can be easily created from LOCC operations, on the opposite end of the spectrum there exist quantum states in finite-dimensional Hilbert spaces that are said to be maximally entangled. These states by definition yield a maximally mixed state when one subsystem is traced out. However in an infinite-dimensional Hilbert space, a maximally entangled state could only be achieved by taking, for example, a two-mode squeezed vacuum state in the limit of infinite squeezing, $r \to \infty$. For any entangled state, the constraint on entanglement is that it cannot emerge nor increase under LOCC operations, although a local unitary operation may have the effect of decreasing entanglement.

3.2 Separability Criteria

As discussed, the definition of an entangled state, and hence entanglement, is based on the concept that if a state cannot be classified as separable, it is entangled. Arising from this are a number of separability criteria which serve as a verification of the presence or absence of entanglement. It is important to note that the resolution power of different separability criteria can vary, leading to an objective definition of the 'border' between separable and entangled states, such that separable according to one criteria can appear non-separable according to another.

Before introducing the main separability criterion used within this Thesis, it is necessary to present the notion of a *positive but not completely positive map*. A positive map, as the name suggests, will act in such a way as to transform a positive matrix[3] i.e. the density matrix, to another positive matrix. The positivity of the resulting state determines its validity as a quantum state. In addition, a map Z is positive if it preserves the property of being Hermitian. Considering a bipartite system with density matrix ρ_{AB}, using Choi's theorem [75], a map Z is defined as positive if,

$$(\mathbb{1} \otimes Z)\rho_{AB} = (\mathbb{1} \otimes Z)\left(\sum_j p_j \rho_{A,j} \otimes \rho_{B,j}\right) = \sum_j p_j \rho_{A,j} \otimes Z\rho_{B,j}. \tag{3.5}$$

If the resulting density matrix is positive, the map is known as *completely positive*. However, to utilise this theorem for the purposes of identifying entanglement, those maps which are positive but not completely positive are of interest. A quantum state is then considered to be separable if and only if

$$(\mathbb{1} \otimes Z)\rho_{AB} \geq 0, \tag{3.6}$$

for positive but not completely positive maps.

[3] A positive matrix is defined as one possessing positive eigenvalues.

3.2.1 Peres-Horodecki Criterion (PPT)

One of the most recognised separability criteria for bipartite and multipartite quantum systems is the Peres-Horodecki criterion [76, 77]. Popularly known as the PPT criterion due to its use of a positive partial transpose[4], this criterion is based on a positive but not completely positive map. It was demonstrated in [77] that the PPT criterion is necessary and sufficient for quantum states ρ_{AB} defined in the Hilbert space $\mathcal{H}_{AB} = \mathcal{H}_A \otimes \mathcal{H}_B$ as in Eq. (3.3) for dimensions $d_A = 2$ or 3 and $d_B = 2$ where the PPT of one subsystem, say ρ_A, simply defined by the density matrix

$$\rho_{AB}^{\top_A} = \sum_j p_j \rho_{A,j}^{\top} \otimes \rho_{B,j}, \tag{3.7}$$

corresponds to a valid density matrix, with the superscript $\top_n$ indicating with respect to which subsystem the transpose is being performed. It was also shown that the Peres-Horodecki criterion is sufficient for separability when $d_A \cdot d_B \leq 6$.

The Peres-Horodecki criterion has been extended to continuous variable systems by Simon [78], where it is interpreted as the time reversal of one subsystem. Consider a bipartite state with a covariance matrix basis $(x_A,\ p_A,\ x_B,\ p_B)$, PPT on subsystem B will result in a change of basis as $(x_A,\ p_A,\ x_B,\ -p_B)$. Note that although performing a time reversal on an individual quantum system will lead to a valid density matrix, this is not guaranteed when performing time reversal on a subsystem of a larger global system.

In respect to the symplectic formalism for Gaussian states, PPT can be represented by a symplectic Gaussian map as

$$\lambda_{A|B} = \left(\bigoplus_{j=1}^{N} \mathbb{1}_j \right) \oplus \left(\bigoplus_{k=1}^{M} \sigma_{z,k} \right) \tag{3.8}$$

where N and M denote Hilbert dimensions of subsystems A and B respectively and σ_z is the third Pauli spin matrix. From Ref. [78] the separability criterion for a bipartite Gaussian state is fully characterised by the lower symplectic eigenvalue of the partially transposed system, $\tilde{\nu}_-$. The state ρ_{AB} is considered separable if and only if $\tilde{\nu}_- \geq 1$, thus $\tilde{\nu}_-$ fully characterises the entanglement, a fact which is considered in a later following Section introducing a range of basic entanglement measures.

3.2.2 Other Separability Criteria

This Section will serve as a brief introduction to other popular existing separability criteria, chosen due to their simplicity as well as their frequent use in literature [79].

[4]The partial transpose simply refers to the transpose of one subsystem whilst the remaining subsystems are unchanged.

Duan's Inseparability Criterion

Duan *et al.* introduced an inseparability criterion for continuous variable systems and proved that it provides a sufficient condition for entanglement in any bipartite states, and for all Gaussian states the criterion provides a necessary and sufficient condition for inseparability [80]. Consider two operators

$$\hat{u} = |m|\hat{x}_1 + \frac{1}{m}\hat{x}_2, \quad \text{and} \quad \hat{v} = |m|\hat{p}_1 - \frac{1}{m}\hat{p}_2, \tag{3.9}$$

for $\forall m > 0$ and $m \in \mathbb{R}$, the variance of these operators is then given by

$$\langle(\Delta\hat{u})^2\rangle_\rho + \langle(\Delta\hat{v})^2\rangle_\rho \geq m^2 + \frac{1}{m^2}. \tag{3.10}$$

The Gaussian counterpart relies on the state being expressed in a standard form covariance matrix similar to Eq. (2.70) but with $a_1 \neq a_2$ and $b_1 \neq b_2$. The operators then become [81, 82]

$$\hat{u} = |m_0|\hat{x}_1 - \frac{c_+}{|c_+|}\frac{1}{m_0}\hat{x}_2, \quad \text{and} \quad \hat{v} = |m_0|\hat{p}_1 - \frac{c_-}{|c_-|}\frac{1}{m_0}\hat{p}_2, \tag{3.11}$$

where $m_0 = \sqrt[4]{\dfrac{b_1 - 1}{a_1 - 1}} = \sqrt[4]{\dfrac{b_2 - 1}{a_2 - 1}}$ and so the inseparability criterion becomes,

$$m_0^2\frac{a_1 + a_2}{2} + \frac{b_1 + b_2}{2m_0^2} - |c_+| - |c_-| \geq m_0^2 + \frac{1}{m_0^2}. \tag{3.12}$$

for bipartite Gaussian states.

Range Criterion

Consider a state ρ_{AB} where the dimensions of the two subsystem yield $d_A \cdot d_B > 6$. In this case there exists states that are entangled but separable according to PPT, therefore another, separability criterion is required to detect the entanglement of these states independent of the PPT criterion. One such criterion based on positive but not completely positive maps where the chosen map is not decomposable is the range criterion [83].

The range criterion states that if the state ρ_{AB} is separable, then by definition, there exists a set of product vectors $\{\psi_A^i \otimes \phi_B^i\}$ that span the range of ρ_{AB}, while $\{\psi_A^i \otimes (\phi_B^i)^*\}$ spans the range of the partial transpose $\rho_{AB}^{\top_B}$, where the complex conjugate is taken in the same basis as the partial transposition on ρ_{AB}.

Reduction Criterion

A reduction map is defined as a linear map $\Lambda_r : \mathcal{S}_{d_A \times d_B} \to \mathcal{S}_{d_A \times d_B}$ such that $\Lambda_r[\rho_{AB}] = \mathbb{1}(\mathrm{Tr}[\rho_{AB}]) - \rho_{AB}$, with $\rho_{AB} \in \mathcal{S}_{d_A \times d_B}$ and $\mathbb{1}$ the identity operator. The reduction criterion [84, 85] then states that if a state $\rho_{AB} \in \mathcal{S}_{d_A \times d_B}$ is separable, then $(\mathbb{1} \otimes \Lambda_r)[\rho_{AB}] \geq 0$, i.e., the following two conditions hold

$$\rho_A \otimes \mathbb{1}_B - \rho_{AB} \geq 0, \qquad \mathbb{1}_A \otimes \rho_B - \rho_{AB} \geq 0,$$

where ρ_A and ρ_B are the reduced density matrices of the subsystems S_A and S_B respectively.

3.3 Entanglement Measures

Now that quantum entanglement has been defined and discussed, it is necessary to continue by introducing some quantitative measures of entanglement. Those to be introduced are considered to be the core measures relevant to this Thesis, however there exist a wide range of general and tailored entanglement measures outlined in Ref. [86].

3.3.1 Entropy of Entanglement

The most fundamental measure of quantum entanglement in a bipartite pure state is that defined by the *entropy of entanglement* [5]. This measure is simply defined as the von Neumann entropy of one of the reduced subsystems, i.e.,

$$\mathcal{E}_R(\rho_{AB}) = \mathcal{S}(\rho_A) = \mathcal{S}(\rho_B), \tag{3.13}$$

where, for instance, $\rho_A = \mathrm{Tr}_B[\rho_{AB}]$. Of course $\mathcal{E}_R(\rho)$ cannot increase under LOCC as necessary. Note that for a pure state the entropy of the global system is zero; implying that the disorder of the reduced systems will be greater than that of the global system. The entropy of entanglement is typically rarely used as a measure in itself, but rather is implemented in more sophisticated measures seen in Section 3.3.3.

3.3.2 Distillable Entanglement and Entanglement Cost

The concept of *distillable entanglement* is based on the transformation of N copies of a combined state ρ_{AB} by LOCC, to a minimum of M copies of a maximally entangled state. The best possible conversion rate over all possible LOCC schemes is defined as the distillable entanglement [86–88]

$$\mathcal{E}_D(\rho_{AB}) = \max_{\{LOCC\}} \lim_{N\to\infty} \frac{M_{out}}{N_{in}}. \tag{3.14}$$

In being sent by a noisy channel, $\mathcal{E}_D(\rho_{AB})$ will indicate the rate at which a noisy mixed state can be converted into maximally entangled states e.g., Bell pairs. In the continuous variable setting, although the concept of distillable entanglement can be understood, it is impossible to compute, even for the special case of Gaussian states.

The converse to distillable entanglement would be the number of maximally entangled states necessary to create a state ρ_{AB} using LOCC, this is a process knowing as 'dilution' and defines the *entanglement cost* as [89],

$$\mathcal{E}_C(\rho_{AB}) = \min_{\{LOCC\}} \lim_{N\to\infty} \frac{M_{in}}{N_{out}}. \tag{3.15}$$

Although the entanglement cost and distillable entanglement are in general considered to be converses of one another, performing dilution then distillation (or vice versa) would not be classified as a unitary operation since the initial and output state would differ,

essentially it can be stated that the entanglement cost acts as an upper bound to the distillable entanglement for a bipartite state ρ_{AB}.

3.3.3 Entanglement of Formation

The entanglement of formation represents the minimum achievable entanglement over all possible pure state decompositions of a bipartite state ρ_{AB},

$$\mathcal{E}_F(\rho_{AB}) = \inf \left\{ \sum_j p_j \mathcal{E}_R(|\psi_j\rangle\langle\psi_j|) : \quad \rho_{AB} = \sum_j p_j |\psi_j\rangle\langle\psi_j| \right\}, \tag{3.16}$$

where the entanglement in the pure states is measured using the entropy of entanglement Eq. (3.13).

Recently, progress has been made in the extension of the entanglement of formation to a Gaussian setting. The first established definition was for mixed symmetric bipartite states, remarkably solved and found to yield a simple analytical form for Gaussian states, reading as,

$$\mathcal{E}_F(\rho_{AB}) = \max\{0, h(\tilde{\nu}_{-opt})\}, \tag{3.17}$$

with

$$h(x) = \frac{(1+x)^2}{4x} \log\left[\frac{(1+x)^2}{4x}\right] - \frac{(1-x)^2}{4x} \log\left[\frac{(1-x)^2}{4x}\right], \tag{3.18}$$

so that the entanglement of formation is a monotonically decreasing function of the minimum symplectic eigenvalue of the partially transposed covariance matrix $\tilde{\gamma}$. Marian & Marian [90] expanded this by defining the Gaussian entanglement of formation (GEoF) for a number of arbitrary bipartite Gaussian states, defined by specific relations between standard form parameters [5]. These derivations follow the Gaussian interpretation suggested in [91].

Most recently, Adesso *et al.* [92, 93] presented a Gaussian entanglement of formation formalism for a generally mixed bipartite Gaussian state, defined using the von Neumann entropy, as

$$\mathcal{E}_F^{vN}(\rho) = h(\tilde{\nu}_{-opt}) \tag{3.19}$$

with $\tilde{\nu}_{-opt}$ being the symplectic eigenvalue of the partial transpose of the corresponding optimal pure state defined as

$$\tilde{\nu}_{-opt} = \sqrt{m_{opt}} - \sqrt{m_{opt} - 1}, \tag{3.20}$$

[5] 1. symmetric two mode Gaussian states (TMGS) whose standard form parameters are $b1 = b2 =: b$, $c = |d| = -d > 0$; 2. two mode squeezed thermal states (TMSTS) whose standard form parameters are $b1 \geq b2$, $c = |d| = -d > 0$; 3. TMGS at the separability boundary such that $\tilde{\nu}_- = \frac{1}{2}$; 4. TMGSs whose smallest symplectic eigenvalue $\nu_- = \frac{1}{2}$.

where

$$m_\theta(\gamma_{sf}) = \left(c_+\left(ab-c_-^2\right)-c_-+\cos(\theta)\sqrt{\left(b-a\left(ab-c_-^2\right)\right)\left(a-b\left(ab-c_-^2\right)\right)}\right)^2 \times\left[2\left(ab-c_-^2\right)\left(\left(a^2+b^2+2c_-c_+\right)+\left(a^2-b^2\right)\sin(\theta)\sqrt{1-\frac{\left(c_+\left(ab-c_-^2\right)+c_-\right)^2}{\left(b-a\left(ab-c_-^2\right)\right)\left(a-b\left(ab-c_-^2\right)\right)}}\right.\right. \left.\left.-\frac{\cos(\theta)\left(c_-^2c_+\left(a^2+b^2\right)+c_-\left(a^2\left(1-2b^2\right)+b^2\right)-abc_+\left(a^2+b^2-2\right)+2abc_-^3\right)}{\sqrt{\left(b-a\left(ab-c_-^2\right)\right)\left(a-b\left(ab-c_-^2\right)\right)}}\right)\right]^{-1}+1 \tag{3.21}$$

and $m_{opt} \equiv \min_\theta\{m_\theta(\gamma_{sf})\}$, where $\theta \in [0, 2\pi]$ and a, b and $c_\pm$ are elements of the standard form covariance matrix γ_{sf} given by Eq. (2.70).

Using a similar formalism, the GEoF defined using Rényi-2 entropy was also developed as

$$\mathcal{E}_F^{R-2}(\rho) = \frac{1}{2}\ln\left(\inf_\theta m_\theta(a,b,c_+,c_-)\right). \tag{3.22}$$

The optimal θ minimising m_{opt} can be found numerically for general two-mode Gaussian states, and analytically for relevant sub-classes of states, including symmetric states, squeezed thermal states, and so-called GLEMS (Gaussian Least Entangled Mixed States for given local and global purities).

3.3.4 Squashed Entanglement

The squashed entanglement was first introduced in a series of papers by Tucci [94–99] and is defined for a tripartite system ρ_{ABE} as

$$\mathcal{E}_S = \inf_E\left[\frac{1}{2}\mathcal{I}(\rho_{ABE})\right], \quad \text{with} \quad \mathrm{Tr}_E\left[\rho_{ABE}\right] = \rho_{AB}, \tag{3.23}$$

where the quantum conditional mutual information (CMI) defined as

$$\mathcal{I}(\rho_{ABE}) = \mathcal{I}(A;B|E) = \mathcal{S}(\rho_{AE}) + \mathcal{S}(\rho_{BE}) - \mathcal{S}(\rho_{ABE}) - \mathcal{S}(\rho_E), \tag{3.24}$$

satisfies a strong subadditivity property and $\mathcal{I}(A;B|E) \geq 0$ [100]. The squashed entanglement is a convex entanglement monotone serving as a lower bound to the entanglement of formation $\mathcal{E}_F(\rho)$ and an upper bound to the distillable entanglement $\mathcal{E}_D(\rho)$ defined previously. As a direct result of this the squashed entanglement will be equivalent to the entropy of entanglement $\mathcal{E}_R(\rho)$ for pure states [101].

3.3.5 Relative Entropy of Entanglement

The quantum relative entropy is often considered to be a pseudo-distance measure between one quantum system and another possessing specific properties. The relative entropy is defined as

$$\mathcal{S}(\rho \parallel \sigma) := \mathrm{Tr}[\rho\log\rho - \rho\log\sigma]. \tag{3.25}$$

Although the relative entropy is considered to be a measure of correlations, this is not strictly true since $\mathcal{S}(\rho \parallel \sigma) \neq \mathcal{S}(\sigma \parallel \rho)$. The relative entropy of entanglement is then defined as

$$\mathcal{E}_{RE}(\rho_{AB}) := \inf_{\sigma \in \chi} \mathcal{S}(\rho_{AB} \parallel \sigma), \tag{3.26}$$

where χ is the set of separable states. Therefore the relative entropy of entanglement asks for the minimum distance between the state ρ_{AB} and the closest separable state belonging to χ. The Gaussian relative entropy of entanglement for particular classes of Gaussian states can be found in Ref.'s [102, 103].

3.3.6 Negativity and Logarithmic Negativity

The Negativity of a quantum state ρ_{AB} was first introduced by Zyckowski *et al.* [104] and later verified as a legitimate entanglement measure by Vidal and Werner [105]. It is defined as the sum of the eigenvalues of the partially transposed state and can be written, in reference to the density matrix ρ and the covariance matrix γ of a Gaussian state, as

$$\begin{aligned} \mathcal{N}(\rho_{AB}) &= \frac{1}{2}\mathrm{Tr}\left(\sqrt{(\rho_{AB}^{\top_A})^2} - \rho_{AB}^{\top_A}\right) = \frac{1}{2} \parallel \rho_{AB}^{\top_A} \parallel -1, \\ \mathcal{N}(\gamma_{AB}) &= \frac{1}{2}(\prod_k \tilde{\nu}_k^{-1} - 1), \quad \text{for} \quad k : \tilde{\nu}_k < 1, \end{aligned} \tag{3.27}$$

where $\parallel \cdot \parallel$ denotes the trace norm, and if $\tilde{\nu}_k \geq 1$ then $\mathcal{N}(\gamma_{AB}) = 0$. The usefulness of the Negativity is in its simplicity to compute for both discrete and continuous variables, however it lacks the desirable property of additivity. This is overcome by the *Logarithmic Negativity* [106] defined as

$$\begin{aligned} \mathcal{LN}(\rho_{AB}) &= \log_2(1 + 2\mathcal{N}(\rho_{AB})) = \log(\parallel \rho_{AB}^{\top_A} \parallel), \\ \mathcal{LN}(\gamma_{AB}) &= -\sum_k \ln \tilde{\nu}_k, \quad \text{for} \quad k : \tilde{\nu}_k < 1, \end{aligned} \tag{3.28}$$

where $\mathcal{LN}(\gamma_{AB}) = 0$ if $\tilde{\nu}_k \geq 1$. Interesting properties of the Logarithmic Negativity to note are that it acts as an upper bound to the distillable entanglement (see Section 3.3.2) and also that a PPT entangled state can still indicate zero Logarithmic Negativity.

The purpose of this Chapter was to introduce the origin and concept of quantum entanglement as the fundamental phenomenon in quantum information theory. We discovered not only indicators, but explicit quantitative measures of this remarkable property. The information presented here will prove to be essential in the discussion of more complex and less investigated characteristics of a quantum system. Throughout this Chapter the strict distinction has been made between what one may consider to be classically correlated or quantum correlated, and that these are the only realms in which a state may exist. In the next Chapter we will discover the incompleteness of this description and explore the general concept of non-classicality. Particular focus will be placed on mixed bipartite states, where there exists a more broad description of quantumness, of which quantum entanglement is a subset.

Chapter 4

Non-Classicality

Disclaimer: Note the slightly unconventional use of the terms "non-classically correlated" and "quantum correlated". I shall define the set of non-classically correlated states as those exhibiting non-zero quantum discord, and the set of quantum correlated states to be a subset of these states explicitly possessing quantum entanglement. Therefore entangled states are covered under the umbrella of discordant states. This is further illustrated in Fig. 4.1.

The concept of the non-classicality of physical bipartite systems has long been established, but has soley focused on what is now known to be subset of states defined by quantum entanglement. In actuality it is the discrepancy of what is considered as *quantum correlated* or *non-classically correlated* which has been a relatively recent development. In previous Chapters, suggestions have been made regarding the incompleteness of the case in which if a state does not possesses quantum entanglement, it is considered classical. Whilst this is the case for bipartite pure states, for more realistic bipartite mixed states there can arise the situation whereby a state will be separable, but possesses non-classical correlations not defined by quantum entanglement. Within the context of this Thesis, the general distinction is made between quantum correlated and non-classically correlated. Quantum correlated states are those which have entanglement and are a subset of states which are classified as non-classically correlated. So when a state is classified as non-classical, it may or may not exhibit entanglement properties (see Fig. 4.1). It is well known that there exist a discrepancy between separable states and those considered to be truly classical [107].

An early example of the implementation of non-classical correlations beyond entanglement is within the *deterministic quantum computation with one quantum bit* (DQC1) protocol [69] later developed in [108, 109]. The protocol involves a collection of qubits in the completely mixed state coupled to a single control qubit that has non-zero purity. The initial state, operations, and measurements in the protocol appear to indicate a natural bipartite split between the control qubit and the mixed collection. Although there is no entanglement present, it has been shown that non-classical correlations of some degree are present which may play a role in a computational speed-up.

Various indicators of the presence of non-classicality beyond entanglement have been

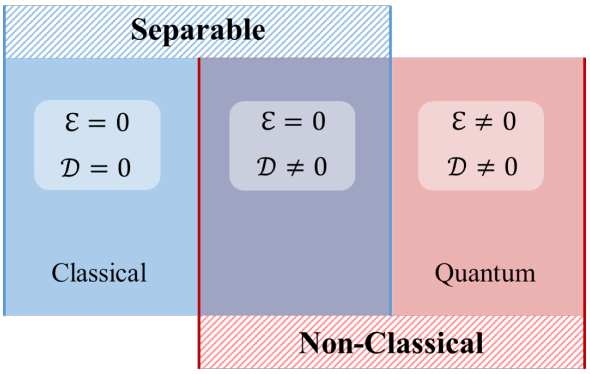

Figure 4.1: Classification of physical states according to the presence of classical, quantum or general non-classical properties. $\mathcal{E}$ denotes quantum entanglement and $\mathcal{D}$ quantum discord. In what remains states classified as quantum are those exhibiting quantum entanglement and are considered a subset of non-classical states.

established and proven imperative in the attempt to understand non-classicality in greater depth. There has been a huge expansion in the interest of non-classicality within quantum information theory in recent years, but still the official significance of non-classical correlations, particularly within separable states, is largely unknown and is the topic of some controversy when considering the usefulness of the phenomenon relative to quantum entanglement. There exists a vast body of literature indicating that these correlations may prove not only useful, but more robust than entanglement within the context of noisy channels [108–119].

4.1 Non-Classicality Indicators

In this Section a selection of non-classicality indicators will be presented. Particular focus will be placed on quantum discord, as this is currently the most predominant measure and as such, is the only one used in later Chapters. Non-zero quantum discord will then serve as an analogy to non-classically correlated states in the discussion of what one defines as a classical state.

4.1.1 Quantum Discord

There are in general two classes of quantum discord, a measurement-based discord and a distance-based discord. Although both shall be introduced in this Section, a particular focus will be placed on the measurement-based approach. Quantum discord has been extensively discussed is various literature such as [120–125].

Measurement-Based Quantum Discord

In 2001 Ollivier and Zurek first introduced the notion of a measurement-based quantum discord [126] as another kind of non-classical correlation different from entanglement[1]. It was defined as the discrepancy of two quantities, which in a classical context, are equivalent. Consider a classical bipartite state composed of two variables A and B, the total mutual information and the classical correlation present in this system are defined respectively as

$$\mathcal{I}(A:B) = \mathcal{H}(A) + \mathcal{H}(B) - \mathcal{H}(A:B) \tag{4.1a}$$

$$\mathcal{J}^{\leftarrow}(A:B) = \mathcal{H}(A) - \mathcal{H}(A:B) \tag{4.1b}$$

where $\mathcal{H}$ denotes the Shannon entropy, which can be interpreted as the ignorance of the observers (in the essence that if the Shannon entropy is non-zero the state is considered as mixed) and where the left arrow indicates an averaging of the entropy over possible values of B and a right arrow for an averaging over possible values of A. Whilst in the classical setting one can, in principle, obtain all information of the system without disturbing it, these quantities will be equivalent, which is intuitive since the total correlations in the system must only be classical. Considering now the quantum setting, the quantum analogies of these quantities are as defined in Eq.'s (2.76, 2.77),

$$\mathcal{I}(\rho_{AB}) = \mathcal{S}(\rho_A) + \mathcal{S}(\rho_B) - \mathcal{S}(\rho_{AB}), \tag{4.2a}$$

$$\mathcal{J}^{\leftarrow}(\rho_{AB}) = \mathcal{S}(\rho_A) - \inf_{\{\hat{\Pi}_j\}} \mathcal{H}_{\{\hat{\Pi}_j\}}(\rho_A|\rho_B). \tag{4.2b}$$

where $\mathcal{S}$ is considered as the von Neumann entropy and so the determination of value now constitutes a measurement. The quantum conditional entropy will be optimised over all possible measurements. Galve *et al.* [127] proved for qubits the optimality of orthogonal measurements for rank-2 states in calculating discord. Clearly, as we are now considering a quantum state, measurements will disturb the system. There will exist more than merely classical correlations, therefore these quantities are no longer equivalent. It is this discrepancy that defines quantum discord,

$$\begin{aligned} \mathcal{D}^{\leftarrow}(\rho_{AB}) &= \mathcal{I}(\rho_{AB}) - \mathcal{J}^{\leftarrow}(\rho_{AB}), \\ &= \mathcal{S}(\rho_B) - \mathcal{S}(\rho_{AB}) + \inf_{\{\hat{\Pi}_j\}} \mathcal{H}_{\{\hat{\Pi}_j\}}(\rho_A|\rho_B) \end{aligned} \tag{4.3}$$

often referred to *"one-way quantum discord"*.

Significant properties of the original measurement-based discord include:

1. non-symmetry i.e., $\mathcal{D}^{\leftarrow}(\rho_{AB}) \neq \mathcal{D}^{\rightarrow}(\rho_{AB})$. Although a symmetric version exists defined simply as

   $$\mathcal{D}^{\leftrightarrow}(\rho_{AB}) = \max\{\mathcal{D}^{\leftarrow}(\rho_{AB}), \mathcal{D}^{\rightarrow}(\rho_{AB})\} \tag{4.4}$$

   appropriately named the *"two-way quantum discord"* which will be zero for classical-classical (CC) states only [128, 129].

[1] Quantum discord was also independently introduced by Henderson and Vedral in Ref. [130].

2. non-negativity i.e., $\mathcal{D}^{\leftarrow}(\rho_{AB}) = \mathcal{D}^{\rightarrow}(\rho_{AB}) \geq 0$.

3. the majority of physical bipartite states have non-zero discord such that the set of CC states are negligible in the whole Hilbert space. Also, any such CC state requires only a small generic perturbation to drive it to a positive-discord state [107].

4. $\mathcal{D}(\rho_{AB}) = 0$ if and only if the state is completely classical and thus measurement cannot cause disruption. It has been proven however that a non-unitary operation may lead to the emergence of discord from a classical state [131].

5. unaffected by local unitary transformations e.g. beamsplitter transformations.

6. equivalence to the entropy of entanglement for bipartite pure states.

7. quantum discord cannot be shared [132]. This property is based on Bohr's postulate using modern tools from quantum information theory. Bohr's idea that if a measurement device is in a non-classical state the measurement results cannot be communicated perfectly by classical means. In this, part of the information in the measurement apparatus is lost and the amount of lost information coincides with the quantum discord. In Ref. [132] it was shown that for pure system-apparatus states quantum communication does not provide any advantage when measurement results are communicated to more than one party. In addition it was demonstrated that quantum communication to two parties on a mixed system-apparatus state appeared to be superior.

A popular example of a quantum state which is defined as separable whilst possessing quantum discord is the Werner state [72], defined as

$$\rho(\psi, p) = \frac{\mathbb{1}}{4}(1-p) + p|\psi\rangle\langle\psi|, \tag{4.5}$$

where $|\psi\rangle$ is a maximally entangled Bell state as presented in Eq. (3.2). If $p < 1/3$ then the Werner state is not entangled, however for values of $0 < p < 1/3$ the state will have non-zero quantum discord.

A pivotal moment in the evolution of the notion of quantum discord was within a paper by Ferraro *et al.* [107]. In this the authors aimed to discredit discord as a useful resource within quantum information. It is claimed that states with zero discord are in fact negligible in any Hilbert space dimension. It is likely that a state chosen at random will have non-zero discord and that if a state has zero discord, a generic arbitrary perturbation transforms the state into one with non-zero discord. Whilst for some this result indeed did raise serious doubts regarding the potential application of quantum discord, for most, this was seen as a remarkable and encouraging result. Ferraro *et al.*'s result demonstrates that zero quantum discord states are rare to find, and consequently the mere presence of quantum discord does not imply its usefulness. But this of course does not exclude the possibility of a valuable association of discord to the usefulness in some task [107].

Gaussian Quantum Discord

An extension to the original definition has been made to continuous variable Gaussian states by Adesso *et al.* [133] and Giorda *et al.* [134] simultaneously (although in the latter a definition is only given for bipartite Gaussian squeezed thermal states). The purpose of defining a Gaussian discord is due to the simple symplectic formalism used in their analysis, described in Section 2.3.2. In addition, Gaussian states are seen to be the most physically realisable of quantum states, since vacuum, coherent and squeezed states are all Gaussian. The *Gaussian quantum discord* as introduced in Ref. [133] is defined as

$$\mathcal{D}^{\leftarrow}(\gamma_{AB}) = \underbrace{f\left(\sqrt{B}\right)}_{\mathcal{S}(\rho_B)} - \underbrace{\left(f(\nu_+) + f(\nu_-)\right)}_{\mathcal{S}(\rho_{AB})} + \underbrace{\inf_{\sigma_0} f\left(\sqrt{\det\epsilon}\right)}_{\inf_{\{\hat{\Pi}_j\}}\mathcal{H}_{\{\hat{\Pi}_j\}}(\rho_A|\rho_B)}, \tag{4.6}$$

where $\nu_\pm$ are the symplectic eigenvalues of the two-mode covariance matrix γ_{AB} from Eq. (2.72) and $f(x)$ is given by Eq. (2.84).

The measurements performed are assumed to be a set of local projective measurements $\{\Pi_B^{(j)}\} = \{|j_B\rangle\langle j_B|\}$ on subsystem B. The state of the whole system related to the measurement is

$$\rho_{AB|j} = \frac{1}{p_j}(\mathbb{1}_A \otimes \Pi_B^{(j)})\rho_{AB}(\mathbb{1}_A \otimes \Pi_B^{(j)}), \tag{4.7}$$

with $\mathbb{1}_A$ the identity matrix and $p_j = \mathrm{Tr}[(\mathbb{1}_A \otimes \Pi_B^{(j)})\rho_{AB}(\mathbb{1}_A \otimes \Pi_B^{(j)})]$ the probability of obtaining outcome j. The conditional entropy component can thus be written as $\mathcal{S}(\rho_A|\{\Pi_B^{(j)}\}) = \sum_j p_j \mathcal{S}(\rho_{A|j})$, with $\rho_{A|j} = \mathrm{Tr}_B[\rho_{AB|j}]$ being the reduced density matrix.

The quantum conditional entropy is restricted to generalised Gaussian positive operator valued measurements (POVMs) on subsystem B written, in general, as

$$\rho_B(\nu) = \frac{1}{\pi}\hat{W}_B(\nu)\rho_B^0(\nu)\hat{W}_B^\dagger(\nu), \tag{4.8}$$

where $\hat{W}_B(\nu)$ is the Weyl operator (Eq. (2.92)), and ρ_B^0 is the density matrix of a single-mode Gaussian state. It was shown to be sufficient to restrict to pure single-mode Gaussian states with covariance matrix Γ_0. The conditional state of subsystem A after the measurement on subsystem B has a covariance matrix given by the Schur complement $\epsilon = \gamma_A - \gamma_C(\gamma_B + \Gamma_0)^{-1}\gamma_C^\top$. The optimised post-measurement state $\inf_{\sigma_0}\det\epsilon$ is given by

$$\inf_{\sigma_0}\det\epsilon = \begin{cases} \frac{2C^2+(B-1)(D-A)+2|C|\sqrt{C^2+(B-1)(D-A)}}{(B-1)^2} \\ \text{if} \quad (D-AB)^2 \le (1+B)\,C^2\,(A+D)\,, \\ \frac{AB-C^2+D-\sqrt{C^4+(D-AB)^2-2C^2(AB+D)}}{2B} \\ \text{Otherwise.} \end{cases} \tag{4.9}$$

where $A = \det\gamma_A$, $B = \det\gamma_B$, $C = \det\gamma_C$ and $D = \det\gamma_{AB}$. The term '$\inf_{\sigma_0}\det\epsilon$' represents the optimised quantum conditional entropy of two systems over the set of Gaussian measurements. The separate scenarios refer to different types of Gaussian measurements, a notable class of states falling under the first case are squeezed thermal states for which the

conditional measurement is minimised by heterodyne measurements (as introduced in [134]), the second case corresponds to homodyne measurements. Key properties of Gaussian quantum discord include (in addition to those applicable to the original discord):

1. almost all bipartite Gaussian states have Gaussian quantum discord.

2. for bipartite mixed separable states, Gaussian discord is less than or equal to 1.

Gaussian measurements are generally thought to be optimal for Gaussian quantum discord in that a Gaussian measurement will tend to disturb the state the least. However, studies are still ongoing regarding the implementation of non-Gaussian measurements (such as photon counting[2]) on Gaussian states and whether they may be least disturbing for certain states [135, 136]. Pirandola *et al.* in Ref. [137] proved that, for a large set of Gaussian states, that the Gaussian quantum discord is optimised by Gaussian measurements.

Operational Gaussian Discord (OGD)

More recently an "operational Gaussian discord" definition has been established by S. Rahimi-Keshari *et al.* in Ref. [138]. This is a discord measure which can be experimentally measured by using local and joint Gaussian measurements and is defined as

$$\mathcal{D}_{OGD}(B \to A) = \mathcal{H}_{GL}^{min}(\tilde{A}|\tilde{B}) - \mathcal{H}_{GJ}^{min}(\tilde{A}|\tilde{B}), \tag{4.10}$$

where $\mathcal{H}_{GL}^{min}(\tilde{A}|\tilde{B})$ is the minimum conditional entropy of A after performing local Gaussian measurements on A and B, and $\mathcal{H}_{GJ}^{min}(\tilde{A}|\tilde{B})$ is the minimum conditional entropy of the same subsystem after performing a joint Gaussian measurement on A and B. The entropies are the continuous (differential) Shannon entropy of Gaussian probability distributions, which for a single mode are given by $\frac{1}{2}\ln(\det\tilde{\gamma}) + \ln(2\pi e)$ [138], with $\tilde{\gamma}$ being the covariance matrix of the probability distribution. In this notation, $\tilde{A}$ and $\tilde{B}$ denote the entropies calculated using outcome probability distributions of the measurements, since all the probability distributions are Gaussian. To calculate the OGD one must simply minimise the determinants of the covariance matrices of the conditional Gaussian probability distributions for the outcomes of local and joint Gaussian measurements. It is suggested that this measure might be useful for quantifying non-classical correlations in resources of other Gaussian protocols that involve Gaussian states, operations, and measurements.

Distance-Based Quantum Discord

Another definition of quantum discord is as a distance-based measure. The *relative entropy-based discord* was introduced by Modi *et al.* [139] and defined as

$$\mathcal{D}^{rel}(\rho) = \min_{\chi \in C} \mathcal{S}(\rho \parallel \chi) = \min_{\chi \in C}[\mathcal{S}(\chi) - \mathcal{S}(\rho)], \tag{4.11}$$

[2]Photon counting is a technique where individual photons are counted using some single photon detector (SPD). Counting efficiency is determined by any electronic losses that are present in the system and the quantum efficiency. An SPD can be a configured photodetector such as a photomultiplier.

where C denotes the set of all classical states and

$$\mathcal{S}(\rho \parallel \chi) = \mathrm{Tr}[\rho \log_2 \rho - \rho \log_2 \chi] \tag{4.12}$$

is the relative entropy. Qualitatively speaking, this measure will seek for the minimum pseudo-distance between a state ρ and the closest classical state χ. Hence if the state ρ is completely classical, $\mathcal{D}^{rel}(\rho)$ will be zero. This resource has the advantage of placing all correlations on an equal footing from its pseudo-distance nature, this allows a quantitative comparison of different classes of correlations.

An additional distance-based measure of quantum discord is the *geometric discord* [140] which is defined by

$$\mathcal{D}^{geo}(\rho) = \min_{\chi} \parallel \rho - \chi \parallel^2, \tag{4.13}$$

where the classical states χ are of the form $p_1|\psi_1\rangle\langle\psi_1|\otimes\rho_1 + p_2|\psi_2\rangle\langle\psi_2|\otimes\rho_2$ with $\sum_i p_i = 1$. The square norm of the Hilbert-Schmidt space is denoted $\parallel \cdot \parallel$, $|\psi_i\rangle$ are the orthonormal basis of subsystem A and ρ_i are the density matrices of subsystem B. A disadvantage of geometric discord is that it is in general difficult to experimentally measure, however a tight lower bound has been established by Girolami and Adesso [141] without the need for full state tomography.

4.1.2 Dynamics of Quantum discord

This Section will serve as a brief introduction to examples illustrating the dynamics of quantum discord in Markovian and non-Markovian environments, enabling further insight into the nature of quantum discord and its complexities. Let us first consider discord in cavity quantum electrodynamics (QED) [142–146]. It has been extensively proven that entanglement, during the evolution of a two-qubit state, may disappear for a finite time, in a phenomenon known as "*entanglement sudden death*" [147–153]. However, it has been established that almost all quantum states are discordant states, and that discord proves to be more robust than entanglement in Markovian environments, to such a degree that there is no quantum discord sudden death [154–157].

For a system of two non-interacting atoms within a dissipative cavity, the level of quantum discord can reach asymptotic values even when the average photon number of the cavity field is relatively large [142]. In [143] two spatially separated and dissipative cavities contained a two-level system in each. In a weak coupling limit, discord will essentially remain at zero for the finite time. Contrary to this, when a strong coupling limit is considered, quantum discord sudden death is non-existent whilst entanglement sudden death persists.

Most studies of quantum discord are set within Markovian environments. However, it has been witnessed that a proportion of quantum discord can be temporarily stored in a non-Markovian environment, and then later returned back into the system. This phenomenon has been referred to as "*sudden birth of discord*", noting that however the existence of "*sudden birth of entanglement*" has not yet been confirmed [158].

Recently, the propagation of quantum correlations via a spin-1/2 chain was investigated [159]. The role of magnetic field in the dynamics of quantum discord was also dis-

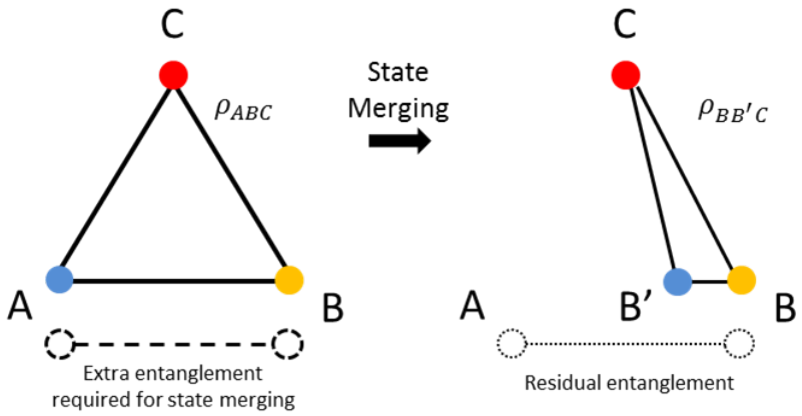

Figure 4.2: State merging protocol for a tripartite state ρ_{ABC} aiming to transfer A to B at the possible cost of using some extra entanglement. The amount of entanglement used is equal to the discord between A and a common reference system C.

cussed. Quantum discord can be transported more efficiently than entanglement for many initial conditions and working points. The effects of Dzyaloshinskii-Moriya interaction[3] upon quantum discord of a spin-star system has been investigated in [145]. The results of this show that strong Dzyaloshinskii-Moriya interaction can increase quantum discord and thermal entanglement. However, a strong magnetic field and high temperature can decrease quantum discord and thermal entanglement.

The dynamics of quantum entanglement and discord of two coupled double quantum dots interacting with an oscillator bath has been investigated in [146]. The results of this paper show that quantum discord is more robust to dissipation than entanglement of formation of this system. Particularly, they pointed out that, even in the case of high temperatures, quantum discord could be finite in the asymptotic limit [146].

From these examples it clear that quantum discord appears to have significance in a broad range of protocols which indicates its dynamicity. Edging further, let us now consider some well known operational implementations and interpretations of quantum discord.

4.1.3 Operational Interpretation of Quantum Discord

The operational interpretation of quantum discord has attracted much attention in recent years with some interesting developments given in Ref. [162].

Extended State Merging If one starts with a tripartite state ρ_{ABC}, state merging is a process by which A and B transfer part-A of the state to B whilst maintaining coherence with a reference C [163]. The entanglement consumption due to this merging will correspond to the discord present (see Fig. 4.2). Both parties A and B have knowledge of the state they

[3]The anti-symmetric exchange defined as the contribution to the total magnetic exchange interaction between two neighbouring magnetic spins, $\mathbf{S}_i$ and $\mathbf{S}_j$ [160, 161].

share and can carry out arbitrary LOCC on the state. The end goal is to create n copies of ρ_{ABC} such that the resulting state $\rho_{BB'C}$ possesses a state B' which essentially plays the same role as state A. The total entanglement consumption used in state merging of A to B is defined as

$$\Gamma(A\rangle B) = \mathcal{E}_F(A:B) + \mathcal{S}(A|B), \tag{4.14}$$

where $\mathcal{S}(A|B)$ is the conditional entropy with a measurement on subsystem B and $\mathcal{E}_F(A:B)$ is the entanglement of formation, which defines the minimum pure state entanglement that A and B need to consume to create ρ_{AB} by LOCC. By use of the Koashi-Winter relation defined later in Section 4.4, the discord can be defined as $\mathcal{D}^{\leftarrow}(AC) = \Gamma(A\rangle B)$. This states that the discord between states A and C, with a measurement on C, is equal to the total entanglement consumption in extended state merging from A to B [162]. This was seen to be the first link between the value of quantum discord and the information about the performance or cost of a particular task.

Dense Coding Consider a sender A and receiver B sharing a quantum state ρ_{AB}. In this, the sender has the ability to transmit more classical information than if the system was merely classical. If encoding is performed on A by unitary rotations, the correction that the sender could achieve by sending a classical system with an equal dimension to that of subsystem ρ_A is exactly the coherent information

$$\mathcal{I}(A\rangle B) = \mathcal{S}(B) - \mathcal{S}(AB). \tag{4.15}$$

The coherent information thus describes the usefulness of a quantum state as a resource for dense coding. However, in the most general scenario described in Ref's. [164–167], A encodes a message by means of general quantum operations $\Lambda_A : M_{d_A} \to M_{d'_A}$, where d_A is the dimension of the original subsystem of A, d'_A is the dimension of the subsystem sent to B and M_d denotes the set of $d \times d$ complex matrices.

If the encoding is applied at the level of single copies of the shared state ρ_{AB}, the dense coding single-copy capacity is equal to

$$\chi(A\rangle B) := \log_2 d'_A + \max_{\Lambda_A} \mathcal{I}(A'\rangle B), \tag{4.16}$$

where the maximisation is over all quantum operations with output dimension d'_A and $\mathcal{I}(A'\rangle B)$ is the coherent information of $(\lambda_A \otimes \mathbb{1}_B)[\rho_{AB}]$. From this $\log_2 d'_A$ can be considered as a classical contribution to the capacity, thus one can focus on the quantum advantage associated with dense coding given by

$$\Delta(A\rangle B) := \max_{\Lambda_A} \mathcal{I}(A'\rangle B). \tag{4.17}$$

The following connection between quantum discord and dense coding was given in Ref. [162] as

$$\mathcal{D}^{\leftarrow}(AC) - \mathcal{D}^{\leftarrow}(BC) = \Delta(C\rangle A) - \Delta(C\rangle B). \tag{4.18}$$

This provides an operational meaning in terms of performance to the differences in discord,

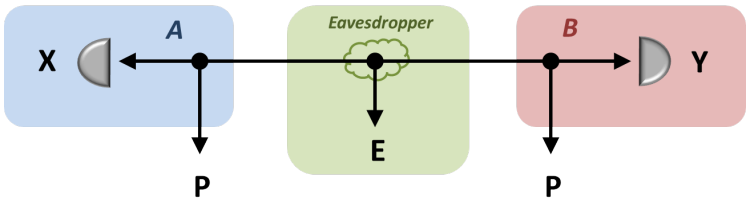

Figure 4.3: Output state from a device-independent QKD protocol. Local systems A and B have correlated variables X and Y, respectively, which are processed into a secret key. Secret key extracted by applying POVMs on local systems A and B. Eavesdropper steals information from system E, while the extra system P is controlled by eavesdropper and completes the purification of the global state Φ_{ABEP}.

stating that the difference in the discord of AC and BC, both measured by C, is the same as the difference in the dense coding capacity from C to either A or B. Note that if C sends subsystems with the same dimension to A and B, this difference can be written as

$$\mathcal{D}^{\leftarrow}(AC) - \mathcal{D}^{\leftarrow}(BC) = \chi(C\rangle A) - \chi(C\rangle B), \tag{4.19}$$

i.e., in terms of the dense coding capacity itself. The same difference in discord can be related to the coherent information,

$$\mathcal{D}^{\leftarrow}(AC) - \mathcal{D}^{\leftarrow}(BC) = I(A\rangle C) - I(B\rangle C) = I(C\rangle A). \tag{4.20}$$

Quantum Cryptography Quantum key distribution (QKD) is a process at the heart of quantum cryptography, traditionally reliant on the presence of quantum entanglement, distillable or bound. In Ref. [168] Pirandola considered a general form of a device-dependent QKD protocol in which noise affecting the device or apparatus is assumed to be trusted, i.e. not coming from an eavesdropper but from the action of the environment. Moreover a so-called device-independent version was also considered. In contrast to the former the device-independent protocol captures minimal requirements related to security and robustness against inefficiencies, and attributes it to an eavesdropper that cannot be trusted. The aim of this work was to align the non-orthogonal properties of a discordant state to the orthogonality essential to QKD. It was found that although the inefficiencies and noise may disrupt the distribution or distillation of entanglement, a secure key is still extractable due to the presence of non-zero quantum discord.

The device-independent protocol discussed in [168] (see Fig. 4.3) considered when locations A and B share a bipartite state ρ_{AB} which can be purified by two systems. One system (ρ_E) accessible to an eavesdropper at location E, while the other system (ρ_P) is inaccessible and accounts from the presence of trusted noise, e.g., coming from imperfections in the state preparation and/or detections.

In the device-independent protocol the system P is controlled by the eavesdropper. The

secret key rates are given by

$$\mathcal{K}^{\rightarrow}(AB) := \sup_{\{M_x\}} \mathcal{K}(B|X) = \mathcal{I}_c(A\rangle B) \tag{4.21a}$$

$$\mathcal{K}^{\leftarrow}(AB) := \sup_{\{M_y\}} \mathcal{K}(A|X) = \mathcal{I}_c(B\rangle A) \tag{4.21b}$$

where $\mathcal{K}(B|X) := \mathcal{I}(B,X) - \mathcal{I}(E,X)$ and $\mathcal{I}(A,B) = \mathcal{S}(A) - \mathcal{S}(A|B)$ is the Holevo bound[4] and coherent information $\mathcal{I}_c(A\rangle B)$ and its reverse $\mathcal{I}_c(B\rangle A)$ quantify the maximum distillable entanglement by LOCC. The discord acts as an upper bound to these secret key rates such that

$$\mathcal{K}^{\rightarrow}(AB) = \mathcal{D}(A|B) - \mathcal{E}_F(A,E) \leq \mathcal{D}(A|B) \tag{4.22a}$$

$$\mathcal{K}^{\leftarrow}(AB) = \mathcal{D}(B|A) - \mathcal{E}_F(B,E) \leq \mathcal{D}(B|A). \tag{4.22b}$$

This is a scenario where key distribution may occur in the complete absence of entanglement, provided that there is non-zero discord. Moreover, it was discussed that any manner of 'prepare and measure' QKD protocols — with a security based on the non-orthogonality of quantum states — can be recast into an "entanglement-free device-dependent form" based on a classical-quantum (CQ) state[5], with non-zero discord transmitted through the imperfect channel.

Although quantum discord is the most prominent measure of non-classical correlation, other measures exist and are well established. The following Section will aim to provide a brief insight into the more popular alternative measures on offer.

4.2 Other Non-Classicality Indicators

Measurement induced disturbance (MID) was first introduced by Luo [169] and was based on the fundamental principle that one can obtain all the information of a classical system by performing measurements without causing disruption. The post-measurement state will be completely classical and as such, any correlations contained within the state can be described fully by the classical mutual information. MID is defined as

$$\mathcal{M}(\rho_{AB}) = \min_{\Pi} \left\{ \mathcal{I}(\rho_{AB}) - \mathcal{I}(\rho_{AB}^{\Pi}) \right\}, \tag{4.23}$$

with $\rho_{AB}^{\Pi} = \sum_{i,j}[(\Pi_A^{(i)} \otimes \Pi_B^{(j)})\rho_{AB}(\Pi_A^{(i)} \otimes \Pi_B^{(j)})]$. Clearly, MID can be considered easy to calculate since it involves no optimisations as in the original definition of quantum discord. An improved indicator followed this, aptly named an *ameliorated measurement-induced disturbance (AMID)* [170–172], which serves as a more faithful symmetric indicator optimised over joint local POVM measurements $\Pi_{AB} = \Pi_A \otimes \Pi_B$ on both subsystems, and therefore reads as

$$\mathcal{M}_{\mathcal{A}}(\rho_{AB}) = \inf_{\Pi_{AB}} \{\mathcal{I}(\rho_{AB}) - \mathcal{I}(\rho'_{AB})\}. \tag{4.24}$$

[4]The upper bound to the amount of information which can be known about a quantum state.
[5]A classical-quantum (CQ) state is one defined as $\rho_{AB} = \sum_i p_i |i\rangle\langle i| \otimes \rho_{B,i}$.

Hence AMID will capture the quantumness of correlations signalled by minimal state disturbance after optimised local measurements.

The *Gaussian ameliorated measurement induced disturbance (GAMID)* was introduced by Mišta *et al.* in [173], which looks at the optimised gap between the classical and quantum mutual information after local Gaussian measurements. In this, an analytic form of GAMID was found for important subclasses of bipartite Gaussian states including symmetric states and squeezed thermal states, including pure states. GAMID was also compared the Gaussian entanglement of formation, which identified lower and upper bounds for GAMID as a function of the GEoF. Moreover, GAMID appeared to consistently exceed the GEoF for all two-mode Gaussian states, enforcing a hierarchy between these two forms of non-classicality.

Another popular indicator of non-classicality is *quantum deficit*, based on the work extraction from a quantum system in a heat bath. When considering a classical system with no quantum correlations, the total work (W_T) that can be extracted from the entire system is the same amount of work, which could be extracted from individual subsystems by local operations and classical correlations, W_{LOCC}. However, this equality does not hold for those systems which possess quantum correlations, i.e. $W_T \neq W_{LOCC}$. The quantum deficit is then defined as the difference between these two amounts of extracted work.

Now that the definition of non-classicality has been full established it is interesting to note different, more intricate definitions of what one may consider to be classical, and by association, non-classical.

4.3 Differing Definitions of Non-Classicality

The essence of the definition of measurement-based Gaussian quantum discord is that a classical state is defined as one which possesses zero discord. This occurs when the standard form covariance matrix becomes diagonal and thus contains no x or p correlations between systems A and B, i.e. $c_- = c_+ = 0$ in Eq. (2.70). States defined as classical in this sense are known as Classical-Classical (CC) states, and constitute the main class of classical states in an information theoretic context. Ferraro and Paris discussed in [174] the discrepancy of the set of C-classical states and $\mathcal{P}$-classical states. $\mathcal{P}$-classical states are mixtures of Glauber coherent states, having a well-defined $\mathcal{P}$-function (see Section 2.2.2). The authors show that the sets of C-classical and $\mathcal{P}$-classical states are almost disjoint and that the two definitions are not only inequivalent, but maximally so. Generic CC states appear to exhibit quantumness in their $\mathcal{P}$-function, and $\mathcal{P}$-classical states have non-zero quantum discord. Recently this has been extended to an experimental setting and shown that almost all $\mathcal{P}$-classical input states generate outputs that are not C-classical. In fact, the more $\mathcal{P}$-classical the resources at the input, the less C-classicality at the output. It was also shown that the $\mathcal{P}$-classicality at the input determines the potential of generating output entanglement [175].

Moreover, aside from this discrepancy between an information theoretic and quantum optics definition of classicality, there exist even more subtle differences in the definition of classicality within CC states. CC states are defined as those which possess zero quantum discord, however, this is found to be dependent on the exact definition of quantum discord.

The original definition of quantum discord and the Gaussian extension were presented in terms of the von Neumann entropy, the quantum equivalent of the Shannon entropy. It was not until recently that Adesso *et al.* introduced Gaussian quantum discord in terms of a Rényi-α entropy for the case of $\alpha = 2$ [50] (see Section 2.4.1). The quantum mutual information and classical correlation have been defined in terms of Rényi-2 entropies in Eq.'s (2.90, 2.94). Hence the Gaussian quantum discord can be written as

$$\begin{aligned}\mathcal{D}_2(\rho_{(A|B)}) &= \mathcal{I}_2(\rho_{(A:B)}) - \mathcal{J}_2(\rho_{(A|B)}) \\ &= \frac{1}{2}\ln\left(\frac{\det\gamma_A \det\gamma_B}{\det\gamma_{AB}}\right) - \sup_{\Gamma_B^{\Pi}} \frac{1}{2}\ln\left(\frac{\det\gamma_A}{\det\tilde{\gamma}_A^{\Pi}}\right) \\ &= \inf_{\Gamma_B^{\Pi}} \frac{1}{2}\ln\left(\frac{\det\gamma_B \det\tilde{\gamma}_A^{\Pi}}{\det\gamma_{AB}}\right)\end{aligned} \tag{4.25}$$

with $\tilde{\gamma}_A^{\Pi} = \gamma_A - \gamma_C(\gamma_B + \Gamma_B^{\Pi})^{-1}\gamma_C^{\top}$ is the covariance matrix of subsystem A after an optimised Gaussian measurement is performed on subsystem B, defined as

$$\inf_{\Gamma_B^{\Pi}} \det\tilde{\gamma}_A^{\Pi} = \begin{cases} a\left(a - \frac{c_+^2}{b}\right) \\ \text{if} \quad (ab^2c_-^2 - c_+^2(a+bc_-^2))(ab^2c_+^2 - c_-^2(a+bc_+^2)) < 0, \\ \\ \frac{2|c_-c_+|\sqrt{(a(b^2-1)-bc_-^2)(a(b^2-1)-bc_+^2)} + (a(b^2-1)-bc_-^2)(a(b^2-1)-bc_+^2) + c_-^2c_+^2}{(b^2-1)^2} \\ \text{Otherwise.} \end{cases} \tag{4.26}$$

Form this definition, zero discord (and hence a CC state) exists when *either* there are no position *or* momentum correlations between subsystem A and B, i.e., $c_- = 0$ *or* $c_+ = 0$, proving as a result that the Rényi-2 definition appears to be a less sensitive indicator of quantum discord. Therefore one must be careful to clarify the exact definition of what is classified as classical.

Thus far a number of fundamental properties have been defined for continuous variable states and some remarkable relationships recognised. The next Section will serve to provide an introduction to the most focused upon relation in this Thesis, the *Koashi-Winter relation*.

4.4 Koashi-Winter Relation

The Koashi-Winter relation stems from the unique property of monogamy of entanglement [176], capturing the trade-off between entanglement and classical correlation. The monogamy of entanglement implies that if a pair of systems A and B are maximally entangled, e.g. $|\Psi^-\rangle = (|01\rangle - |10\rangle)/\sqrt{2}$, neither system can be entangled to a third system C. In addition to this, it is found that neither system can possess even classical correlations with C. Similarly, if a pair of systems A and B contains a maximum amount of classical correlations, then neither system can possess entanglement with any third party.

In [176] Koashi and Winter considered a tripartite state ρ_{ABC} and an ensemble $\{p_i|\psi_i\rangle\}$ which minimises the entanglement of formation (EoF) (see Section 3.3.3). There exists a

measurement outcome i with probability p_i which leaves the state of A and B in $|\psi_i\rangle$. From the definition of $\mathcal{J}^{\leftarrow}(\rho)$,

$$\begin{aligned}\mathcal{J}(\rho_A : \rho_C) &\geq \mathcal{S}(\rho_A) - \sum_i p_i \mathcal{S}(\mathrm{Tr}[|\psi_i\rangle\langle\psi_i|]), \\ &= \mathcal{S}(\rho_A) - \mathcal{E}_F(\rho_{AB}),\end{aligned} \tag{4.27}$$

where $\mathcal{S}(\rho)$, $\mathcal{E}_F(\rho)$ and $\mathcal{J}^{\leftarrow}(\rho)$ represent the marginal entropy, entanglement of formation and one-way classical correlation, respectively. This equality holds for all pure states ρ_{ABC} since the concept of non-classical states with zero entanglement has not been taken into account.

Linking this equality to discord can be simply done by substituting Eq. (4.3) into Eq. (4.27) giving

$$\begin{aligned}\mathcal{S}(\rho_A) &= \mathcal{E}_F(\rho_{AB}) + \mathcal{I}(\rho_{AC}) - \mathcal{D}^{\leftarrow}(\rho_{AC}), \\ \Rightarrow \mathcal{S}(\rho_{AC}) + \mathcal{D}^{\leftarrow}(\rho_{AC}) &= \mathcal{E}_F(\rho_{AB}) + \mathcal{S}(\rho_C).\end{aligned} \tag{4.28}$$

The relation thus allows for the illustration of how general non-classical correlation flows within a tripartite system. A number of relations can arise from this connection such as the difference in the marginal entropies of two subsystems in terms of discord,

$$\mathcal{S}(\rho_{BC}) - \mathcal{S}(\rho_{AC}) = \mathcal{D}^{\leftarrow}(\rho_{AC}) - \mathcal{D}^{\leftarrow}(\rho_{BC}) \tag{4.29a}$$

$$\mathcal{S}(\rho_A) - \mathcal{S}(\rho_B) = \mathcal{D}^{\leftarrow}(\rho_{AC}) - \mathcal{D}^{\leftarrow}(\rho_{BC}). \tag{4.29b}$$

where use has been made of the purity relation $\mathcal{S}(\rho_{ij}) = \mathcal{S}(\rho_k)$ for a tripartite state ρ_{ijk}. These relations were used in an interesting analysis of tripartite Gaussian states in Ref. [177].

In this Chapter the notion of non-classicality was introduced. A notable class of states which are strictly non-classical, while remaining separable, were identified. The most developed and widely accepted measure of non-classicality in bipartite mixed states, quantum discord, was extensively discussed. This Chapter also included a general definition of what one may consider as classical, and how this definition must be strictly laid in place, since there exists a wide array of definitions for the set of classical states. The concepts, definitions and tools defined here, particularly Gaussian quantum discord, will now be implemented into specific schemes to attempt to identify new information in regards to its usefulness as a quantum resource.

Part II

Quantum Nature of Gaussian Discord

Chapter 5

Gaussian Discord in a Dissipative Quantum System

The Gaussian formalism is being constantly expanded in order to strengthen quantum information theory, this extends to Gaussian quantum discord. Gaussian quantum discord is receiving increasing attention and is believed to aid in an ultimate conclusion to the practical usefulness of non-classical correlations in a quantum system. It has recently been shown that for a number of popular classes of Gaussian states, the Gaussian quantum discord corresponds to the true quantum discord[1] [137]. Theoretically speaking, Gaussian mixed states are of specific interest since it is possible to fully describe each state by its first and second moments, i.e. a covariance matrix. Experimentally, mixed Gaussian states are readily realisable, being constructible from pure coherent, squeezed and vacua states. Mixed states are also considered to be more realistic in the sense that they can be perceived as pure states following some degree of mixing with the environment, which is rather infeasible to prevent in reality.

The following presents original work, formally introduced in Ref. [178], focused on the study of Gaussian quantum discord in a realistic, noisy environment. The scheme considered is designed so to be as basic as possible, to allow focus on the fundamental properties of the correlations present therein. A deeper insight into the complexities of the system, and in particular how Gaussian discord can increase under local loss, is achieved by considering a globally pure state in which the bipartite separable discordant system is contained. We find that the discord dynamics can be attributed to the flow of correlations with the global system (system and environment) using the Koashi Winter relation. We thus pinpoint the role of system-environment correlations and the manner in which the flow of correlations to the environment affects the system. The theoretical establishment of general non-classical correlations from system-environment correlations was discussed for qubits in [179]. Recently, experimental evidence has been proposed linking the open-system dynamics of entanglement to correlations with environment and discord [180].

This Chapter will unveil, experimentally and in theory, how the environment can con-

[1] *True* quantum discord is defined as that which is optimised over all general local measurements.

tribute to the manifestation of quantum properties. As a final factor, a conceptual discussion will be presented on the optimisation of this counter-intuitive property of the system, determining the ideal properties a state must possess to benefit most from controlled local dissipation. A conclusion is then held regarding the hidden quantum features within the system in relation to the possible recovery of entanglement in a separable discordant state using classical communication based on initial state preparation.

5.1 Quantumness of Gaussian Discord Under Loss

5.1.1 State Preparation and Scheme Outline

The main aim of the scheme outlined below is gain insight into the characteristics of quantum discord under the influence of a noisy channel. What is the limiting case where robustness of discord is witnessed? What properties of the system are responsible for this robust nature and what are its advantages? To begin our analysis of Gaussian quantum discord we must first construct a bipartite mixed state, possessing the property of being both separable and discordant. This is achieved in two separate scenarios, both of which involve a single interaction with a vacuum state on a beamsplitter.

The first scenario involves the preparation of a squeezed coherent state denoted as $\rho_A^{0,sq}$ and constructed as a polarisation squeezed beam[2] generated by exploiting the non-linear Kerr effect of a polarisation maintaining fibre[3] [181–184]. To this state, we add a Gaussian distributed modulation, which can be seen as random displacements of the original state along either the x– or p–axis of phase-space with an overall Gaussian distribution. This state is considered as a classical state, and so represented by a convex mixture of coherent states. The first consideration of this scheme requires that the Gaussian modulation be primarily applied to the x–quadrature of the input state. This generation of discord is in contrast to all previous discord experiments such as [185–187]. This modulation is applied by an electro-optical modulator (EOM)[4] and adjusted via the half-wave plate such that the modulation occurs along the $\hat{S}_\theta$-axis[5], i.e., the x–axis. A quarter-waveplate after the EOM is necessary to compensate for the residual birefringence of the EOM without an applied voltage. The second scenario is essentially the same but with the vital difference that the initial prepared state is a pure coherent state denoted as $\rho_A^{0,coh}$ which stems directly from the pump source, which is a soliton laser.

Note that in this scheme, the modulation of the input modes in the $(x - p)$ plane

[2]The concept of squeezing can be translated to other variables such as the polarisation of light, such that the intuitive idea of squeezing implies that polarisation fluctuations are reduced below some prescribed level.

[3]The Kerr effect is the case where the electric field is a result of the light itself. This causes a variation in refractive index, proportional to the local irradiance of the light.

[4]An EOMs creates sidebands in a monochromatic laser beam. Imagine that a laser beam with frequency ω with the strength entering the EOM given by $Ae^{i\omega t}$ to which a sinusoidally varying potential voltage is applied with frequency Ω and small amplitude β. This will add a time-dependent phase to this expression such that $Ae^{i\omega t+i\beta\sin(\Omega t)}$.

[5]Stokes showed in Ref's. [188, 189] that a beam of light can be described completely by four parameters. Light is in general partially elliptically polarised, and the four parameters can be, for example, the size (I) and shape (M) of the ellipse, its orientation with respect to some fixed spatial axes (C), and the direction of rotation of the ellipse (S).

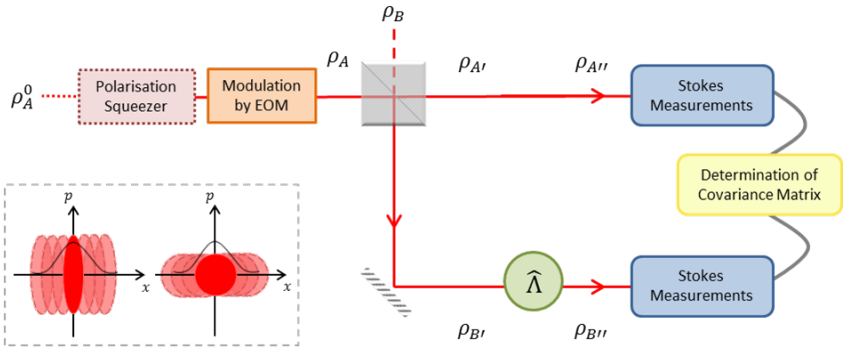

Figure 5.1: Mixed Gaussian state ρ_A prepared by Gaussian distributed modulation of pure coherent or squeezed state ρ_A^0, then mixed on a beamsplitter with a vacuum state ρ_B. Gaussian quantum discord between resulting bipartite state $\rho_{A'B'}$ is evaluated before and after the mode $\rho_{B'}$ undergoes the action of variable local loss $\hat{\Lambda}$ modelled by variable attenuation. Gaussian discord can grow under this local operation.

requires not only EOM, but involves also a down-mixing procedure and a post-processing of the measured data. By applying a sinusoidal voltage the birefringence of the EOM changes. With the help of a phase-matched electronic local oscillator, the modulation of the individual states is transformed into a displacement. In combining the measured data for differently displaced states appropriately, we prepare a Gaussian mixed state. The performed Stokes measurements allow the determination of its complete covariance, where the Stokes observable $\hat{S}_\theta$ is identified with $\hat{x}$ and $\hat{S}_{\theta+\pi/2}$ with $\hat{p}$.

The modulated state ρ_A, whether it be originally squeezed or coherent, is then superimposed on a beamsplitter with a vacuum state, labelled as state ρ_B. The input mixed state ρ_A and vacuum state ρ_B read in covariance matrix form as,

$$\gamma_A = \begin{pmatrix} V_x & 0 \\ 0 & V_p \end{pmatrix} \quad \text{and} \quad \gamma_B = \mathbb{1}, \tag{5.1}$$

where the quadrature variances are defined as $V_x = 2\langle(\Delta x_A)^2\rangle$ and $V_p = 2\langle(\Delta p_A)^2\rangle$ with $V_x V_p \geq 1$, encompassing both the original variances and the addition due to modulation. The composite system is constructed as the direct sum of subsystems, i.e. $\gamma_{AB} = \gamma_A \oplus \gamma_B$, which is a solely classically correlated bipartite mixed state (since all non-product Gaussian states were proved to possess non-zero Gaussian discord [133, 190]). The beamsplitter interaction is described by the symplectic transformation, Eq. (2.58), as

$$\hat{U}_{AB} = \begin{pmatrix} T\mathbb{1} & R\mathbb{1} \\ R\mathbb{1} & -T\mathbb{1} \end{pmatrix}, \quad \text{with} \quad T^2 + R^2 = 1, \tag{5.2}$$

with T and R are the transmittivity and reflectivity, respectively. As a direct result of the specifically chosen modulation, in the case of ρ_A^{sq} the initial squeezing is destroyed and any opportunity of entanglement creation between a modulated squeezed state and vacuum following a beamsplitter interaction is prevented. Alternatively, an interaction of

a coherent state ($\rho_A^{0,coh}$) and vacuum state should yield a bipartite classical state, however, modulation leads to the emergence of a separable non-classical state. Gaussian quantum discord is thus present between output modes for both cases of input state, ρ_A. Note also that following [137], for this bipartite state, Gaussian quantum discord corresponds to true quantum discord (see Appendix A). It can be interpreted that the quantumness of the post-interaction bipartite state originating from $\rho_A^{0,coh}$ can be seen as enhanced by modulation and the quantumness of the state originating from $\rho_A^{0,sq}$ seen to be dampened.

From a quantum optical perspective this is not as intuitive since the modulated state and vacuum state are seen as being purely classical objects, defined as such by a positive $\mathcal{P}$-function for mixed states and a positive delta $\mathcal{P}$-function for a vacuum state. Thus a unitary operation should not yield a non-classical object. Formally, this result is rather anticipated since in the language of covariance matrices any introduction of modulation (or squeezing) on ρ_A will result in non-zero x and/or p covariance terms between systems, and hence non-zero Gaussian quantum discord. The discussion of differing classicality definitions has been covered in Chapter 4.

The covariance matrix of the output state of the beamsplitter interaction, denoted as $\gamma_{A'B'}$, is thus given by $\gamma_{A'B'} = \hat{U}_{AB}\gamma_{AB}\hat{U}_{AB}^{\top}$,

$$\gamma_{A'B'} = \begin{pmatrix} \alpha & \sigma \\ \sigma^{\top} & \beta \end{pmatrix} = \begin{pmatrix} T^2\gamma_A + R^2\mathbb{1} & TR(\gamma_A - \mathbb{1}) \\ TR(\gamma_A - \mathbb{1}) & R^2\gamma_A + T^2\mathbb{1} \end{pmatrix}. \tag{5.3}$$

In order to study the effect of loss on separable non-classical states, subsystem $\rho_{B'}$ will undergo the action of a controlled local loss modelled by variable attenuation (beamsplitter interaction with a variable ratio, superimposing $\rho_{B'}$ and a vacuum state). The covariance matrix, $\gamma_{A''B''}$, representing the final state is then measured and is of the form,

$$\gamma_{A''B''} = \begin{pmatrix} T^2\gamma_A + R^2\mathbb{1} & \tau TR(\gamma_A - \mathbb{1}) \\ \tau TR(\gamma_A - \mathbb{1}) & \tau^2(R^2\gamma_A + T^2\mathbb{1}) + \rho^2\mathbb{1} \end{pmatrix}. \tag{5.4}$$

where τ and ρ are the transmittivity and reflectivity of the second beamsplitter modelling local loss $\hat{\Lambda}$ as shown in Fig. 5.1. This is the final measured covariance matrix, noting that the attenuation on subsystem B' can be modelled by adjusting τ such that when $\tau = 1$, $\gamma_{A''B''}$ corresponds to $\gamma_{A'B'}$ since the beamsplitter is essentially removed. Next let us draw attention to a number of imperfections within the experimental setup that were explored and modelled.

5.1.2 Dissipation and Imperfections

Noise and losses are introduced into the system by a number of possible sources. The scheme is designed with two intentional and controlled sources, these are:

- The modulation of the initial state modelled as an increase of the input quadrature variances, V_x, in subsystem A before the first beamsplitter.
- The local loss applied to subsystem $\rho_{B'}$ denoted as $\hat{\Lambda}$ in Fig. 5.1, and modelled as a

beamsplitter interaction with a vacuum state with a variable attentuation defined as $Att = \rho^2 = 1 - \tau^2$.

There are however some unintentional experimental losses which result in rather significant impacts. These are present due to:

- An apparent additional noise due to propagation of the light mode through the squeezing fibre added to the non-squeezed quadrature of the initial state. This is modelled as an increase of the concerned quadrature variance i.e., V_p, such that the exponential relationship in Eq. (2.57) no longer exists.

- Imperfect common mode rejection (CMR). Common mode rejection refers to the rejection of unwanted input signals common to both input modes. Imperfections in this process will lead to residual noise present in both output modes of the beamsplitter involved in homodyne detection (see Section 2.3.1).

  In mode A, measuring the photo-current difference should cancel out any noise. However, if this is not done perfectly, there will be some residual excess noise introduced. Therefore the measured quadrature is, $\hat{x}_A = \hat{x}_{A,p} + \hat{x}_{A,N}$, where $\hat{x}_{A,p}$ is the quadrature that would be measured with perfect CMR and $x_{A,N}$ is the excess noise. The imperfect CMR will be the same in both modes, so $2\langle(\Delta\hat{x}_{A,N})^2\rangle = 2\langle(\Delta\hat{x}_{B,N})^2\rangle = a$. Also, there is no feasible explanation for the imperfectly cancelled noise in mode A to be correlated to that in mode B, therefore $2\langle\Delta\hat{x}_{A,N}\ \Delta\hat{x}_{B,N}\rangle = 0$.

  Common mode rejection is modelled as linearly decreasing with attenuation and therefore is introduced as,

$$\gamma_{A''B''} \to \gamma_{A''B''} + \gamma^N_{A''B''}, \quad \text{where} \quad \gamma^N_{A''B''} = \begin{pmatrix} a\mathbb{1} & 0_2 \\ 0_2 & \tau^2 a\mathbb{1} \end{pmatrix}, \tag{5.5}$$

  where $\gamma_{A''B''}$ is given by Eq. (5.4) and 0_2 is the 2×2 null matrix. Imperfect CMR will linearly decrease with attenuation since attenuation is carried out on mode B, and so the excess noise is also attenuated. Therefore the measured quadrature is, $\hat{x}_B = \hat{x}_{B,p} + \tau\hat{x}_{B,N}$. Combining all this gives an addition to the elements of the theoretical covariance matrix as $\gamma^N_{1,1} = a$, $\gamma^N_{3,3} = \tau^2 a$, and $\gamma^N_{1,3} = 0$.

- In addition to imperfect shot noise calibration, there is a statistical error in the measurement of the Stokes observables performed for the determination of the covariance matrices and Duan's separability criterion [80] made use of later. To analyse these errors the results of the measurements performed on pure coherent states are compared to the theoretical expectations. With the use of Monte-Carlo simulations the discrepancies are used to estimate the errors in the further determined quantities, for example the Gaussian quantum discord. The possible errors are shown as error bars in Fig.'s 5.2, and reflect both the error in the calibration as well as the statistical error.

  We must assume that any additional systematic error must be present due to further imperfections in the measurement system, as well as due to the modulation performed by the EOM and drifts in the setup over the long measurement times. As a

result, the elements of the covariance matrix deviate from what we would expect theoretically. This also applies to the eigenvalues of the covariance matrices. Both for the states $\rho_A^{0,coh}$ and $\rho_A^{0,sq}$ we found the lowest eigenvalue after PPT give $\tilde{nu}_- < 1$, indicating weak global squeezing in the bipartite state $\rho_{A'B'}$, which indicates an inseparable state. This appears surprising since the state prepared by displacing coherent states is separable and classical by construction. Moreover, the squeezing in the mixed state prepared from a squeezed state is reliably destroyed due to the amount of imprinted modulation. Thus, the eigenvalue lower than 1 is clearly an artefact of a systematic error present in the setup.

An attempt was held in order to justify and correct natural imperfections inherent in determining an experimental covariance matrix which caused theoretically null elements to be measured as non-zero. Two linked imperfections where considered to explain these entries, but were found to not play a significant role, and were subsequently excluded. The considered imperfections were:

- Measurement of slightly rotated quadratures when constructing the covariance matrix $\gamma_{A'B'}$. The measurement can be modelled by phase shifts as in Eq. (2.56),

$$\hat{U}_j(\theta_j) = \begin{pmatrix} \cos\theta_j & \sin\theta_j \\ -\sin\theta_j & \cos\theta_j \end{pmatrix}, \tag{5.6}$$

  performed on modes A' and B' followed by measurement of the correct quadratures. The phase shifts give

$$\gamma_{A'B'} = \begin{pmatrix} \hat{U}_A \alpha \hat{U}_A^\top & \hat{U}_A \sigma \hat{U}_B^\top \\ \hat{U}_B \sigma^\top \hat{U}_A^\top & \hat{U}_B \beta \hat{U}_B^\top \end{pmatrix}. \tag{5.7}$$

  If the phase shifts $\hat{U}_{A,B}^\top$ are chosen such that they diagonalise all of the sub-blocks of the covariance matrix, then it is clear that the appearance of non-zero elements $\gamma_{1,2}, \gamma_{1,4}, \gamma_{2,3}$ and $\gamma_{3,4}$ arise from the measurement of rotated quadratures.

- *Phase fluctuations* are present meaning that instead of mixing a state ρ_A with covariance matrix (5.1) on a beam splitter, we mix a state,

$$\rho_A^\varphi = \int P(\varphi)\hat{U}(\varphi)\rho_A\hat{U}^\dagger(\varphi)d\varphi, \tag{5.8}$$

  where $P(\varphi)$ is the distribution of the random phase and $\hat{U}(\varphi)$ is the operator of the phase shift. Typically, P is Gaussian with the mean $\langle\varphi\rangle$, the variance $\langle(\Delta\varphi)^2\rangle$, and the integration is performed over the entire real axis. The elements of the corresponding

covariance matrix can be expressed as

$$\begin{aligned}\gamma_{ij}^{\varphi} &= \mathrm{Tr}[(\xi_i\xi_j + \xi_j\xi_i)\rho_A^{\varphi}] \\ &= \int P(\varphi)\mathrm{Tr}[(\xi_i\xi_j + \xi_j\xi_i)\rho_A(\varphi)]d\varphi \\ &= \int P(\varphi)(\gamma_A(\varphi))_{ij}d\varphi,\end{aligned} \tag{5.9}$$

where $\gamma_A(\varphi) = \hat{U}(\varphi)\gamma_A\hat{U}^{\top}(\varphi)$ is the rotated covariance matrix (5.1). The modulation causes tilting in the squeezed ellipsis. The larger the modulation the more prominent the tilt. Since the modulated state is a mixture of states with the positive displacements of the position quadrature we mix states with a different non-zero tilt and hence our phase distribution has a non-zero mean $\langle\varphi\rangle \neq 0$. Assuming only a small tilt we can expand the trigonometric functions in $\gamma_A(\varphi)$ as $\cos(\varphi) = 1-\varphi^2/2$ and $\sin(\varphi) = \varphi$. Excluding terms greater than second order we get:

$$\gamma_A^{\varphi} = \begin{pmatrix} V_x(1-\langle\varphi^2\rangle) + V_p\langle\varphi^2\rangle & (V_p - V_x)\langle\varphi\rangle \\ (V_p - V_x)\langle\varphi\rangle & V_p(1-\langle\varphi^2\rangle) + V_x\langle\varphi^2\rangle \end{pmatrix}. \tag{5.10}$$

If we require $\sigma_{12} = \sigma_{21}$, where σ_{ij} are the matrix elements of the sub-block σ of $\gamma_{A'B'}$, we can compensate the unwanted angles of rotation of measured quadratures, this requirement is satisfied if:

$$\tan(\theta_A - \theta_B) = \frac{\sigma_{12} - \sigma_{21}}{\sigma_{11} + \sigma_{22}}, \tag{5.11}$$

which of course should be zero in an ideal case.

In fully describing the preparation of the state and the possible imperfections included in the scheme, it is now appropriate to begin our analysis of the effect of discord increase under the action of local loss, and a number of ways in which the effect may be amplified.

5.1.3 Scheme Analysis and Optimisation

After allowing the systems ρ_A and ρ_B to interact, the resultant bipartite state, $\rho_{A'B'}$, was found to exhibit a counter-intuitive increase of Gaussian discord as the local loss was applied and increased on one subsystem. This implies that if the noisy channel is intensified, the quantumness of the system is not only hugely robust, but actually appears to strengthen, contrary to expectations. The local loss is realised by a variable attenuation on $\rho_{B'}$ denoted as $\hat{\Lambda}$ in Fig. 5.1, where maximum attenuation would correspond to $\rho_{B'}$ being fully absorbed. Gaussian discord was calculated using the formulation introduced in Section 4.1.1 and in Ref. [133]. Results of this for both squeezed and coherent states are presented in Fig. 5.2 (left) and Fig. 5.2 (right), respectively. Focusing on the scenario with an initial state ρ_A^{sq} with quadrature variances $V_x = 9.84$ and $V_p = 38.4$, depicted by a blue solid line, with corresponding experimental results and associated statistical errors. Note that although discord

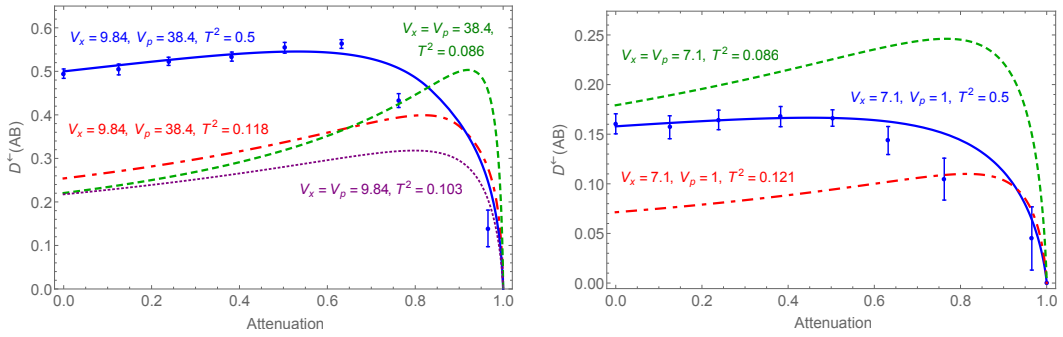

Figure 5.2: (left) Gaussian quantum discord versus attenuation in mode $\rho_{B'}$ for modulated squeezed state. Theory curve (blue solid) and experiment (blue dots) for modulation in $\hat{x}$-quadrature, $V_x = 9.84$, $V_p = 38.4$ and $T^2 = 0.4982$. Theory curves: for the same input and $T^2 = 0.14$ (red dot-dashed); for $V_x = V_p = 38.4$ and $T^2 = 0.081$(green dashed); for $V_x = V_p = 9.84$ and $T^2 = 0.085$ (purple dotted).
(right) Gaussian quantum discord versus attenuation in mode $\rho_{B'}$ for modulated coherent state. Theory curve (solid blue) and experiment (blue dots) for modulation in $\hat{x}$-quadrature, $V_x = 7.1$, $V_p = 1$ and $T^2 = 0.5006$. Theory curves for the same input state and $T^2 = 0.16$ (red dot-dashed) and for modulation in both quadratures, $V_x = V_p = 7.1$, and $T^2 = 0.08$ (green dashed).

increase is seen for both ρ_A^{sq} and ρ_A^{coh}, the achievable discord when implementing a coherent state is significantly lower than the squeezed state scenario. This can be attributed to the quantumness of the state being introduced by the squeezing and the imprinted modulation preventing the creation of a quantum state (containing quantum entanglement) rather than creating quantumness from a classical state, as in the coherent state scenario.

Let us first attempt a better understanding of the optimal conditions under which the effect is most pronounced. This can be done by generalising the scheme and considering two hypothetical cases;

i The asymmetric case where ρ_A is modulated in one quadrature only.

ii The symmetric case where ρ_A is modulated equally in both quadratures.

Note that whether ρ_A^0 is prepared as a squeezed or coherent state is irrelevant as both of the above cases can be constructed from either. Fig.'s 5.2 show the discord in the theoretical model with corresponding experimental results (blue), with the most influential of the aforementioned imperfections implemented (i.e., CMR)[6], for a squeezed (left) and coherent (right) input states. Although the Gaussian discord value and relative increase can be enhanced by increasing the modulation in the x-quadrature, this however will only improve the effect to a small degree. At further inspection it appears that having a symmetric input state will lead to a more pronounced Gaussian discord increase (see green dashed curves in Fig.'s 5.2). This appears to only be true provided that the quadrature variances in the symmetric input state do not fall below that of the smallest quadrature variance of the asymmetric input state, e.g., if the asymmetric state has variances $V_x = 10$ and $V_p = 40$ then the use of

[6]Not all of the imperfections could be included into the model as this proved to be computationally exhaustive.

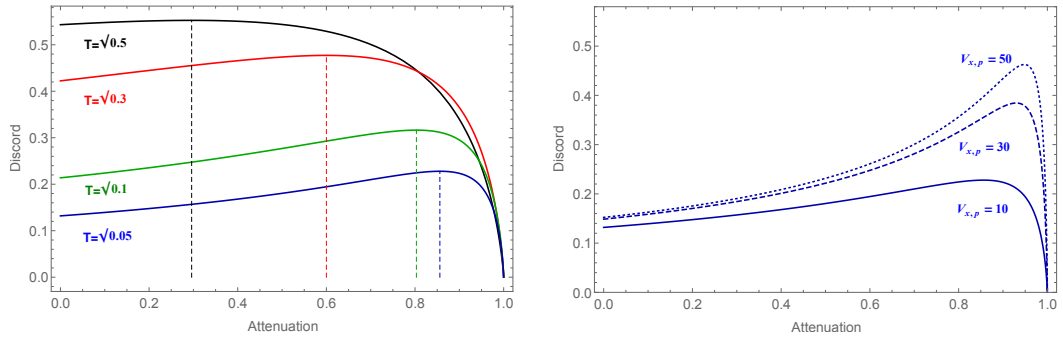

Figure 5.3: (left): (Solid lines) Gaussian quantum discord versus attenuation in mode $\rho_{B'}$ for symmetric input state ρ_A with $V_x = V_p = 10$, for different beamsplitter ratios; (black) $T = \sqrt{0.5}$, (red) $T = \sqrt{0.3}$, (green) $T = \sqrt{0.1}$ and (blue) $T = \sqrt{0.05}$. Dashed lines indicate the corresponding attenuation at which maximum discord is achieved for each case.
(right): Gaussian quantum discord versus attenuation in mode $\rho_{B'}$ for symmetric input state ρ_A with $T = \sqrt{0.05}$, for different variances; (solid) $V_x = V_p = 10$, (dashed) $V_x = V_p = 30$ and (dotted) $V_x = V_p = 50$.

a symmetric state is only advantageous provided that it has variances $V_x = V_p > 10$. As the symmetric modulation is increased, the overall Gaussian discord value and growth due to increased attenuation will increase and converge to an optimal value. This is rather intuitive as Gaussian discord is fundamentally connected to the non-compatibility of observables, so modulation in both quadratures should be preferable to achieve greater Gaussian discord.

It is interesting to note that the Gaussian discord increase can be further improved by preparing the output state of the beamsplitter, $\gamma_{A'B'}$, such that the subsystems are maximally indistinguishable. The obvious method of doing so is to instead implement an asymmetric beamsplitter i.e., $T < 1/\sqrt{2}$. In fact we can conclude that a highly asymmetric beamsplitter proves to provide the best case of Gaussian discord increase[7] (see Fig. 5.3 (left)). However, note that as the beamsplitter becomes more asymmetric, the overall level of Gaussian discord lowers. An increase in the overall level is only achievable at stronger levels of modulation, and hence larger variances (see Fig. 5.3 (right)). Also, the degree of attenuation where the maximum discord value is achieved is in general inversely proportional to the beamsplitter ratio, i.e., as the transmittivity is lowered, the point where maximum discord is present, appears at stronger attenuations, as seen by the dashed lines in Fig. 5.3 (left).

Since the local loss is applied to subsystem $\rho_{B'}$ only, the total variance (V_x and V_p) of the mode will always decrease with increasing local loss. When an optimised asymmetric beamsplitter is implemented, the total variance of mode $\rho_{B'}$ will decrease more dramatically as $Att \to 1$. The higher the rate of decrease of the total variance of $\rho_{B'}$ with respect to the level of local loss, the more pronounced the increase of the Gaussian discord. The maximum value of Gaussian discord in each case is obtained as the total variances of $\rho_{A'}$ and $\rho_{B'}$ become less distinguishable. In the optimised asymmetric beamsplitter case the variances

[7]Optimisation of the beamsplitter ratio is done on the basis of maximising the possible increase of Gaussian quantum discord.

of $\rho_{A'}$ and $\rho_{B'}$ are converging, as opposed to the case of a balanced beamsplitter, where the variances of states diverge from one another. This is seen for all possible input states.

In summary, since Gaussian states such as $\rho_{A'B'}$ are convex mixtures of non-orthogonal over complete coherent basis states, the impossibility to deterministically discriminate between them is a seminal example of quantumness in separable bipartite states. Thus, intuitively the discord growth under the action of local loss can be attributed to these non-orthogonal basis states becoming less distinguishable with attenuation, modelled by a large symmetric initial variance in ρ_A and a highly asymmetric beamsplitter such that most of the input mode A is reflected into the attenuated mode B'. Although it is difficult to reduce the mechanism behind this effect to a simple single phenomenon since in Ref.'s [131, 159, 191] it has been explained without the use of orthogonality arguments. This is remarkable since asymmetrising the beamsplitter will clearly significantly reduce the level of discord, but an increase of local loss can counteract this negative impact and restore the discord to levels seen for a symmetric beamsplitter.

An increase of Gaussian quantum discord $\mathcal{D}^{\leftarrow}(\rho_{A'B'})$ with growing loss on one subsystem $\rho_{B'}$ was only recently first demonstrated by Madsen *et al.* [185]. In this the authors only considered a symmetrically modulated coherent state. However, the discord increase was remarkably pronounced and unlike anything achievable with the basic theoretical model implied in the article. A probable explanation is that a highly asymmetric beamsplitter was modelled, and then attributed to a limited balancing of the homodyne detectors — although no indication of the type or degree of noise was discussed. Fig. 5.4 illustrates how similar results are achievable when implementing an asymmetric beamsplitter for variances provided ($V_x = V_p = \langle n \rangle$). Note that slight differences will be largely attributed to the estimation of the discord value at zero attenuation. The inset shows for comparison the noiseless model with a balanced beamsplitter for the same variances. Thus an asymmetric beamsplitter (or noise simulating the same effect) has an essential role in amplifying the feature of discord increase under local loss which cannot be attributed to varying modulation alone. This acts to reinforce our analysis that a decreased discord caused by imperfections can be regained by introducing controlled local loss.

Recently, Marian *et al.* examined the decay of quantum correlations in a two-mode squeezed thermal state in contact with a local thermal reservoir. Two measures of quantum correlations were compared, namely the entanglement of formation and the quantum discord. One of the cases considered was when a single reservoir acts on one mode only. From this it was shown that in the evolution of the Gaussian quantum discord, when it is defined by local measurements on the attenuated mode and the input state is mixed, the discord can increase in time above its initial value. This enhancement of discord was seen to be stronger for zero-temperature reservoirs and increases with the degree of input mixing [192].

In the following Section the bipartite mixed state $\rho_{A'B'}$ will be expanded to its globally pure system. This will allow further insight into how classical and non-classical correlations flow throughout the system in order to seek an explanation of the unexpected effect of discord increase under the action of local loss.

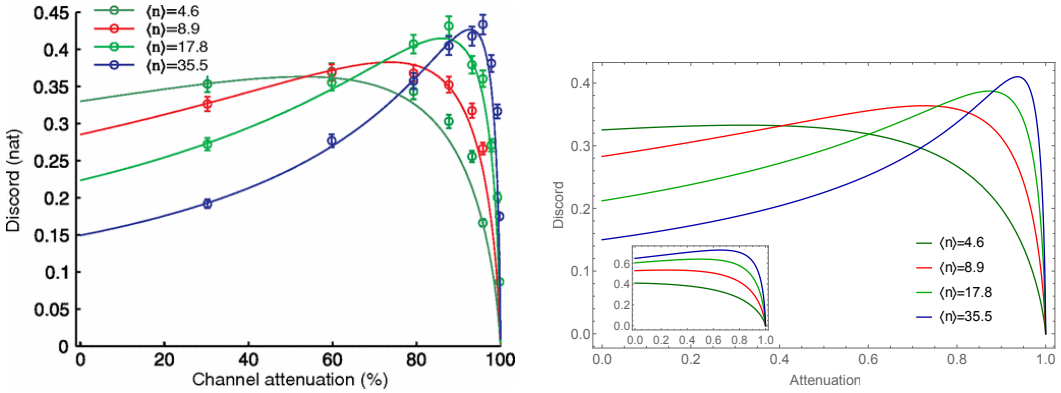

Figure 5.4: (left) Discord increase for varying levels of symmetrically modulated input state as presented in [185]. (right) Comparison using theoretical model presented above for matching levels average photon number $\langle n \rangle$ and fitted using zero attenuation point (left). The curves are achieved when beamsplitter is highly asymmetric, $\langle n \rangle = 35.5, T^2 = 0.05$, $\langle n \rangle = 17.8, T^2 = 0.09$, $\langle n \rangle = 8.9, T^2 = 0.16$ and $\langle n \rangle = 4.6, T^2 = 0.29$. Inset: symmetric beamsplitter case for same average photon numbers.

5.2 Flow of correlations in Global System

The previous Section sought to explain the factors which appear to most significantly affect the gain of Gaussian discord from local loss, and how is it possible to optimise this gain. In contrast, this Section will aim to provide insight to the source of these additional correlations as a flow of hidden correlations within a larger global system.

It is clear from the construction of the state that $\gamma_{A'B'}$ must possess two symplectic eigenvalues of the form $\nu_{A'} = \sqrt{\det \gamma_{A'}} = \sqrt{V_x V_p}$ and $\nu_{B'} = 1$. Alternatively, the eigenvalues can be calculated from Eq. (2.72). The purification process can be thought of as the search for the necessary additional quantum system required to expand a mixed state to a larger pure state system. Due to this, and since system ρ_B is already pure, the purification of the state involves the addition of one extra system in order to purify ρ_A, i.e., the purification of $\rho_{A'B'}$ is tripartite. The third purifying subsystem $\rho_{E'}$ is then interpreted as the environment and the purification is obtained by characterising the input state, ρ_A, as a subsystem of a two-mode squeezed thermal state $|\psi_{TMSTS}\rangle_{AE}$ (Eq. 2.60) with the covariance matrix

$$\gamma_{AE}^{(TMSTS)} = \begin{pmatrix} a\mathbb{1} & c\sigma_z \\ c\sigma_z & a\mathbb{1} \end{pmatrix}, \tag{5.12}$$

where

$$\begin{aligned} a &= \cosh(2r) = \nu_{A'} = \sqrt{V_x V_p}, \\ c &= \sinh(2r) = \sqrt{\nu_{A'}^2 - 1} = \sqrt{V_x V_p - 1}, \end{aligned} \tag{5.13}$$

r is the squeezing parameter and σ_z is the Pauli diagonal matrix. Thus the state ρ_{ABE} is pure.

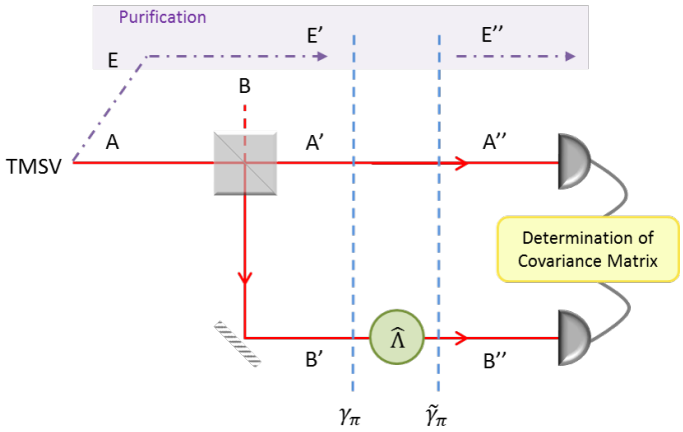

Figure 5.5: Subsystem ρ_A taken as subsystem of a TMSTS ρ_{AE}, then prepared by Gaussian distributed modulation and is split up on a beamsplitter. The Gaussian quantum discord between resulting modes $\rho_{A'}$ and $\rho_{B'}$ is evaluated before and after the mode $\rho_{B'}$ undergoes the action of variable local loss modelled by variable attenuation. Gaussian discord can grow under this LO. Two purifications must be performed before and after local noise, denoted γ_π and $\tilde{\gamma}_\pi$, these involve two different "environmental" modes, E' and E'', respectively.

Following the purification process outlined in Section 2.3.2 we apply now a symplectic transformation S^{-1} to modes A' and B', such that S symplectically diagonalises $\gamma_{A'B'}$, i.e., $S\gamma_{A'B'}S^\top = (\nu_{A'}\mathbb{1}) \oplus \mathbb{1}$ and satisfies the symplectic condition $S\Omega S^\top = \Omega$. The transformation S will read as

$$S = (S_A \oplus \mathbb{1})\hat{U}_{AB}^\top, \quad S_A = \begin{pmatrix} \sqrt[4]{\frac{V_p}{V_x}} & 0 \\ 0 & \sqrt[4]{\frac{V_x}{V_p}} \end{pmatrix}, \tag{5.14}$$

where $\hat{U}_{AB}$ a beamsplitter transformation given by Eq. (5.2). Therefore the covariance matrix of the purification then reads:

$$\gamma_\pi = \begin{pmatrix} \gamma_{A'B'} & D \\ D^\top & \nu_{A'}\mathbb{1} \end{pmatrix}, \quad \text{where} \quad D = \sqrt{\nu_{A'}^2 - 1}\begin{pmatrix} TS_A^{-1}\sigma_z \\ RS_A^{-1}\sigma_z \end{pmatrix}. \tag{5.15}$$

This purification then satisfies the cyclic purity condition $\mathrm{Det}(\gamma_{ij}) = \Delta_{ij} - 1$ given in Eq. (2.75).

In the next step of the scheme, mode B' of the state $\rho_{A'B'}$ is subjected to a local variable attenuation, modelled by superimposing $\rho_{B'}$ with a vacuum mode on a beamsplitter. We require the global system to consistently comprise of three systems, as we wish to ultimately use the Koashi-Winter equality (see Section 4.4) valid for tripartite pure systems. Since the attenuation is modelled with the addition of another vacuum mode, a second purification is required modelling the global state again as tripartite. This proved to be slightly more complex, but essentially required following the same process as above. The final bipartite

mixed composite state possesses a covariance matrix of the form:

$$\gamma_{A''B''} = \begin{pmatrix} \alpha' & \sigma' \\ \sigma'^{\top} & \beta' \end{pmatrix}, \tag{5.16}$$

with $\alpha' = \alpha$, $\beta' = \tau^2\beta + \rho^2\mathbb{1}$, and $\sigma' = \tau\sigma$, as presented in Eq. (5.4). Consequently, Eq.'s (2.72) reveals that $\nu_{B''} = 1$ and

$$\nu_{A''} = \sqrt{(T^2 + \tau^2R^2)^2 v_x v_p + (T^2 + \tau^2R^2)(v_x + v_p) + 1}, \tag{5.17}$$

where $v_{x,p} = V_{x,p} - 1$. Thus, the state $\gamma_{A''B''}$ has again only a tripartite purification. The purification can be constructed exactly as in the case of the covariance matrix (5.12).

First, a matrix $\tilde{S}$ must be found that symplectically diagonalises $\gamma_{A''B''}$. The matrix attains the form $\tilde{S} = \tilde{H}(\tilde{S}_A \oplus \tilde{S}_B)$, where $\tilde{S}_A = \mathrm{diag}(\lambda, 1/\lambda)$ and $\tilde{S}_B = \mathrm{diag}(\mu, 1/\mu)$. Here λ and μ are defined as,

$$\lambda = \sqrt[4]{\frac{T^2 v_p + 1}{T^2 v_x + 1}} \quad \text{and} \quad \mu = \sqrt[4]{\frac{\tau^2 R^2 v_p + 1}{\tau^2 R^2 v_x + 1}}, \tag{5.18}$$

acting as local squeezing transformations bringing the covariance matrix (5.16) into the standard form as seen in Eq. (2.70), with

$$\begin{aligned} \tilde{a} &= \sqrt{(T^2 v_x + 1)(T^2 v_p + 1)}, \\ \tilde{b} &= \sqrt{(\tau^2 R^2 v_x + 1)(\tau^2 R^2 v_p + 1)}, \\ \tilde{c}_1 &= \tau T R \lambda \mu v_x, \quad \tilde{c}_2 = \frac{\tau T R v_p}{\lambda \mu}. \end{aligned} \tag{5.19}$$

From this, the symplectic matrix $\tilde{H}$ symplectically diagonalises the standard form (5.19). By introducing the auxiliary parameters $M \equiv \tilde{a}\tilde{c}_1 + \tilde{b}\tilde{c}_2 \neq 0$, $L_A \equiv -(\tilde{a}^2 + \tilde{c}_1\tilde{c}_2 - 1)$, and $L_B \equiv \tilde{b}^2 + \tilde{c}_1\tilde{c}_2 - 1$, the matrix can be expressed in the form [193]

$$\tilde{H} = \sqrt{2} \begin{pmatrix} x_1 & 0 & x_2 & 0 \\ 0 & x_3 & 0 & x_4 \\ x_5 & 0 & x_6 & 0 \\ 0 & x_7 & 0 & x_8 \end{pmatrix}, \tag{5.20}$$

where the elements x_n are defined using the auxiliary parameters as,

$$x_1 = -\frac{(\tilde{a}L_A - \tilde{c}_2 M)x4}{M\nu_{A''}}, \qquad x_5 = -\frac{(\tilde{a}L_A - \tilde{c}_2 M)x_8}{M\nu_{B''}},$$
$$x_2 = \frac{(\tilde{b}M - \tilde{c}_2 L_B)x_4}{M\nu_{A''}} \qquad x_6 = \frac{(\tilde{b}M - \tilde{c}_2 L_B)x_8}{M\nu_{B''}},$$
$$x_3 = -\frac{L_A x_4}{M}, \qquad x_7 = -\frac{L_B x_8}{M},$$
$$x_4 = \frac{\sqrt{-\frac{M^2\nu_{A''}}{-\tilde{a}L_A^2 - \tilde{b}M^2 + 2\tilde{c}_2 L_A M}}}{\sqrt{2}}, \qquad x_8 = \frac{\sqrt{-\frac{M^2\nu_{B''}}{-\tilde{a}L_B^2 - \tilde{b}M^2 + \tilde{c}_2 L_B M}}}{\sqrt{2}}.$$

Hence, the purification of the state $\gamma_{A''B''}$ after the attenuating beamsplitter is of the form:

$$\tilde{\gamma}_\pi = \begin{pmatrix} \gamma_{A''B''} & \tilde{D} \\ \tilde{D}^\top & \nu_{A''}\mathbb{1} \end{pmatrix}, \quad \text{where} \quad \tilde{D} = \sqrt{\nu_{A''}^2 - 1}\tilde{S}^{-1}\begin{pmatrix} \sigma_z \\ 0_2 \end{pmatrix}. \tag{5.22}$$

From the latter purification constructed here, it is possible to analyse the system as a whole as opposed to a mixed subsystem. Note that the second purification $\tilde{\gamma}_\pi$ when $\tau = 1$ is equivalent to the first purification γ_π since it is models the situation where the second beamsplitter is essentially removed. It is now possible to investigate the change of several fundamental quantities under local attenuation, and connect these quantities using the Koashi-Winter inequality defined in Section 4.4. However, before doing so, we must discuss the significance of entropy usage.

Entropic Measure Selection

In Fig. 5.6 the Gaussian entanglement of formation (defined in Section 3.3.3) is shown for squeezed and coherent states, calculated using both the Rényi-2 and von Neumann entropies, using the variance values used in Fig. 5.2. The entanglement between system $\rho_{A'}$ and the environment will always increase with local loss. It is interesting also to note that any quantity utilising the von Neumann entropy will act as an upper bound for Rényi-2 entropy case i.e., $\mathcal{S}_1(\rho) \geq \mathcal{S}_2(\rho) \geq \ldots \geq \mathcal{S}_\infty(\rho)$ since

$$\mathcal{S}_2(\rho) = -\ln \mathrm{Tr}[\rho^2] \leq -\mathrm{Tr}[\rho \ln \rho] = \mathcal{S}_1(\rho) \tag{5.23}$$

for any physical state represented by the density matrix ρ.

As discussed in Section 4.3, non-classicality criteria can vary for Gaussian states in respect to which entropy is used in defining Gaussian quantum discord, since classicality is defined by zero discord. When using von Neumann entropy, a completely classical state in an information theoretic context, with zero Gaussian discord, is seen to possess a covariance matrix in product form i.e., having no x or p correlations between subsystems ($c_+, c_- = 0$ of the standard form). Now, when using the Rényi-2 entropy, the same bipartite state will be seen to be completely classical when there exists *either* no position or no momentum correlations between subsystems, i.e., $c_+ = 0$ or $c_- = 0$). Thus the classicality criteria

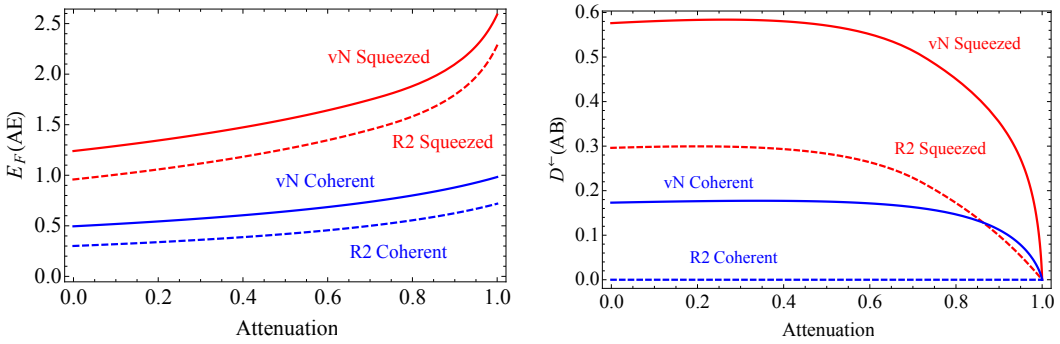

Figure 5.6: (left) Gaussian entanglement of formation $\mathcal{E}_F(\rho_{AE})$ with growing attenuation for squeezed (red) and coherent (blue) Gaussian modulated input state for Rényi (solid) and von Neumann (dashed) entropies. Squeezed state: $V_x = 9.84$, $V_p = 38.4$ and $T^2 = 0.4982$. Coherent: $V_x = 7.1$, $V_p = 1$ and $T^2 = 0.5006$.
(right) Gaussian discord $\mathcal{D}^{\leftarrow}(\rho_{AB})$ with growing attenuation for squeezed (red) and coherent (blue) Gaussian modulated input state for Rényi (solid) and von Neumann (dashed) entropies. Squeezed state: $V_x = 9.84$, $V_p = 38.4$ and $T^2 = 0.4982$. Coherent: $V_x = 7.1$, $V_p = 1$ and $T^2 = 0.5006$.

according to Gaussian quantum discord as defined by Rényi-2 entropy is less sensitive than that of von Neumann entropy. Within the context of the scheme being discussed, if we consider the case where ρ_A is a Gaussian modulated coherent state, the output state of the beamsplitter $\gamma_{A'B'}$ will, according to the von Neumann definition of Gaussian discord, possess non-classical correlations. However, according to Rényi-2 entropy, the state will in fact be classical and thus possess zero Gaussian discord as seen in Fig. 5.6.

Due to this discrepancy, as well as discussions reflecting the optimality of Gaussian discord for von Neumann entropy in Ref. [137], for the remainder of this analysis, we shall solely focus on von Neumann definitions of fundamental constituents of the Koashi-Winter relation in Eq. (4.27). Although we have proven the equality to hold for either entropic measure for any arbitrary Gaussian state.

As previously mentioned, we make use of the Koashi-Winter inequality, which becomes an equality when dealing with globally pure tripartite systems. If we consider the permutation given in Eq. (4.27),

$$\mathcal{S}(\rho_A) = \mathcal{E}_F(\rho_{AE}) + \mathcal{J}^{\leftarrow}(\rho_{AB}), \tag{5.24}$$

we know that the marginal entropy of subsystem $\rho_{A'}$ will remain constant with growing attenuation since no interaction is being performed here. We also know that because we are introducing local loss on subsystem $\rho_{B'}$, and hence losing information about the system, the classical correlations within system $\rho_{A'B'}$ will decrease. Relying on conservation of correlations in a pure state we know then that the entanglement existing between $\rho_{A'E'}$ must increase in order for the equality to hold.

From Adesso *et al.* [93], the Gaussian entanglement of formation can be explicitly cal-

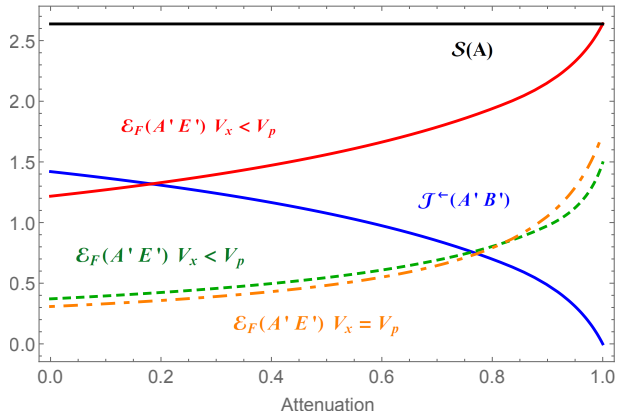

Figure 5.7: Components of Koashi-Winter equality against attenuation for squeezed initial state $V_x = 9.84$, $V_p = 38.4$ and $T^2 = 0.4982$: (black dot-dashed) marginal entropy of subsystem $\rho_{A'}$, (blue dashed) classical correlation in system $\rho_{A'B'}$, (red solid) Gaussian entanglement of formation between subsystem $\rho_{A'}$ and the environment $\rho_{E'}$. The perforated curves show system-environment EoF for same input state and $T^2 = 0.118$ (green dashed) and a symmetric input state with $Vx = Vp = 38.4$ and $T^2 = 0.086$ (orange dot-dashed).

culated as given by Eq. (3.19). Fig. 5.7 displays the constituents of the Koashi-Winter equality for a modulated squeezed input state (solid). From this it is clear that the quantum correlations between subsystem $\rho_{A'}$ and the environment increase monotonically as local loss is introduced to subsystem $\rho_{B'}$. This can be seen as intuitive since the quantum correlations will decrease between $\rho_{B'E'}$ as local loss is introduced, for both squeezed and coherent states, since local loss is applied to $\rho_{B'}$[8]. It then appears feasible that the additional non-classical correlation gained by $\rho_{A'B'}$, have been induced by the strengthening of entanglement between subsystem $\rho_{A'}$ and the environment, and that in performing a local operation on $\rho_{B'}$, a transfer of correlations occurs. The flow of correlations from the environment into a connected system has been discussed for qubits in [179] and Gaussian states in [177].

Comparing quantum discord and entanglement of formation one can clearly see that discord appears not to be a monotonically increasing function with respect to attenuation. The explanation behind this is that as the attenuation increases above approximately 60-90%[9] the system B' will become absorbed so that at maximum attenuation, the discord measured is between A' and the additional vacuum state, which will clearly be zero. The entanglement of formation will not be affected by this since it exists between system A' and the environment E'.

[8] Monotonically increasing system-environment entanglement is witnessed for squeezed and coherent state with both von Neumann and Rényi-2 entropies as seen in Fig. 5.6.

[9] The level of attenuation at which non-monotonic behaviour begins is dependent on the state as discussed earlier in reference to Fig. 5.3

5.3 Entanglement Recovery

We recall that if an unmodulated squeezed state is superimposed on a beamsplitter with a vacuum state, the resulting bipartite state will possess entanglement. In the scenario above, the creation of entanglement is prevented by the Gaussian distributed modulation. In this remaining Section a specialised scenario, depicted in Fig. 5.8, will be considered, in which an interaction of the system $\rho_{A'B'}$ with a separable environmental mode $\rho_{\tilde{E}}$ causes a partial elimination of the displacement noise and recovers entanglement between systems ρ_A and ρ_B[10]. The experimentally measured covariance matrix for the state $\rho_{A''B''}$ reads as

$$\gamma^{\mathrm{sq}}_{A''B''} = \begin{pmatrix} 5.42 \pm 0.05 & 0.23 \pm 0.02 & 4.06 \pm 0.03 & 0.04 \pm 0.01 \\ 0.23 \pm 0.02 & 19.28 \pm 0.17 & 0.45 \pm 0.01 & 17.29 \pm 0.15 \\ 4.06 \pm 0.03 & 0.45 \pm 0.01 & 4.73 \pm 0.04 & 0.55 \pm 0.02 \\ 0.04 \pm 0.01 & 17.29 \pm 0.15 & 0.55 \pm 0.02 & 17.70 \pm 0.16 \end{pmatrix}. \tag{5.25}$$

Despite the absence of local squeezing, the covariance matrix appears to exhibit a weak global squeezing. The squeezing occurs in the diagonal direction with respect to x and p quadratures and thus cannot originate from the input squeezing. We measure the covariance matrix of a state, which was created by mixing with vacuum state and therefore lies on the boundary of the set of squeezed states. Hence the effect of global squeezing can be attributed to the systematic error caused by drifts during the long measurement times of the covariance matrix. As a result of the lack of squeezing in the local covariance matrices we verify that the displacements in the direction of squeezing destroyed the squeezing. The non-zero off-diagonal entries of sub-block C may be attributed to the inconsistency of CMR in the different modes. The state of modes A and B is then inevitably separable [194] as witnessed by the non-negativity of the minimal eigenvalue, $\min\{\mathrm{eig}[(\gamma^{\mathrm{sq}}_{A'B'})^{(\top_A)} + i\Omega]\} = 0.84 \pm 0.02$. However the state contains quantum correlations as evidenced by Gaussian quantum discord $\mathcal{D}^{\leftarrow}(A'B') = 0.49 \pm 0.01$. The correlations originate from two sources, each have the capability to generate correlations independent of the other. First source is the random displacement $\bar{x}$ of the x-quadrature of the input mode ρ^0_A that yields quantum correlations between separable modes A' and B' exactly as in the case of coherent initial state. Secondly, the initial squeezing of mode ρ^0_A alone has the capacity to create entanglement between A' and B'.

As above, preparation of the state with covariance matrix (5.3) is achieved by splitting a randomly displaced squeezed input mode ρ_A on a beamsplitter. Imagine that encoded in the $\hat{x}$-quadrature of a separable system, $\rho_{\tilde{E}}$, is the random displacement $\bar{x}$ as

$$x_{\tilde{E}} \to x_{\tilde{E}} - \bar{x}. \tag{5.26}$$

In contrast to the previously considered purifying mode E, mode $\tilde{E}$ has been created by local operations and classical communication (LOCC) and hence it is separable from the subsystem. It is important to note that the exact level of displacement does not need to be known, the only essential constraint is that the displacements in ρ_A and $\rho_{\tilde{E}}$ are classically

[10]Note, that in this case, the system $\rho_{\tilde{E}}$ does not possess purifying qualities

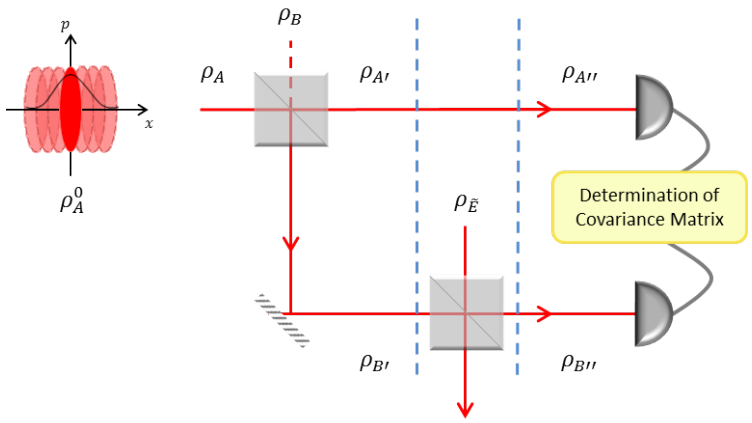

Figure 5.8: Entanglement recovery by interference. Subsystem ρ_A taken as Gaussian distributed modulated pure squeezed state is split on a beamsplitter. Gaussian quantum discord is present in output bipartite state. Due to the tailored modulation, entanglement creation is prevented. $\rho_{B'}$ interacts with non-purifying system $\rho_{\tilde{E}}$ created by LOCC. Displacements encoded in $\hat{x}$-quadrature of $\rho_{\tilde{E}}$ which will partially cancel out initial modulation, leading to recover the entanglement within system $\rho_{A''\tilde{r}B''}$.

correlated. Next, similar to above, mode $\rho_{B'}$ is superimposed on a beamsplitter with $\rho_{\tilde{E}}$. As a consequence, the noise caused by the random displacements is partially cancelled and the potential entanglement between modes $\rho_{A''}$ and $\rho_{B''}$ is recovered. To verify this, instead of physically imprinting a displacement on the third quantum mode $\rho_{\tilde{E}}$ and interfering the mode with mode $\rho_{B'}$ on a beamsplitter, we have superimposed $\rho_{B'}$ with vacuum state $\rho_{\tilde{E}}$ on a beamsplitter and implemented equivalent displacement electronically on the measured data. This gives us a violation of Duan's separability criterion (Section 3.2.2) $0.91\pm0.01 < 1$, which certifies entanglement between $\rho_{A''}$ and $\rho_{B''}$.

Now, consider the instance where we have access to the displacement $\bar{x}$ encoded on mode $\tilde{E}$, entanglement between modes $\rho_{A''}$ and $\rho_{B''}$ can be recovered by directly performing the reverse displacement on mode $\rho_{B'}$ to cancel the modulation. Entanglement can again be recovered. Initially we have pure squeezed state ρ_A^0 with quadratures $\hat{x}_A = e^{-r}\hat{x}_A^{(0)}$, $\hat{p}_A = e^{r}\hat{p}_A^{(0)}$, and state ρ_B in a vacuum state with quadratures $\hat{x}_B = \hat{x}_B^{(0)}$, $\hat{p}_B = \hat{p}_B^{(0)}$, with r being the squeezing parameter. Displacements are applied to the $\hat{x}$-quadrature of ρ_A^0 such that

$$\hat{x}_A \to \hat{x}_A + \bar{x} \tag{5.27}$$

After undergoing a beamsplitter transformation the resulting output quadratures are

$$\begin{aligned} \hat{x}'_A &= T\hat{x}_A + R\hat{x}_B + T\bar{x}, \quad \hat{p}'_A = T\hat{p}_A + R\hat{p}_B, \\ \hat{x}'_B &= R\hat{x}_A - T\hat{x}_B + R\bar{x}, \quad \hat{p}'_B = R\hat{p}_A - T\hat{p}_B. \end{aligned} \tag{5.28}$$

The "demodulation" required for entanglement recovery can be found using Duan's separa-

bility criterion (Section 3.2.2), also known as the *product inseparability criterion* [80]:

$$\langle (g\hat{x}'_A + \hat{x}'_B)^2 \rangle \langle (g\hat{p}'_A - \hat{p}'_B)^2 \rangle < \frac{1}{4}(g^2+1)^2. \tag{5.29}$$

where g is the variable gain. The operators on the left-hand side read as

$$\begin{aligned} g\hat{x}'_A + \hat{x}'_B &= \hat{x}_A(gT+R) + \hat{x}_B(gR-T) + \bar{x}(gT+R) \\ g\hat{p}'_A - \hat{p}'_B &= \hat{p}_A(gT-R) + \hat{p}_B(gR+T). \end{aligned} \tag{5.30}$$

Hence the general "demodulation" to be applied to mode $\rho_{B'}$ is of the form

$$\hat{x}''_B \to \hat{x}'_B - (gT+R)\bar{x}, \tag{5.31}$$

which gives,

$$g\hat{x}'_A + \hat{x}'_B = \hat{x}_A(gT+R) + \hat{x}_B(gR-T). \tag{5.32}$$

Rearranging Eq. (5.29) and using Eq. (5.30) we have a recast criterion as

$$\frac{[e^{2r}(gT-R)^2 + (gR+T)^2][e^{-2r}(gT+R)^2 + (gR-T)^2]}{(g^2+1)^2} < 1. \tag{5.33}$$

In the ideal case of a balanced beamsplitter, i.e., $T = R = \frac{1}{\sqrt{2}}$, the left-hand side of the inequality (5.33) is minimised with a gain of $g = 1$. Therefore

$$e^{-2r} < 1, \quad \forall\, r > 0, \tag{5.34}$$

and thus entanglement is recovered for any $r > 0$. In this ideal case the demodulation to be applied to mode ρ_B is given by

$$\begin{aligned} \hat{x}''_B &\to \hat{x}'_B - (gT+R)\bar{x} \\ &= \hat{x}'_B - \sqrt{2}\bar{x}. \end{aligned} \tag{5.35}$$

Hence the prefactor in the ideal case is $-\sqrt{2}$.

This entanglement recovery reveals two important facts about quantum correlations in the global system $(AB\tilde{E})$. First, it demonstrates that there must exist entanglement across the $A' - (B'\tilde{E})$ splitting before the beamsplitter, as otherwise it would not create entanglement between systems $\rho_{A'}$ and $\rho_{B'}$. Second, it is a proof that system $\rho_{B'}$ shared quantum correlations with the subsystem $(\rho_{A'\tilde{E}})$ and therefore realised a true quantum communication between locations of systems $\rho_{A'}$ and $\rho_{\tilde{E}}$, which cannot be replaced by LOCC. Indeed, if system $\rho_{B'}$ was only classically correlated with subsystem $(A'\tilde{E})$, it would be possible to replace its transmission by a measurement of its state (which does not disturb the global state), followed by a recreation of the state in the location of subsystem $\rho_{\tilde{E}}$. This is, however, a LOCC operation which cannot establish entanglement across the $A'' - (B''\tilde{E})$ splitting.

To place these results in context, consider some counter-intuitive protocols recently suggested and experimentally demonstrated using separable discordant states, e.g., distribu-

tion of entanglement by separable states [195–198] and entanglement activation from discord [199]. These protocols typically begin with multipartite discordant but otherwise fully separable states. Entanglement is then shown to emerge after some local operations on parts of the state. Our description of entanglement recovery by direct displacement of system $\rho_{B'}$ using classical information traveling from parties A to B crystallises the core mechanism behind such protocols; the emergence of more powerful correlations is inherently linked to the presence of entanglement along a single bi-partition including a separable system.

Implausible effects in separable discordant states often have their roots in the preparation of the initial discordant state. More precisely, the preparation always contains communication of classical information between parties A and B which they use for imposing correlated noise onto their quantum systems (equivalent with discord in the case outlined in this Chapter). In the subsequent stages of the protocol, the noise is removed by interference of the correlated subsystems and hence entanglement is recovered. The essence of this effect is demonstrated in this Chapter by entanglement recovery using interference with the "environmental mode" $\tilde{E}$. Further, we have obtained a better entanglement recovery compared to the quantum interference scenario by imprinting the classical information directly on a relevant quantum system, which can be done by anybody having access to the classical communication because it can be read without disturbance. This features even more clearly the important role of exchange of classical information. It is our belief that the same mechanism is behind the performance of the qubit versions of the discussed protocols but the structure of the communicated classical information can be much more involved in comparison with communication of just a single real number $\bar{x}$ in our case.

It is interesting to note that the emergence of entanglement from discord was reviewed and developed for the tripartite qubit case by Tatham and Korolkova in [179]. This work was inspired by that of Campbell *et al.* [159], Ciccarello and Giovannetti [191], and Streltsov *et al.* [131]. In the latter it was discussed that if two states (A and C) initially have no quantum correlations, it is possible to perform a local operation on one subsystem (C) to create non-classical correlations between the two subsystems (A and C). That is, the state goes from having zero discord to non-zero discord. The focus of [179] was on the flow of quantum correlations in the purified tripartite state, which emerged to be a three-qubit GHZ state[11] [200]

$$|GHZ\rangle = \frac{1}{\sqrt{2}}(|000\rangle + |111\rangle). \tag{5.36}$$

In this pure system, initially no two subsystems are entangled, but all systems possess strong classical correlations. The entanglement existing across any bi-partition i.e., $A-BC$, $B-AC$ and $C-AB$, of the pure state is maximum. Through implementation of the Koashi-Winter relation a direct relationship was found between the discord and the entropy of the system on which an operation is performed,

$$\mathcal{D}^{\leftarrow}(AC) = 2\mathcal{S}(C) - 1 \quad \text{where} \quad \mathcal{S}(C) = \frac{\ln[8] - \sqrt{2}\coth^{-1}[\sqrt{2}]}{\ln[4]}. \tag{5.37}$$

[11] One of the most remarkable properties of the GHZ states is that by tracing out only one subsystem entanglement will be completely destroyed in the state and the result is a fully mixed separable state.

After the local operation on C its entropy must decrease but no entanglement can form between $A(B)$ and C as there was none initially present. As a result only classical correlations can be present which prove to be weaker than previously. However, the capacity of $A(B)$ to be correlated is not consumed by this so entanglement must emerge between A and B. Alternatively, the local measurement on C can be seen as a non-local measurement on A and B from the condition of purity $\mathcal{S}(\rho_{ij}) = \mathcal{S}(\rho_k)$ for a tripartite state ρ_{ijk}.

Thus far in this Chapter a counter-intuitive effect of Gaussian discord increase under the action of local loss was presented. Experimental evidence correlating with a simple theoretical model validated this observation in a bipartite system. It was uniquely found, contrary to previous expectations, that this enhancement of discord can be generated without having to distort each quadrature variance in a similar manner, it is sufficient to affect only one. For the first time, action was then taken to explain the increase of non-classical correlations in this environment leading to an optimisation through the introduction of noisy channels. Two main conclusions of this are that, Gaussian discord proves to show great robustness as local loss in intensified. Moreover, in a more imperfect setting Gaussian discord between two systems can – when depleted by imperfections – be regained by introduction of controlled losses. This leads to the new insight that Gaussian discord proves to be a hugely robust quantum resource compared to entanglement, and can be of huge benefit in the context of an imperfect setup.

Next a discussion was held on the restoration of entanglement, lost due to the Gaussian distributed displacements imposed on the input squeezed state. This can be viewed in a number of ways, all of which lead to the conclusion that there must exist hidden quantum correlations between system and environment in order to restore entanglement from discord. We prove that continuous variables are unique in unveiling the simple mechanism behind some puzzling effects and lead to a clear intuition of how to exploit quantum correlations in separable states.

The remainder of this Chapter will focus within the well-established protocol of Entanglement Distribution by Separable States. This investigation will use the concepts introduced previously to study the flow of correlations within the global system. The aim of this is to gain insight into the origin of the emerging entanglement and to link the mechanism to the flow of discord within the system, thus establishing its fundamental role.

5.4 Entanglement Distribution by Separable States

Quantum entanglement, although complex in nature, requires only a surprising simple interaction to establish. To explore entanglement further, protocols were developed to investigate possible formation techniques. In the continuous variable setting one can create entanglement by superimposing a vacuum state with a squeezed state on a beamsplitter, for any small amount of squeezing. A more sophisticated protocol is entanglement distribution by separable states first proposed by Cubitt *et al.* [196] for discrete variable systems[12]. The most defining feature of this protocol is that no entanglement is necessary to distribute

[12]In addition Cubitt *et al.* [196] similarly demonstrated that two systems can also become entangled by continuous interaction with a highly mixed mediating particle that never becomes entangled itself.

entanglement i.e., two distant systems can be entangled by sending a third ancillary system that is consistently separable from the other two. The procedure is schematically illustrated in Fig. 5.9 and is as follows; view a bipartite separable state in a finite-dimensional Hilbert space composed of two distant subsystems A and B, the *sender's* system (A) locally interacts with a separable ancillary system (C), where this interaction allows the ancilla to remain unentangled[13]. Next this separable ancillary system is sent to the distant *receiver's* subsystem (B), where it again undergoes a local non-entangling interaction. The result of this transfer is that the separable bipartite state is now entangled, whilst the ancillary system remains completely separable.

In the following work we aim to explain the mechanism behind entanglement distribution by separable state in terms of quantum discord. We hypothesise that it is not only the initial presence of discord between A and B, but also the flow of non-classical correlations between system and environment that is essential for the distribution of entanglement, and thus discord plays a key role similar to what has been proven in the discrete variable case.

5.4.1 Continuous Variable Entanglement Distribution

The phenomenon of entanglement distribution is actually not bounded to finite-dimensional Hilbert space. The infinite-dimensional Gaussian version of the entanglement distribution by separable states was first presented by Mišta and Korolkova in [201,202] and is schematically depicted in Fig. 5.10. It was shown that there exist tripartite mixed Gaussian fully separable state (ρ_{ABC}) allowing to entangle two subsystems A and B by mixing them stepwise with a third consistently separable mode C on two beamsplitters. This continuous variable implementation of the protocol proved to give a clearer insight into the actual mechanism of the phenomenon as described already for qubits. The initial Gaussian states A_0, B_0 and C_0 are prepared as a momentum squeezed, position squeezed and vacuum state respectively, shown by the green elliptical/circular contours in Fig. 5.10. The essential component of the Gaussian version is embedded in the classically correlated noise implemented to these initial states (Stage 1). This is encoded such that neither system has knowledge of the noise on the other, which creates an extra interesting point that A and B need not communicate on any level, even to form classical correlations. In actual fact the correlated noise is designed such that the tripartite state possesses a set of desirable properties after the first interaction (Stage 2). At this stage it is required that the state exhibits the following properties across bi-partitions,

$$\mathcal{E}_{B-AC}(\rho_2) = 0, \quad \mathcal{E}_{C-AB}(\rho_2) = 0, \tag{5.38a}$$

$$\text{and} \quad \mathcal{E}_{A-(BC)}(\rho_2) \neq 0. \tag{5.38b}$$

[13]The type of interaction performed is a controlled NOT (CNOT) operation. The CNOT operation flips the configuration of a second qubit (known as the target qubit) if and only if the first qubit (known as the control qubit) is in a predefined configuration. Typically an entangling operation but the states were chosen such that this would not be the case.

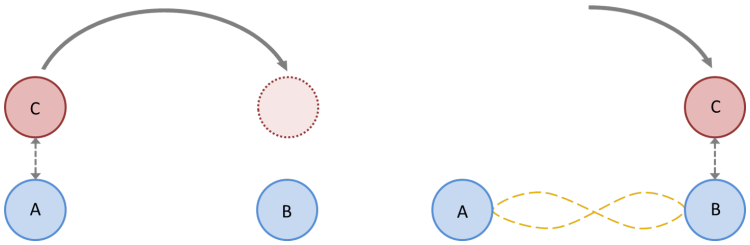

Figure 5.9: Schematic depiction of the qubit entanglement distribution by separable states protocol [196]. Qubits A and C interact while allowing C remaining separable. System C then interacts with B which establishes entanglement between A and B (yellow dashed lemniscata). C will finally remain separable from AB and may be traced out.

The correlated noise is modelled as displacements to the position and momentum quadratures of the form

$$\hat{x}_B \to \hat{x}'_B = \hat{x}_B + v, \tag{5.39a}$$
$$\hat{x}_C \to \hat{x}'_C = \hat{x}_C + v\sqrt{2}, \tag{5.39b}$$
$$\hat{p}_A \to \hat{p}'_A = \hat{p}_A - u\sqrt{2}, \tag{5.39c}$$
$$\hat{p}_B \to \hat{p}'_B = \hat{p}_B + u, \tag{5.39d}$$

where u and v are classical displacements which obey the Gaussian distribution $\mathcal{P}(u,v) = \exp[-(u^2+v^2)/4x]/(4\pi x)$.

It was found that the possibility of distribution of entanglement originates from the structure of the initial mixed state. The sender's system A_0 carries originally a potential to be entangled with the separable auxiliary mode C_0 that is used to distribute entanglement. The entanglement is however prevented by the aforementioned local correlated displacements that make the auxiliary system separable from the sender's system. The resultant state is then a tripartite mixed Gaussian fully separable state (ρ_{ABC}), as mentioned above. The separable ancilla is then sent to the receiver who partially restores the entanglement by mixing it with their suitably classically correlated system. The separability at Stage 2 is verified by the minimum symplectic eigenvalue in the PPT criterion (see Section 3.2.1) such that the separability of the necessary bi-partitions in 5.38a hold if the displacement satisfies

$$\bar{x}_{sep} = \frac{e^{2r-1}}{2} \tag{5.40}$$

The desired tripartite state γ_2 satisfying Eq.'s (5.38a, 5.38b) is of the form

$$\gamma_2 = \underbrace{\begin{pmatrix} \cosh(2r)\mathbb{1} & \underline{0} & \sinh(2r)\sigma_z \\ \underline{0} & \mathbb{1} & \underline{0} \\ \sinh(2r)\sigma_z & \underline{0} & \cosh(2r)\mathbb{1} \end{pmatrix}}_{\gamma_{ABC}} + \bar{x}K = \begin{pmatrix} a\mathbb{1} & 2x\sigma_z & b\sigma_z \\ 2x\sigma_z & (1+4x)\mathbb{1} & -2x\mathbb{1} \\ b\sigma_z & -2x\mathbb{1} & a\mathbb{1} \end{pmatrix} \tag{5.41}$$

where γ_{ABC} is therefore the tripartite state of non-displaced states after the beamsplitter

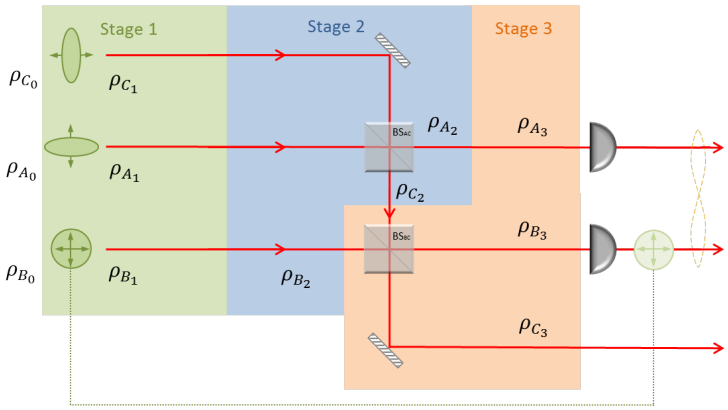

Figure 5.10: Schematic of the Gaussian entanglement distribution via separable ancilla protocol. Initial states prepared as a momentum squeezed vacuum mode A_0, a position squeezed vacuum mode C_0, and a vacuum mode B_0. Random displacements then applied (green box) to the $\hat{x}$ quadrature (horizontal arrow) and the $\hat{p}$ quadrature (vertical arrow), which are correlated via a classical communication channel. Modes A_1 and C_1 superimposed on a balanced beam splitter BS_{AC} with output mode C_2 remaining separable. Mode C_2 then superimposed with mode B_2 on another balanced beam splitter BS_{BC}, which establishes entanglement between the output modes A_3 and B_3 (black dotted lemniscata). Note the position of the displacement on mode B. In the original protocol, the displacement is performed before BS_{BC}. Equivalently, this displacement on mode B can be performed after the second beamsplitter (the dashed green line indicates the respective relocation of the displacement) on mode B_3, and even a posteriori after the measurement of mode B_3 [195].

BS_{AC} and the correlated noise matrix K is of the form

$$K = \kappa_1\kappa_1^\top + \kappa_2\kappa_2^\top \quad \text{and} \quad \begin{matrix}\kappa_1 = (0,-1,0,2,0,-1)^\top \\ \kappa_2 = (1,0,2,0,-1,0)^\top\end{matrix}. \tag{5.42}$$

The initial state γ_1 and the final state γ_3 can be extrapolated from the appropriate reverse and forward beamsplitter transformations such that

$$\gamma_1 = \underbrace{\gamma_A \oplus \gamma_A \oplus \gamma_A}_{\gamma_0} + \tilde{M} \tag{5.43a}$$

$$\text{and} \quad \gamma_3 = \hat{U}_{BC}\gamma_2\hat{U}_{BC}^\top = \begin{pmatrix} a\mathbb{1} & \frac{2x+b}{\sqrt{2}}\sigma_z & \frac{2x-b}{\sqrt{2}}\sigma_z \\ \frac{2x+b}{\sqrt{2}}\sigma_z & \frac{1+a}{2}\mathbb{1} & \frac{1+4x-a}{2}\mathbb{1} \\ \frac{2x-b}{\sqrt{2}}\sigma_z & \frac{1+4x-a}{2}\mathbb{1} & \frac{1+8x+a}{2}\mathbb{1} \end{pmatrix} \tag{5.43b}$$

where $\tilde{M} = \bar{x}\hat{U}_{AC}^\top K\hat{U}_{AC}$ and $\hat{U}_{ij}$ denotes a three mode symplectic beamsplitter interacting systems i and j.

The theoretical results in [202] were experimentally verified later by Peuntinger *et al.* [195], in which it was discussed the possibility of the equivalence of the displacements on mode B_0 to be performed after BS_{BC} on mode B_3, and even *a posteriori* after the measurement of mode B_3 (depicted by the green dotted line in Fig. 5.10), thus verifying that

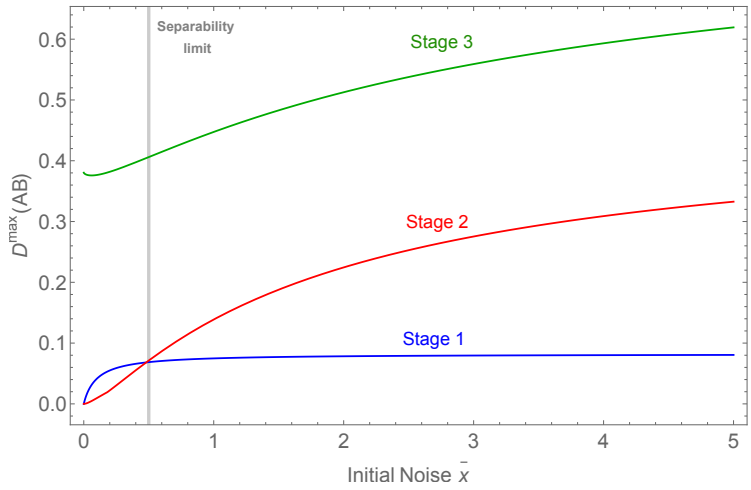

Figure 5.11: Maximum Gaussian quantum discord between systems A and B at three stages in the scheme shown in Fig. 5.10. Level of discord present will always increase, with respect initial noise $\bar{x}$, as system AB propagates through protocol. The instance shown coincides with the use of a balanced beamsplitter and squeezing of magnitude $r = 0.5$. According to Eq. (5.40) the separability limit for C to be separable will be at $\bar{x} = 0.859$ (grey vertical line).

entanglement distribution is truly performed via a dual classical and quantum channel, by a classical information exchange alongside the transmission of separable quantum states.

5.4.2 Role of Gaussian Quantum Discord in Entanglement Distribution

Along with such an interpretation of the scheme, the mechanism can be also described by using the notion of quantum discord. Initially, we have three Gaussian pure independent systems A_0, B_0 and C_0 with zero discord in AB_0 since it is a product state. To this tripartite state correlated noise is added causing non-zero discord in $(AB)_1$, which was proved to be an essential component in this mechanism by Chuan *et al.* in [203]. The decisive juncture is the Stage 2 of the protocol, after the interaction of the ancilla mode C_1 with the sender's mode A_1 on the first beamsplitter (see Fig. 5.10). As already mentioned in [202], the tripartite state in Stage 2 is a Gaussian bi-separable state, separable across $C_2 - (A_2B_2)$ and $B_2 - (A_2C_2)$ bi-partitions and entangled across $A_2 - (B_2C_2)$, that is, it is a bound entangled state [204]. Naturally, this state should also exhibit non-zero discord between A and B. It is this quantumness which is then, in a way, activated into entanglement by the interaction on the second beamsplitter, coupling the ancilla C_2 with the receiver's system B_2 (Stage 3 of the protocol).

To analyse the continuous variable version of entanglement distribution we first directly calculated the Gaussian quantum discord between A and B at all stages of the protocol. Fig. 5.11 illustrates how the maximum Gaussian discord $\mathcal{D}^{max}(\rho_{AB})$ (see Eq. 4.4) is affected by varying levels of initial noise. These results clearly confirm not only the presence of Gaussian quantum discord within ρ_{AB} at all stages of the protocol, but also that the level of discord

will increase significantly as the protocol is carried out. However, this is only explicitly the case when the separability limit, which indicates separability of C, given in Eq. (5.40) is satisfied (shown by the grey vertical line). The scenario considered here (and throughout this investigation) is the case of $r = 0.5$ and so $\bar{x}_{sep} = 0.5$. A remarkable point is the emergence of non-zero discord from a product state after admixing of the correlated noise in Stage 1; although surprising at first glance, this phenomenon becomes plausible if the arguments similar to those in [179] are used. Coupling to the correlated noise plays the role of the global unitary operation on modes of interest and it has the same effect a local non-unitary operation in [179].

It is interesting to note that the distribution of entanglement was also linked to quantum discord by Chuan *et al.* in [203]. Similar to the continuous variable case, the progression from Stage 2 to Stage 3 in the distribution was identified as the pivotal step, the transfer of the ancilla corresponds to difference in the entanglement across the bi-partitions $A - BC$ and $B - AC$, which was found to be upper bounded by the discord across the $C - AB$ splitting for any pure tripartite state ρ_{ABC}, i.e.,

$$|\mathcal{E}_{A-BC}(\rho) - \mathcal{E}_{B-AC}(\rho)| \leq \mathcal{D}_{C-AB}(\rho). \tag{5.44}$$

where entanglement is quantified by the relative entropy of entanglement reviewed in Section 3.3.5. This relation is based on the fact that a local operation on AC cannot increase the entanglement across the $B - AC$ partition led to the adapted

$$\mathcal{E}_{A-BC}(\rho_2) \leq \mathcal{E}_{B-AC}(\rho_1) + \mathcal{D}_{C-AB}(\rho_2). \tag{5.45}$$

Directly resulting from this is the implication that the quantum discord $\mathcal{D}_{C-AB}(\rho_2)$ must be non-zero. To see this, consider the instance where $\mathcal{D}_{C-AB}(\rho_2) = 0$, of course this implies that the transfer of the separable ancillary system C equates to classical communication and that entanglement cannot increase under LOCC. Hence the case where $\mathcal{D}_{C-AB}(\rho_2) \neq 0$ reveals the intrinsic role of discord in general quantum communication. Another key property for the possibility of entanglement distribution is the initial existence of quantum discord between systems A and B. This coincides with our results in Fig. 5.11 where it can be seen that above the limit of separability of the ancilla, there exists an almost constant level of non-zero discord.

Unlike the argument given in the qubit case [179], obtaining a simple yet explicit analytic expression for a continuous variable Gaussian discord is far more challenging. Therefore we restrict ourselves to the use of Koashi and Winter inequality and argue that although quantum discord does play a role in entanglement distribution, in a similar way to [179], its role is not fundamental. Discord merely emerges as a side product of the correlation flow originating in local entropy changes due to coupling to some dissipative reservoir, be it correlated noise designed through correlated displacements in phase-space or just the environment in general. To see this in the continuous variable system we must consider a tripartite globally pure system, thus we are first required to construct the purification to the tripartite Gaussian mixed state. This is discussed further in the next Section.

5.4.3 Flow of Correlations in Global System

The particular flow of correlations in a dissipative bipartite system leading to a beneficial quantum outcome discussed previously in this Chapter motivated us to consider the use of a similar approach to unveil the nature of the counter-intuitive phenomenon of entanglement distribution by separable states. This protocol involves the interaction of similar Gaussian states after having undergone Gaussian distributed modulation and are subject to the same set of Gaussian maps. Leading from this, the distribution protocol can be seen as an extension of the discord increase scheme[14]. So, can the flow of system-environment correlations in the globally pure system provide insight to the workings of the mechanism behind entanglement distribution?

In order to analyse the flow of correlations within the system we began by taking a step back in order to have a more general overview of the correlation properties of the initial state. Similar to the beginning of this Chapter, this can be done by enacting a purification. According to [204] this involves the addition of two modes E_1 and E_2 encoding the information from the environment. The consequential pure five-mode (or 'quint-partite') state is given by

$$|\psi\rangle = \int \sqrt{\mathcal{P}(u,v)} \left|-i\frac{u}{2};+r\right\rangle_A \left|\frac{v+iu}{\sqrt{2}};0\right\rangle_B \left|\frac{v}{2};-r\right\rangle_C |v\rangle_{E_1}^{(x)} |u\rangle_{E_2}^{(p)} \, dudv \tag{5.46}$$

where $|\alpha, \pm r\rangle$ is the displaced squeezed state and $|u\rangle^{(x)}$ and $|v\rangle^{(p)}$ are the eigenvectors of the position and momentum quadratures, respectively. This state satisfies the relation $\rho_{ABC} = \mathrm{Tr}_{E_1E_2}(|\psi\rangle\langle\psi|)$. This purification can be fully characterised by its covariance matrix, which is of the form $\Gamma_1 = X_1 \oplus (X_1)^{-1}$ where[15]

$$X_1 = \begin{pmatrix} e^{2r} & 0 & 0 & 0 & \frac{e^{2r}}{\sqrt{2}} \\ 0 & 1+4\bar{x} & 2\sqrt{2}\bar{x} & 4\bar{x} & -1-2\bar{x} \\ 0 & 2\sqrt{2}\bar{x} & e^{-2r}+2\bar{x} & 2\sqrt{2}x & -\sqrt{2}\bar{x} \\ 0 & 4\bar{x} & 2\sqrt{2}\bar{x} & 4\bar{x} & -2\bar{x} \\ \frac{e^{2r}}{\sqrt{2}} & -1-2\bar{x} & -\sqrt{2}\bar{x} & -2\bar{x} & y \end{pmatrix} \tag{5.47}$$

with $y = 1 + \bar{x} + \frac{1}{4\bar{x}} + \frac{e^{2r}}{2}$ and $\mathrm{Det}(X_1) = 1$.

It is now possible to define a single system Z that shall embody the three consolidated systems C, E_1 and E_2, that is ancilla and environment, such that $\rho_{AB} = \mathrm{Tr}_Z[\Gamma_1]$. Implementing this composite system Z into the above protocol would now imply that the first interaction can be seen as the interaction of A with Z and the second interaction with B and Z. Such a global operation between A and Z can be modelled as a single local operation on the remaining subsystem B since purity implies the cyclic property $\mathcal{S}(\rho_{AZ}) = \mathcal{S}(\rho_B)$ from Eq. (2.75).

[14] This of course is not chronologically correct since the entanglement distribution protocol was developed first.

[15] Note this covariance matrix will have a basis of the form $\{x_1 \ldots, x_N, p_1, \ldots, p_N\}$, where N is the dimension of the system, thus requiring a simple symplectic transformation to transform it into the desired form.

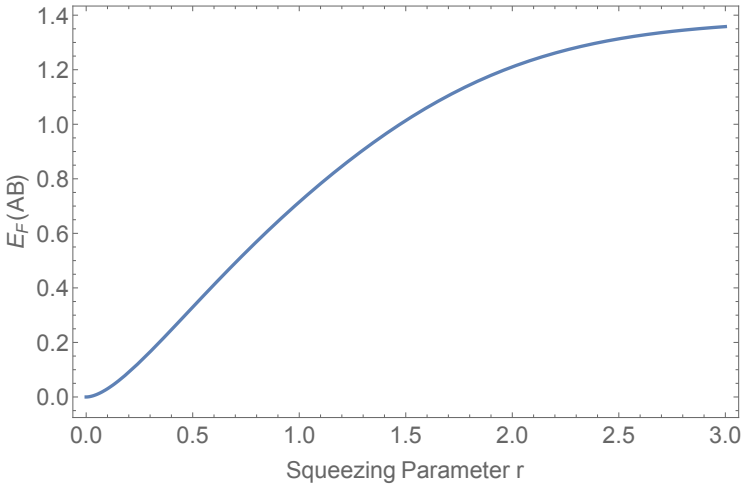

Figure 5.12: Gaussian entanglement of formation between A and B upon measurement following Stage 3 as function of the degree of squeezing.

The protocol is designed such that it possesses the following initial properties:

$$\mathcal{E}_F(\rho_{AB_1}) = \mathcal{E}_F(\rho_{AZ_1}) = \mathcal{E}_F(\rho_{BZ_1}) = 0. \tag{5.48}$$

In the case of a complicated five-mode scheme, it is difficult to verify analytically and exactly that the Koashi-Winter relation holds. Therefore a pivotal assumption must now be made regarding the relative similarity of the pure tripartite system ABZ with that discussed in at the beginning of this Chapter. On the grounds of the success of the Koashi-Winter Relation in analysis of the previous scheme, we will assume that it must also hold for the system ABZ as there is no legitimate justification for it failing.

Using the lack of entanglement across all permutations from the Koashi-Winter Relation Eq. (4.27) we have that

$$\mathcal{S}(\rho_{A_1}) = \mathcal{J}^{\leftarrow}(\rho_{AZ_1}) \Rightarrow \mathcal{S}(\rho_{A_1}|\rho_{Z_1}) = 0, \tag{5.49a}$$
$$\mathcal{S}(\rho_{B_1}) = \mathcal{J}^{\leftarrow}(\rho_{BZ_1}) \Rightarrow \mathcal{S}(\rho_{B_1}|\rho_{Z_1}) = 0, \tag{5.49b}$$
$$\mathcal{S}(\rho_{Z_1}) = \mathcal{J}^{\leftarrow}(\rho_{ZB_1}) \Rightarrow \mathcal{S}(\rho_{Z_1}|\rho_{B_1}) = 0. \tag{5.49c}$$

These relations imply that at this initial stage a measurement of one subsystem will not affect the other. This is intuitive since the system is purely classically correlated across these bi-partitions. Of course when we perform a measurement on a system its capacity to preserve the purity of the total state, and hence entropy, decreases

$$\mathcal{S}(\rho_{A_1}) < \mathcal{S}(\rho_{A_2}) = \mathcal{S}(\rho_{A_3}), \tag{5.50a}$$
$$\mathcal{S}(\rho_{B_1}) = \mathcal{S}(\rho_{B_2}) < \mathcal{S}(\rho_{B_3}). \tag{5.50b}$$

Substituting Eq. (5.50a) into the Koashi-Winter Relation for the final stages of the

protocol, we arrive at

$$\begin{aligned} \mathcal{J}^{\leftarrow}(\rho_{AZ_2}) &= \mathcal{E}_F(\rho_{AB_3}) + \mathcal{J}^{\leftarrow}(\rho_{AZ_3}) \\ \Rightarrow \mathcal{J}^{\leftarrow}(\rho_{AZ_2}) &> \mathcal{J}^{\leftarrow}(\rho_{AZ_3}), \end{aligned} \tag{5.51}$$

where the case of equality is not considered since we know that $\mathcal{E}_F(\rho_{AB_3}) > 0$. The classical correlation of A with the "environment" Z is decreasing. It can be interpreted that the quantum correlations gained within the system AB are due to an exchange of classical correlations in return for quantumness. Tying into the specific case considered in the construction of Fig. 5.11, the achievable entanglement according to Gaussian entanglement of formation is $\mathcal{E}_F(\rho_{AB_3}) \approx 0.33$ for squeezing $r = 0.5$ and $\bar{x} > 0.5$ in accordance with Eq. (5.40). The effect of squeezing on the achievable entanglement is much more pronounced compared to initial noise, as seen in Fig. 5.12 where it can be seen that the level of squeezing, up to a limit, can dramatically increase the level of Gaussian entanglement of formation that can be obtained. Rather intuitive as it is well known that squeezing provides the potential for the creation of quantum correlations. The gradual discord increase seen in Fig. 5.11 — since we are not assuming discord to be initially present between A and B — appears to not be a fundamental phenomenon but a side effect of all the changes in local entropy as predicted, and the mechanism of entanglement distribution by separable states is not a direct result of the flow of quantum discord as originally anticipated.

In this part of the Chapter we are reintroduced to the counter-intuitive protocol of entanglement distribution by separable states. A discussion was held regarding the essential construction of the states and the non-classical correlations required for its success. In an attempt to explore the necessity of quantum discord within the continuous variable setting we sought insight from the Koashi-Winter relation. It was thought that, much like the qubit case, the presence of discord in the initial separable state AB, would prove to be an essential criteria for the success of the protocol. The new insight provided here is that, although discord is present and increases as the protocol progresses, the mechanism witnessed here seems to be explainable by the exchange of classical correlation in lieu of quantum entanglement, without any explicit requirement of discord. Quantum information is passed into the environment via coupling to the common noise reservoir and then retrieved back via a non-local operation on the subsystems which can be replaced by passing classical information on to the noise structure. We can conclude that in the continuous variable setting, the distribution of entanglement appears to not be a direct result of quantum discord. Any presence or flow of non-classical correlations captured by discord seem to be coincidental, and in this particular scenario the flow of quantum discord — although abundantly present — is not as essential as a communication resource compared to the qubit case.

The work presented here serves as a critical analysis of quantum discord in the continuous variable setting. Discordant states have been proved to be commonplace in quantum systems, including those in popular protocols such as entanglement distribution by separable states. However, it is crucial to not immediately associate the presence of discord as

playing a fundamental role in a quantum communication mechanism. We uniquely propose a simple explanation of this protocol by a free flow of both classical and quantum correlations between system and environment. It appears that a systems interaction with its environment plays a more crucial role compared to discord. This is not to say quantum discord has no utilisable properties. The main focus of the work presented here was the study of quantum discord under the conditions of local loss and noisy channels. First, it was remarkably shown that contrary to expectations, the increase of discord under local loss can be witnessed for input states with an asymmetric degree of mixing in its quadratures. Next, it was shown that although particular apparatus imperfections can deplete the level of discord present, attenuation of one system can counteract this loss of quantumness and restore discord to levels close to that of a perfect scenario. Extension of this scheme came in the form of a study of entanglement recovery. Indeed entanglement can be restored from a discordant state by means of a remarkably simple classical-quantum channel. Hence it can be interpreted that converting an entangled state to one which is separable discordant can shield the system against noisy channels that would otherwise destroy entanglement. Once the state has been protected, entanglement can be restored and the system then used for any number of quantum communication protocols.

Chapter 6

Concluding Remarks

"Discord could be like sunlight, which is plentiful but has to be harnessed in a certain way to be useful. We need to identify what that way is." – Kavan Modi

The core focus of this Thesis was the usefulness of non-classical correlations within imperfect decoherent quantum systems. The study of separable non-classical states has become increasingly popular over the past decade, but as yet a consistent and practical usefulness is largely unknown. I saw it important to study their characteristics in more realistic dissipative systems, to gain a fresh insight into possible advantageous behaviour.

The first system involved a bipartite separable discordant state under the action of controlled loss on one subsystem. Under these conditions the Gaussian quantum discord not only proved robust against loss, but actually improves as loss is intensified. Also, although imperfections reduce the achievable level of discord, local loss was remarkably found to vastly improve the level of discord, almost to the degree of fully counteracting the influence of imperfections. Surprising, as decoherence is typically associated with the loss of information, as with the case of quantum entanglement. Through a purification I sought to explain this effect by considering system-environment correlations. I found that classical correlations within the discordant state are exchanged for a strengthening of system-environment entanglement, which in turn increases the quantumness of the state. A discussion was also held in respect to the entanglement recovery possibilities which revealed the importance of hidden quantum correlations along bi-partitions across the bipartite state and a classically prepared "demodulating" third system, acting in such a way as to partially cancel the entanglement preventing noise.

The second protocol assessed was entanglement distribution by separable states. The interpretation of this protocol in discrete and continuous variables was revisited with particular focus on the latter. By a similar framework, we endeavoured to explain the emergence on quantum entanglement by a specific flow of correlations in the globally pure system. Although this presented difficulty in respect to explicit calculations, a more qualitative approach proved sufficient to show that through a loss of classical correlations between the system and environment, non-classical correlations were able to grow resulting in entanglement from previously existing discord. Discord appeared to play a less fundamental role

compared to the qubit version of the protocol. The strengthening of non-classical correlations can be attributed to a flow of classical and quantum correlations between system and environment.

The latter result leads to the warning that one must be cautious when placing importance on quantum discord. The mere presence for flow of discord does not equate to usefulness, particularly since states without discord (CC-classical states) are a rare occurrence. However, the former results reinforce the prospect that non-classical correlations beyond entanglement are more robust than entanglement. Moreover, this work proved that discord can act in such a way as to counteract harmful imperfections in the apparatus, and as a result may ultimately prove to be more applicable in real world applications which are by definition decoherent.

Appendix A

Optimal Gaussian Discord

The question exists whether non-Gaussian measurements can lead to optimal quantum discord. It has been proven that for a particular class of Gaussian states, Gaussian measurements lead to the optimal Gaussian discord. The following will follow the procedure introduced in Ref. [137] and be applied to the first scheme discussed in Chapter 5. Consider the bipartite state created by mixing a vacuum state and a state with covariance matrix γ_A of the form

$$\gamma_{A'B'} = \frac{1}{2}\begin{pmatrix} \gamma_A + \mathbb{1} & \gamma_A - \mathbb{1} \\ \gamma_A - \mathbb{1} & \gamma_A + \mathbb{1} \end{pmatrix}, \quad \text{with} \quad \gamma_A = \text{diag}\left\{V_x,\ V_p\right\}. \tag{A.1}$$

Assuming γ_A has been prepared by Gaussian distributed random displacement of the x-quadrature of a squeezed state with squeezing in the x-quadrature and large anti-squeezing in the p-quadrature, and hence $V_p > V_x > 1$. Since discord is an entropic quantity, it is invariant under local unitaries. Meaning that displacements may be applied to reduce a covariance matrix into normal form. Thus, without loss of generality, discord can be studied for zero-mean Gaussian states. By local squeezing $\gamma_{A'B'}$ can be transformed into standard form with elements

$$a = b = \frac{\sqrt{(V_x+1)(V_p+1)}}{2}, \quad c_+ = \sqrt{\frac{V_p+1}{V_x+1}}\left(\frac{V_x-1}{2}\right), \quad c_- = \sqrt{\frac{V_x+1}{V_p+1}}\left(\frac{V_p-1}{2}\right). \tag{A.2}$$

In Ref. [137] the optimality of Gaussian measurement was proven for all two-mode Gaussian states, which can be decomposed as

$$\gamma_{AB}^{opt} = S(\zeta)\left[KS(r)\gamma^{TMSV}S(r)^\top K^\top + N\right]S(\zeta)^\top. \tag{A.3}$$

Here γ^{TMSV} is the two-mode squeezed vacuum state with covariance matrix

$$\gamma^{TMSV} = \begin{pmatrix} m\mathbb{1} & \sqrt{m^2-1}\sigma_z \\ \sqrt{m^2-1}\sigma_z & m\mathbb{1} \end{pmatrix}, \tag{A.4}$$

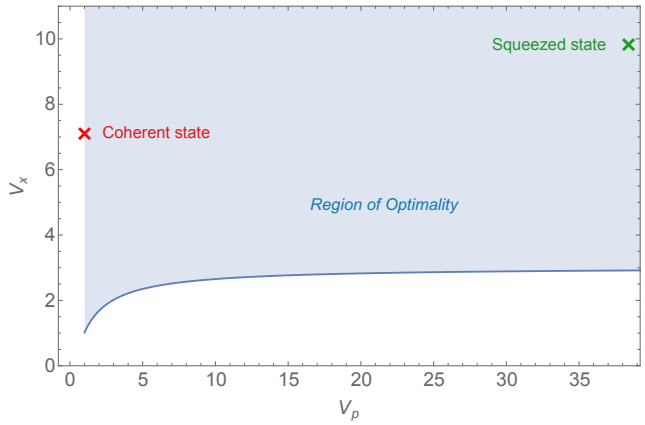

Figure A.1: Region of values of V_x and V_p where the Gaussian discord is optimal for Gaussian measurements. (Red cross) variance values corresponding to coherent state. (Green cross) variance values corresponding to squeezed state.

$S(\zeta)$ and $S(r)$ are single mode local squeezing operators such that $S(x) = \text{diag}\left\{x^{\frac{1}{2}},\ x^{-\frac{1}{2}},\ 1,\ 1\right\}$ and

$$K = \quad \text{diag}\left\{\sqrt{\tau},\ \text{sgn}(\tau)\sqrt{\tau},\ 1,\ 1\right\} \tag{A.5}$$

$$N = \qquad \text{diag}\left\{\eta,\ \eta,\ 1,\ 1\right\}. \tag{A.6}$$

The parameters of which are related as

$$\zeta = r\frac{\theta(r^{-1}}{\theta(r)}, \quad \theta(r) = \sqrt{\eta r + |\tau| m}, \tag{A.7}$$

chosen such that the optimised state with covariance matrix γ_{AB}^{opt} is in standard form with elements

$$a = \theta(r)\theta(r^{-1}), \quad c_+ = \sqrt{|\tau|(m^2-1)\frac{\theta(r^{-1})}{\theta(r)}}, \quad c_- = -\text{sgn}(\tau)\sqrt{|\tau|(m^2-1)\frac{\theta(r)}{\theta(r^{-1})}}. \tag{A.8}$$

These parameters must satisfy the conditions

$$\tau \in \mathbb{R}, \quad \eta \geq |1-\tau|, \quad r \in [m^{-1},\ m]. \tag{A.9}$$

where τ represents the transmittivity of the lossy single-mode channel with thermal noise η, such that for an "amplifier channel" $\tau > 1$ and $\eta \geq \tau - 1$.

Let us now show that under a certain condition of V_x one can express these parameters in terms of V_x and V_p which fulfil the conditions above, and $m = a$, reading as

$$\tau = -\frac{(V_x-1)(V_p-1)}{(V_x+1)(V_p+1)-4}, \quad \eta = \frac{2(V_xV_p-1)}{(V_x+1)(V_p+1)-4}, \quad r = \sqrt{\frac{V_x+1}{V_p+1}}\left(\frac{V_p-1}{V_x-1}\right). \tag{A.10}$$

First, τ is real and therefore the first of conditions Eq.'s (A.9) is satisfied. Second, because $\eta = 1 - \tau$ the second condition in Eq.'s (A.9) is fulfilled and the single-mode channel is the phase-conjugating channel which can be realised by the two-mode squeezer where the idler mode is taken as an output. Third, it can be written that $r = m^{-1}(V_x+1)(V_p-1)/[2(V_x-1)]$, one gets immediately using inequalities $V_x > 1$ and $V_p > V_x$ that $r > m^{-1}$. Finally, we also have $r = 2m(V_p - 1)/[(V_x - 1)(V_p + 1)]$ which gives $r \leq m$ provided that

$$3 - \frac{4}{V_p + 1} \leq V_x. \tag{A.11}$$

Hence this acts as the main condition on the states of which we are concerned. The left-hand side of the inequality A.11 is a monotonically increasing function of V_p which approaches the maximum value of 3 in the limit of infinitely large V_p (see Fig. A.1). Therefore, for states with a sufficiently large modulation in the x-quadrature such that $V_x \geq 3$ also the third condition in Eq.'s (A.9) is fulfilled. Hence the quantum discord of all of the states considered in Chapter 5 are optimised by Gaussian measurements, and thus the Gaussian discord corresponds to the true quantum discord.

Bibliography

[1] M. Planck, Annalen der Physik, **309**:3, pp.564-566, (1901).

[2] A. Einstein. Annalen der Physik, **17**:132, (1905).

[3] J. C. Maxwell, Philosophical Transactions of the Royal Society of London, **155**, pp.459-512, (1865).

[4] A. Einstein, B. Podolsky and N. Rosen, Phys. Rev. **47**:10, (1935).

[5] E. Schrödinger and M. Born, Mathematical Proceedings of the Cambridge Philosophical Society, **31**:4, pp.555-563, (1935).

[6] W. Heisenberg, "Über den anschaulichen Inhalt der quantentheoretischen Kinematik und Mechanik", Zeitschrift für Physik (in German) **43**:(3-4), pp.172-198, (1927).

[7] B. Schumacher, Phys. Rev. A, **51**:2738, (1995).

[8] U. Leonhardt. Essential Quantum Optics. Cambridge University Press, (2010).

[9] M. O'Scully and M. Zubairy. Quantum Optics. Cambridge University Press, (1997).

[10] C. Gerry and P. Knight. Introductory Quantum Optics. Cambridge University Press, (2005).

[11] D. Wallis and G. Milburn. Quantum Optics. Springer, (1995).

[12] L. Mandel and E. Wolf. Optical Coherence and Quantum Optics. Cambridge University Press, (1995).

[13] R. Glauber. Phys. Rev., **130**:2529, (1963).

[14] R. Glauber, Phys. Rev., **131**:2766, (1963).

[15] E. Schrödinger, Naturwissenschaften, **14**:664, (1926).

[16] D. Stoler, Phys. Rev. D, **1**:3217, (1970).

[17] J. N. Hollenhorst, Phys. Rev. D, **19**:1669, (1981).

[18] C. M. Caves, Phys. Rev. D, **23**:1693, (1981).

[19] W. Pauli. Die allgemeinen Prinzipien derWellenmechanik, Handbuch der Physik, Springer, Berlin, (1933).

[20] E. Wigner, Phys. Rev., **40**:749, (1932).

[21] J. Bertrand and P. Bertrand, Foundations of Physics, **17**:397, (1987).

[22] Kôdi Husimi, Proc. Phys. Math. Soc. Jpn. **22** pp.264-314, (1940).

[23] K. E. Cahill and R. J. Glauber. Phys. Rev., **177**:1857, (1969).

[24] K. E. Cahill and R. J. Glauber. Phys. Rev., **177**:1882, (1969).

[25] E. C. G. Sudarshan, Phys. Rev. Lett., **10**:277, (1963).

[26] R. Glauber, Phys. Rev. Lett., **10**:84, (1963).

[27] S. L. Braunstein and P. van Loock, Rev. Mod. Phys., **77**:513, (2005).

[28] G. Adesso, Entanglement of Gaussian states. PhD Thesis, University of Salerno, (2007).

[29] C. Weedbrook, S. Pirandola, R. Garcia-Patron, N. Cerf,T. Ralph, J. Shapiro and S. Lloyd, Rev. Mod. Phys. **84**:621669, (2012).

[30] A. Ferraro, S. Olivares and M. G. A. Paris, "Gaussian states in continuous variable quantum information.", Napoli Series on Physics and Astrophysics (ed. Bibliopolis, Napoli, 2005), (2005).

[31] J. Marcinkiewicz. Math. Z., **44**:612, (1939).

[32] A. K. Rajagopal and E. C. G. Sudarshan. Phys. Rev. A, **10**:1852, (1974).

[33] J. Ivan, M. Kumar and R. Simon, Quant. Inf. Pro., pp. 1, (2011).

[34] M. A. Nielsen and I. L. Chuang, Quantum Computation and Quantum Information. Cambridge University Press, (2000).

[35] J. Williamson. Am. J. Math., **58**:141, (1936).

[36] G. Adesso, A. Serafini and F. Illuminati, Open Systems & Information Dynamics, **12**:189, (2005).

[37] A. S. Holevo and R. F. Werner, Phys. Rev. A, **63**:032312, (2001).

[38] W. H. Cropper, "The Road to Entropy Rudolf Clausius". Great Physicists: The Life and Times of Leading Physicists from Galileo to Hawking. Oxford University Press. pp.93-105. (2004).

[39] I. Devetak and A. Winter, IEEE Trans. Inf. Theory, **50**:3183, (2004).

[40] J. von Neumann, Thermodynamik quantummechanischer Gesamheiten, Gött. Nach. **1**, pp.273-291, (1927).

[41] J. von Neumann, Mathematische Grundlagen der Quantenmechanik, Springer, Berlin, (1932).

[42] A. Rényi, in *Proceedings of the 4th Berkeley Symposium on Mathematics, Statistics and Probability: held at the Statistical Laboratory, University of California, 1960*, edited by J Neyman (University of California Press, Berkeley), pp.547, (1961).

[43] C. E. Shannon, Bell System Technical Journal, **27**:3 pp.379-423, (1948).

[44] J. C. Baez, arXiv: 1102.2098 (2011).

[45] J. Eisert and M. M. Wolf, in *Quantum Information with Continuous Variables of Atoms and Light* edited by N. Cerf, G. Leuchs, and E. S. Polzik (Imperial College Press, London), pp.23 (2007).

[46] V. Giovannetti, S. Guha, S. Lloyd, L. Maccone and J. H. Shapiro, Phys. Rev. A, **70**:032315, (2004).

[47] A. Serafini, J. Eisert and M. M. Wolf, Phys. Rev. A, **71**:012320, (2005).

[48] V. Giovannetti, R. GarcPatrón, N. J. Cerf and A. S. Holevo, Nature Photonics 8, pp. 796-800, (2014).

[49] R. L. Stratonovich, Izv. Vyssh. Uchebn. Zaved, Radiofiz. **8**:116, (1965) [Probl. Inf. Transm. **2**:35 (1966)].

[50] G. Adesso, D. Girolami and A. Serafini, Phys. Rev. Lett. **109**:190502, (2012)

[51] Letter from Einstein to Max Born, 3 March (1947); The Born-Einstein Letters; Correspondence between Albert Einstein and Max and Hedwig Born from 1916 to 1955, Walker, New York, (1971).

[52] L. de Broglie, An Introduction to the Study of Wave Mechanics (E. P. Dutton and Company, Inc., New York, 1930), Chapters 6, 9, and 10 Compt. rend. 183, 447 (1926).

[53] D. Bohm, Phys. Rev. **85**, (1952).

[54] J. S. Bell, Rev. Mod. Phys. **38**:447, (1966).

[55] J. S. Bell, Physics, **1**:3 pp.195-200 (1964).

[56] J. S. Bell, Introduction to the hidden variable question, Proceedings of the International School of Physics 'Enrico Fermi', Course IL, Foundations of Quantum Mechanics, pp.171-81, (1971).

[57] J. S. Bell, Journal de Physique, Colloque C2, suppl. au numero 3, Tome **42** pp.C2 41-61 (1981).

[58] S. J. Freedman and J. F. Clauser, Phys. Rev. Lett. **28**:938, (1972).

[59] A. Aspect, P. Grangier and G. Roger, Phys. Rev. Lett. **47**:460, (1981).

[60] A. Aspect, P. Grangier and G. Roger, Phys. Rev. Lett. **49**:91, (1982).

[61] A. Aspect, J. Dalibard and G. Roger, Phys. Rev. Lett. **49**:1804, (1982).

[62] C. H. Bennett and G. Brassard, "Quantum cryptography: Public key distribution and coin tossing". In Proceedings of IEEE International Conference on Computers, Systems and Signal Processing, **175**, pp.8. New York, (1984).

[63] C. Bennett, G. Brassard, C. Crepeau, R. Jozsa, A. Peres and W. Wootters, Phys. Rev. Lett., **70**:1895, (1993).

[64] D. Bouwmeester, J. W. Pan, K. Mattle, H. Weinfurter and A. Zeilinger, Nature, **390**, pp.575-579, (1997).

[65] D. Boschi, S. Branca, F. De Martini, L. Hardy and S. Popescu, Phys. Rev. Lett., **80**:1121, (1998).

[66] R. Ursin, F. Tiefenbacher, T. Schmitt-Manderbach, H. Weier, T. Scheidl, M. Lindenthal, B. Blauensteiner, T. Jennewein, J. Perdigues, P. Trojek, B. Ömer, M. Fürst, M. Meyenburg, J. Rarity, Z. Sodnik, C. Barbieri, H. Weinfurter and A. Zeilinger, Nature Phys., **3**, pp.481-486, (2007).

[67] K. C. Lee, M. R. Sprague, B. J. Sussman, J. Nunn, N. K. Langford, X.-M. Jin1, T. Champion, P. Michelberger, K. F. Reim, D. England, D. Jaksch and I. A. Walmsley, Science, **334**:6060, pp.1253-1256, (2011).

[68] M. Arndt, O. Nairz, J. Vos-Andreae, C. Keller, G. van der Zouw and A. Zeilinger, Nature, **401**, pp.680-682, (1999).

[69] E. Knill and R. Laflamme, Phys. Rev. Lett. **81**:5672, (1998).

[70] H. Häseler and N. Lütkenhaus, Phys. Rev. A **81**:060306(R), (2010).

[71] I. Khan, C. Wittmann, N. Jain, N. Killoran, N. Lütkenhaus, Ch. Marquardt and G. Leuchs Phys. Rev. A, **88**:010302(R), (2013).

[72] R. F. Werner, Phys. Rev. A, **40**, pp.4277-4281, (1989).

[73] A. Peres, Phys. Rev. Lett. **77**, pp.1413-1415, (1996).

[74] R. F. Werner and M. M. Wolf, Phys. Rev. Lett., **86**:3658, (2001).

[75] M. Choi, Linear Algebra and Its Applications, pp. 285-290, (1975).

[76] A. Peres, Phys. Rev. Lett., **77**, pp.1413-1415, (1996).

[77] M. Horodecki, P. Horodecki and R. Horodecki, Phys. Lett. A, **223**:1, (1996).

[78] R. Simon, Phys. Rev. Lett. **84**:2726, (2000).

[79] O. Gühne and G. Tóth, Physics Reports, **474**:1-6, pp. 1-75, (2009).

[80] L.-M. Duan, G. Giedke, J. I. Cirac and P. Zoller, Phys. Rev. Lett., **84**:2722, (2000).

[81] L. Mišta, Jr., Phys. Rev. A, **7**:062326, (2013).

[82] V. Giovannetti, S. Mancini, D. Vitali and P. Tombesi, Phys. Rev. A, **67**:022320, (2002).

[83] P. Horodecki, Phys. Lett. A, **232**, (1997).

[84] M. Horodecki and P. Horodecki, Phys. Rev. A. **59**:4206, (1999).

[85] N. J. Cerf, C. Adami and R. M. Gingrich, Phys. Rev. A. **60**:898, (1999).

[86] M. B. Plenio and S. Virmani, Quant. Inf. Comp. **1**:1-51 (2007).

[87] C. Bennett, G. Brassard, S. Popescu, B. Schumacher, J. Smolin and W.Wootters, Phys. Rev. Lett., **76**:722, (1996).

[88] C. H. Bennett, D. P. DiVincenzo, J. A. Smolin, and W. K. Wootters, Phys. Rev. A, **54**:3824, (1996).

[89] G. Vidal and J. I. Cirac, Phys. Rev. A, **65**:012323, (2001).

[90] P. Marian and T. A. Marian, Phys. Rev. Lett., **101**:220403 (2008).

[91] G. Giedke, M. M. Wolf, O. Krüger, R. F. Werner and J. I. Cirac, Phys. Rev. Lett., **91**:107901, (2003).

[92] M. M. Wolf, G. Giedke, O. Krüger, R. F. Werner and J. I. Cirac, Phys. Rev. A **69**:052320, (2004);

[93] G. Adesso and F. Illuminati, Phys. Rev. A, **72**:032334, (2005).

[94] R. R. Tucci, arXiv:quant-ph/9909041, (1999).

[95] R. R. Tucci, arXiv:quant-ph/0005119, (2000).

[96] R. R. Tucci, arXiv:quant-ph/0005119, (2000).

[97] R. R. Tucci, arXiv:quant-ph/0101123, (2001).

[98] R. R. Tucci, arXiv:quant-ph/0103040, (2001).

[99] R. R. Tucci, arXiv:quant-ph/0202144, (2002).

[100] E. H. Lieb, M. B. Ruskai, J. Math. Phys., **14**, pp. 1938-1941, (1973).

[101] M. Christandl and A. Winter, J. Math. Phys., **45**:3, pp. 829-840 (2004).

[102] X.-yu Chen, Phys. Rev. A, **71**:062320, (2005).

[103] L. Huai-Xin and Z. Bo, Chinese Physics, **15**:9, (2006).

[104] K. Zyczkowski, P. Horodecki, A. Sanpera and M. Lewenstein, Phys. Rev. A, **58**:883, (1998).

[105] G. Vidal and R. F. Werner, Phys. Rev. A, **65**:032314, (2002).

[106] M. B. Plenio, Phys. Rev. Lett., **95**:090503, (2005).

[107] A. Ferraro, L. Aolita, D. Cavalcanti, F. M. Cucchietti and A. Acín, Phys. Rev. A, **81**:052318, (2010).

[108] A. Datta, A. Shaji and C. M. Caves, Phys. Rev. Lett. **100**:050502 (2008).

[109] B. P. Lanyon, M. Barbieri, M. P. Almeida, and A. G. White, Phys. Rev. Lett., **101**:200501, (2008).

[110] C. H. Bennett, D. P. DiVincenzo, C. A. Fuchs, T. Mor, E. Rains, P. W. Shor, J. A. Smolin and W. K. Wootters, Phys. Rev. A, **59**:1070, (1999).

[111] M. Horodecki, P. Horodecki, R. Horodecki, J. Oppenheim, A. Sen, U. Sen and B. Synak-Radtke, Phys. Rev. A, **71**:062307, (2005).

[112] J. Niset and N. J. Cerf, Phys. Rev. A, **74**:052103, (2006).

[113] S. L. Braunstein, C. M. Caves, R. Jozsa, N. Linden, S. Popescu and R. Schack, Phys. Rev. Lett., **83**:1054, (1999).

[114] D. A. Meyer, Phys. Rev. Lett., **85**:2014, (2000).

[115] A. Datta, S. T. Flammia and C. M. Caves, Phys. Rev. A, **72**:042316, (2005).

[116] A. Datta and G. Vidal, Phys. Rev. A, **75**:042310, (2007).

[117] R. Dillenschneider, Phys. Rev. B, **78**:224413, (2008).

[118] M. S. Sarandy, Phys. Rev. A, **80**:022108, (2009).

[119] J. Cui and H. Fan, J. Phys. A: Math. Theor., **43**:045305, (2010).

[120] S. Gharibian, M, Piani, G. Adesso, J. Calsamiglia and P, Horodecki, Int. J. Quant. Inf., **9**:7-8, pp.1701-1713, (2011).

[121] M, Piani, S. Gharibian, G. Adesso, J. Calsamiglia, P, Horodecki and A. Winter, Phys. Rev. Lett. **106**:220403, (2011).

[122] B. Groisman, D. Kenigsberg and T. Mor, arXiv:quant-ph/0703103, (2007).

[123] B. Bylicka and D. Chruscinski, Open Syst. Inf. Dyn., **19**:1250006, (2012).

[124] S. Rahimi-Keshari, C. M. Caves and T. C. Ralph, Phys. Rev. A, **87**:012119, (2013).

[125] L. A. Correa, A. A. Vaildo and D. Alonso, Phys. Rev. A, **86**:012110, (2012).

[126] H. Ollivier and W. H. Zurek, Phys. Rev. Lett., **88**:017901 (2001).

[127] F. Galve, G. Giorgi, R. Zambrini, Europhys. Lett., **96**:40005, (2011).

[128] M. Piani, P. Horodecki and R. Horodecki, Phys. Rev. Lett., **100**:090502, (2008).

[129] D. Girolami, M. Paternostro, G. Adesso, J. Phys. A: Math. Theor., **44**:352002, (2011).

[130] L. Henderson and V. Vedral, Journal of Physics A, **34**:6899, (2001).

[131] A. Streltsov, H. Kampermann and D. Bruß, Phys. Rev. Lett., **107**:170502, (2011).

[132] A. Streltsov and W. H. Zurek, Phys. Rev. Lett. **111**:040401, (2013).

[133] G. Adesso and A. Datta, Phys. Rev. Lett., **105**:030501, (2010).

[134] P. Giorda and M. G. A. Paris, Phys. Rev. Lett., **105**:020503, (2010).

[135] P. Giorda, M. Allegra and M. G. A. Paris, Phys. Rev. A, **86**:052328, (2012).

[136] J. Fiurášek and L. Mišta Jr., Phys. Rev. A, **75**:060302(R), (2007).

[137] S. Pirandola, G. Spedalieri, S. L. Braunstein, N. J. Cerf and S. Lloyd, Phys. Rev. Lett., **113**:140405, (2014).

[138] S. Rahimi-Keshari, T. C. Ralph and C. M. Caves, arXiv:1502.02331, (2015).

[139] K. Modi, T. Paterek, W. Son, V. Vedral and M. Williamson, Phys. Rev. Lett., **104**:080501, (2010).

[140] B. Dakic, V. Vedral and C. Brukner, Phys. Rev. Lett., **105**:190502, (2010).

[141] G. Adesso and D. Girolami, Int. J. Quant. Inf., **9**:7-8, (2011).

[142] D. Z. Rossatto, T. Werlang, E. I. Duzzioni and C. J. Villas-Boas, Phys. Rev. Lett., **107**:153601, (2011).

[143] J. S. Zhang, L. Chen, M. Abdel-Aty and A. X. Chen, Eur. Phys. J. D, **66**:2, (2012).

[144] Y. X. Chen and S. W. Li, Phys. Rev. A, **81**:032120, (2010).

[145] X. S. Ma, M. T. Cheng, G. X. Zhao and A. M. Wang, Physica A, **391**:2500, (2012).

[146] F. F. Fanchini, L. K. Castelano and A. O. Caldeira, New J. Phys., **12**:073009, (2010).

[147] S. Scheel, J. Eisert, P. L. Knight and M. B. Plenio, J. Mod. Opt., **50**:881, (2003).

[148] T. Yu and J. H. Eberly, Phys. Rev. Lett., **93**:140404, (2004).

[149] T. Yu and J. H. Eberly, Science (London), **323**:598, (2009).

[150] J. S. Zhang, J.B. Xu, and Q. Lin, Eur. Phys. J. D, **51**:283, (2009).

[151] M. P. Almeida, F. deMelo, M. Hor-Meyll, A. Salles, S. P. Walborn, P. H. Souto Ribeiro and L. Davidovich, Science (London), **316**:579, (2007).

[152] A. Salles, F. de. Melo, M. P. Almeida, M. Hor-Meyll, S. P. Walborn, P. H. Souto Ribeiro and L. Davidovich, Phys. Rev. A, **78**:022322 (2008).

[153] J. Laurat, K. S. Choi, H. Deng, C. W. Chou and H. J. Kimble, Phys. Rev. Lett., **99**:180504, (2007).

[154] B. Wang, Z. Y. Xu, Z. Q. Chen and M. Feng, Phys. Rev. A, **81**:014101, (2010).

[155] A. Auyuanet and L. Davidovich, Phys. Rev. A, **82**:032112, (2010).

[156] Z. Y. Sun, L. Li, K. L. Yao, G. H. Du, J. W. Liu, B. Luo, N. Li and H. N Li, Phys. Rev. A, **82**:032310, (2010).

[157] T. Werlang, S. Souza, F. F. Fanchini and C. J. Villas Boas, Phys. Rev. A, **80**:024103, (2009).

[158] F. F. Fanchini, T. Werlang, C. A. Brasil, L. G. Arruda and A. O. Caldeira, Phys. Rev. A, **81**:052107, (2010).

[159] S. Campbell, T. J. G. Apollaro, C. Di Franco, L. Banchi, A. Cuccoli, R. Vaia, F. Plastina and M. Paternostro, Phys. Rev. A, **84**:052316, (2011).

[160] I. Dzyaloshinskii, Journal of Physics and Chemistry of Solids, **4**:241, (1958).

[161] T. Moriya, Phys. Rev., **120**:91, (1960).

[162] D. Cavalcanti, L. Aolita, S. Boixo, K. Modi, M. Piani and A. Winter, Phys. Rev. A, **83**:032324, (2011).

[163] M. Horodecki, J. Oppenheim and A. Winter, Nature, **436**:7051, pp. 673-676, (2005).

[164] C. H. Bennett and S. J. Wiesner, Phys. Rev. Lett., **69**:2881, (1992).

[165] M. Horodecki, P. Horodecki, R. Horodecki, D. Leung and B. Terhal, Quantum Inf. Comput., **1**:70, (2001).

[166] A. Winter, J. Math. Phys., **43**:4341, (2002).

[167] M. Horodecki and M. Piani, J. Phys. A: Math. Theor., **45**:105306, (2012).

[168] S. Pirandola, Scientific Reports, **4**:6956, (2014).

[169] S. Luo, Phys. Rev. A, **77**:022301, (2008).

[170] D. Girolami, M. Paternostro and G. Adesso, J. Phys. A: Mathematical and Theoretical, **44**:352002, (2011).

[171] S. Wu, U. V. Poulsen and K. Mølmer, Phys. Rev. A, **80**:032319, (2009).

[172] M. Piani, P. Horodecki and R. Horodecki, Phys. Rev. Lett., **100**:090502, (2008).

[173] L. Mišta, Jr., R. Tatham, D. Girolami, N. Korolkova and G. Adesso, Phys. Rev. A, **83**:042325, (2011).

[174] A. Ferraro and M. G. A. Paris, Phys. Rev. Lett., **108**:260403, (2012).

[175] M. Brunelli, C. Benedetti, S. Olivares, A. Ferraro, M. G. A. Paris, arXiv:1502.04996, (2015).

[176] M. Koashi and A. Winter, Phys. Rev. A, **9**:022309, (2004).

[177] S. Olivares and M. G. A. Paris, Int. J. Mod. Phys. B, **27**:1245024, (2012).

[178] V. Chille, N. Quinn, C. Peuntinger, C. Croal, L. Mišta, Jr., C. Marquardt, G. Leuchs and N. Korolkova, Phys. Rev. A, **91**:050301(R), (2015).

[179] R. Tatham and N. Korolkova, Phys. Scr., **T160**:014040, (2014).

[180] G. H. Aguilar, O. Jimenez Farias, A. Valdes-Hernandez, P. H. Souto Ribeiro, L. Davidovich and S. P. Walborn, Phys. Rev. A, **89**:022339, (2014).

[181] N. Korolkova, G. Leuchs, R. Loudon, T. C. Ralph and C. Silberhorn, Phys. Rev. A, **65**:052306, (2002).

[182] R. Dong, O. Glöckl, J. Heersink, U. L. Andersen, J.Yoshikawa and G. Leuchs, New J. Phys. 9, 410 (2007).

[183] T. Eberle, V. Händchen and R. Schnabel, Optics Express **21**:11546 (2013).

[184] R. Dong, J. Heersink, J.-I. Yoshikawa, O. Glöckl, U. L. Andersen and G. Leuchs, New J. Phys., **9**:410, (2007).

[185] L. S. Madsen, A. Berni, M. Lassen and U. L. Andersen, Phys. Rev. Lett., **109**:030402, (2012).

[186] M. Gue, H. M. Chrzanowski, S. M. Assad, T. Symul, K. Modi, T. C. Ralph, V.Vedral and P. K. Lam, Nature Physics, **8**:671, (2012).

[187] U. Vogl, R. T. Glasser, Q. Glorieux, J. B. Clark, N. V. Corzo and P. D. Lett, Phys. Rev. A, **87**:010101(R), (2013).

[188] G. G. Stokes, Trans. Cambridge Philos. Soc., **9**:399, (1852).

[189] G. G. Stokes, Mathematical and Physical Papers, **3**, (1901).

[190] L. Mišta, Jr., D. McNulty and G. Adesso, Phys. Rev. A, **90**:022328, (2014).

[191] F. Ciccarello and V. Giovannetti, Phys. Rev. A, **85**:010102, (2012).

[192] P. Marian, I. Ghiu, T. A. Marian, arXiv:1412.0096, (2014).

[193] A. Serafini, G. Adesso and F. Illuminati, Phys. Rev. A, **71**:032349, (2005).

[194] M. S. Kim, W. Son, V. Bužek and P. L. Knight, Phys. Rev. A, **65**:032323, (2002).

[195] Ch. Peuntinger, V. Chille, L. Mišta, N. Korolkova, M. Förtsch, J. Korger, Ch. Marquardt and G. Leuchs, Phys. Rev. Lett., **111**:230506, (2013).

[196] T. S. Cubitt, F. Verstraete, W. Dür and J. I. Cirac, Phys. Rev. Lett., **91**:037902, (2003).

[197] C. E. Vollmer, D. Schulze, T. Eberle, V. Händchen, Fiurášek and R. Schnabel, Phys. Rev. Lett., **111**:230505, (2013).

[198] A. Fedrizzi, M. Zuppardo, G. G. Gillett, M. A. Broome, M. de Almeida, M. Paternostro, A. G. White and T. Paterek, Phys. Rev. Lett., **111**:230504, (2013).

[199] G. Adesso, V. D'Ambrosio, E. Nagali, M. Piani and F. Sciarrino, Phys. Rev. Lett., **112**:140501, (2014).

[200] D. M. Greenberger, M. A. Horne, A. Zeilinger: Bell's theorem, Quantum Theory, and Conceptions of the Universe, pp.73-76, Kluwer Academics, Dordrecht, The Netherlands, (1989).

[201] L. Mišta, Jr and N. Korolkova, Phys. Rev. A, **77**:050302, (2008).

[202] L. Mišta, Jr and N. Korolkova, Phys. Rev. A, **80**:032310, (2009).

[203] T. K. Chuan, J. Maillard, K. Modi, T. Paterek, M. Paternostro and M. Piani, Phys. Rev. Lett., **109**:070501, (2012).

[204] L. Mišta, Jr and N. Korolkova, Phys. Rev. A, **86**:040305(R), (2012).